



Justus-Liebig-Universität Gießen

Klinik Für Neurologie



**Functional characterization of the protein
kinase MK2 in the pathogenesis of Experimental
autoimmune encephalomyelitis (EAE)**

Inaugural Dissertation

Submitted

In partial fulfillment of the requirements for the
Dr. Degree
To the Faculties of Veterinary Medicine and Medicine
Of the Justus-Liebig-University Giessen, Germany

By

Liza Gupta

Patiala, India

Giessen, 2017

Germany

Multiple sclerosis Research Group

Department of Neurology of the Justus-Liebig-University Giessen

Prof. Dr. Manfred Kaps

First Supervisor:

Prof. Dr. Martin Berghoff

Faculty of Medicine

Multiple Sclerosis Research Group

Neurology Clinic

Justus-Liebig-University Giessen

Second Supervisor:

Prof. Dr. Martin Diener

Faculty of Veterinary Medicine

Institute of Veterinary Physiology and Biochemistry

Justus-Liebig-University Giessen

Committee members:

PD Dr. Christoph Rummel

Institute of Veterinary Physiology and Biochemistry

Justus-Liebig-University Giessen

Prof. Dr. Norbert Weissmann

Medical Clinic II

Excellence Cluster Cardio-Pulmonary System (ECCPS)

Justus-Liebig-University Giessen

Doctoral Defense: 08.12.2017

ABBREVIATIONS

BBB	Blood Brain Barrier
BDNF	Brain-derived neurotrophic factor
BSA	Bovine serum albumin
CNS	Central nervous system
CSF	Cerebrospinal fluid
DNA	Deoxyribonucleic acid
EAE	Experimental autoimmune encephalomyelitis
ECL	Enhanced chemiluminescence
ERK	Extracellular signal-regulated kinases
GA	Glatiramer acetate
GAPDH	Glyceraldehyde 3-phosphate dehydrogenase
h	hour
H and E	Hematoxylin and Eosin
IFN β -1a	Interferon β -1a
IL	Interleukins
iNOS	Inducible Nitric oxide synthase
KA	Kainic acid
LFB/PAS	Luxol fast blue/periodic acid Schiff
LINGO-1	Leucine rich repeat and Immunoglobulin-like domain-containing protein 1

MBP	Myelin Basic protein
min	Minutes
MK2	Mitogen-activated protein kinase activated protein kinase 2 (MK2)
MOG	Myelin oligodendrocyte glycoprotein
mRNA	Messenger Ribonucleic acid
MS	Multiple sclerosis
OLG	Oligodendrocyte
OPC	Oligodendrocyte progenitor cells
p.i.	Post immunization
PBS	Phosphate buffered saline
PFA	Paraformaldehyde
PLP	Proteolipid protein
RT	Room temperature
RT-PCR	Real time-Polymerase chain reaction
SEMA3A	Semaphorin-3A
SDS	Sodium dodecyl sulfate
TBS	Tris buffered saline
TBST	Tris buffered saline with Tween 20
TNF	Tumor necrosis factor
TrkB	Neurotrophic tyrosine kinase receptor, type 2

For my loving Grandmother

DECLARATION

I hereby declare that the present thesis is my original work and that it has not been previously presented in this or any other university for any degree. I have appropriately acknowledged and referenced all text passages that are derived literally from or are based on the content of published or unpublished work of others and all information that relates to verbal communications. I have abided by the principles of good scientific conduct laid down in the charter of the Justus Liebig University of Giessen in carrying out the investigations described in the dissertation.

Liza Gupta

Table of Contents

1	Introduction	1
1.1	Multiple sclerosis	1
1.1.1	Etiology of MS	2
1.1.2	MS symptoms and pathology	3
1.1.3	MS diagnosis	6
1.1.4	Subtypes of MS	8
1.1.5	MS treatment	8
1.2	Animal models of multiple sclerosis	12
1.2.1	Overview	12
1.2.2	Experimental autoimmune encephalomyelitis (EAE)	12
1.3	P38 and MK2 pathway	16
1.3.1	MK2 and Inflammation	17
1.3.2	MK2 glial cells and myelination	18
1.3.3	MK2 and EAE	20
2	Objectives	22
3	Materials and Methods	23
3.1	MATERIALS	23
3.1.1	Animals	23
3.1.2	Cell lines	23
3.1.3	Primary antibodies	23
3.1.4	Secondary antibodies	25
3.1.5	Kits	26
3.1.6	Genotyping Primers	26
3.1.7	Primers used for analysis	27
3.1.8	Ladders	28
3.1.9	Chemicals	28
3.1.10	Laboratory consumables	30
3.1.11	Laboratory instruments	31
3.1.12	Buffers	33
3.1.13	Softwares	34
3.2	Methods	34
3.2.1	Mice	34
3.2.2	Molecular biology	42
3.2.3	Histopathology and immunohistochemistry	44
3.2.4	Cell culture experiments	46

3.2.5	Statistics	47
4	RESULTS	48
4.1	Genotype confirmation of MK2 deletion in C57BL/6J mice	48
4.1.1	Total MK2 was decreased in the MK2 ^{-/-} mice	49
4.2	EAE in MK2^{-/-} and control mice	49
4.2.1	Clinical scoring	49
4.3	Clinical symptoms of MK2^{-/-} mice	50
4.3.2	Assessment of inflammation: Cell infiltration of T-cells, B-cells and macrophages	53
4.3.3	Demyelination and axonal density in MK2 ^{-/-} mice	59
4.3.4	Pattern of cytokines expression in MK2 ^{-/-} mice spinal cord	62
4.3.5	The cytokine expression in the spleen of MK2 ^{-/-} and wild type mice	64
4.3.6	Myelin protein expression in the spinal cord of MK2 ^{-/-} and wild type mice	65
4.3.7	The remyelination markers were altered in MK2 ^{-/-} mice	69
4.3.8	CREB phosphorylation was increased in the MK2 ^{-/-} mice	71
4.3.9	NF-κB phosphorylation is reduced in the MK2 ^{-/-} mice	71
4.3.10	Levels of Akt and STAT-1 remained unchanged in the MK2 ^{-/-} mice	72
4.3.11	Analyzing the growth factor receptor Trk-B in MK2 ^{-/-} mice	73
4.4	In vitro experiments	74
4.4.1	MK2 is required for glatiramer acetate mediated C17.2 neuronal cell survival/proliferation	74
5	DISCUSSION	76
5.1	MK2 knockout mice have a normal phenotype	76
5.2	EAE in MK2^{-/-} mice	77
5.3	Decreased inflammation and infiltration of immune cells	78
5.4	Myelination and axonal density	79
5.5	Cytokine levels	80
5.6	NF-κB protein level	82
5.7	Phosphorylation of CREB	82
5.8	Regulation of myelin proteins and inhibitors of remyelination	83
5.9	Role of MK2 in glatiramer acetate mediated C17.2 neuronal cell proliferation/survival	85
6	Summary	86

List of Figures

Figure 1: World distribution of multiple sclerosis

Figure 2: Symptoms of multiple sclerosis

Figure 3: The inflammation phase of multiple sclerosis

Figure 4: MK2 signaling pathway

Figure 5: MK2 deficiency leads to severity and prolongation of EAE

Figure 6: Induction of MOG₃₅₋₅₅-induced EAE

Figure 7: Strategy applied to mutate the MK2 gene

Figure 8: Genotyping gels

Figure 9: Protein analysis of total MK2 in acute and chronic EAE mice spinal cord

Figure 10: Clinical symptoms of MOG₃₅₋₅₅-induced EAE

Figure 11: Chronic phase clinical course of MOG₃₅₋₅₅-induced EAE

Figure 12: Acute phase clinical course of MOG₃₅₋₅₅-induced EAE

Figure 13: Complete clinical course of MOG₃₅₋₅₅-induced EAE

Figure 14: The inflammatory index of EAE investigated with H & E staining

Figure 15: T cell infiltration in white matter lesions

Figure 16: B cell infiltration in white matter lesions

Figure 17: Macrophages/microglia infiltration in white matter lesions

Figure 18: Demyelination of EAE investigated with LFB/PAS staining

Figure 19: Bielschowsky silver staining for axonal density of white matter lesions

Figure 20: mRNA expression of proinflammatory cytokines in the mice spinal cord

Figure 21: mRNA expression of proinflammatory cytokines in mice spleen

Figure 22: mRNA expression of the myelin proteins in the mice spinal cord

Figure 23: Protein analysis of MBP expression in the mice spinal cord

Figure 24: Histopathological analysis of MBP expression in the mice spinal cord

Figure 25: mRNA expressions of the remyelination inhibitors in the mice spinal cord

Figure 26: CREB phosphorylation in acute and chronic EAE mice spinal cord

Figure 27: NF- κ B phosphorylation in acute and chronic EAE mice spinal cord

Figure 28: AKT, STAT1 phosphorylation in acute and chronic EAE mice spinal cord

Figure 29: TrkB expression in acute and chronic EAE mice spinal cord

Figure 30: GA treatment in MK2 knockdown C17.2 cells

Figure 31: WST proliferation assay of GA treatment in MK2 knockdown C17.2 cells

List of Tables

Table 1: The 2010 McDonald criteria for diagnosis of MS

Table 2: Commonly used rodent EAE models

Table 3: Clinical characteristics of MOG₃₅₋₅₅-induced EAE in MK2^{-/-} mice

Table 4: Immune cell infiltration in spinal cord of EAE mice

Table 5: Histopathological analysis of spinal cord from EAE mice

Abstract

The objective of this study is to characterize the role of MK2 in experimental autoimmune encephalomyelitis (EAE), an animal model for multiple sclerosis (MS). Inflammatory demyelination in the CNS is the pathological hallmark of MS. MK2 is an essential component in the inflammatory response, which regulates biosynthesis of TNF- α at a post-transcriptional level. We hypothesized that MK2 is a negative regulator in EAE. The previous study done in our lab underlines the significance of MK2 in the regulation of CNS inflammatory disease, multiple sclerosis and its animal model, EAE. The initial hypothesis was rejected in the study as MK2 deficiency resulted in a more severe disease course and was associated with more cellular CNS inflammation.

Yet, this study is the first to characterize the morphology, histology and distribution of immune cells in spinal cord lesions of MOG₃₅₋₅₅-EAE of MK2^{-/-} mice. MOG₃₅₋₅₅ peptide was used to induce EAE in 10-12 weeks old MK2^{-/-} and control female mice. No phenotypic changes were observed in MK2^{-/-} mice. The clinical symptoms were seen from day 9-11 after the induction. The MK2^{-/-} mice showed milder symptoms of MOG₃₅₋₅₅-EAE on day 12 and day 14, the acute phase of EAE. Histological analysis of the acute phase EAE showed reduced inflammation, reduced total myelin loss and axonal loss. Acute phase EAE was associated with some regulations, however, no pattern was seen in the chronic phase EAE. These findings suggest that MK2 might not serve as a potential target in the treatment of EAE model.

1 Introduction

1.1 Multiple sclerosis

There have been descriptions of multiple sclerosis (MS) since the 14th century. It was, Jean-Martin Charcot (1825–1893) the French neurologist, who made the first definite connections between the symptoms of MS and the pathological changes seen in post-mortem samples (Lublin & Reingold, 1996). The first recognizable case of multiple sclerosis appears to be that of Augustus d'Este (1794–1848), the grandson of George III of England and cousin of Queen Victoria (Weiner, 2005). This ambiguous, relapsing and progressive disorder of the central nervous system continues to be challenging in not only understanding the pathogenesis of the disease but also its prevention and progression. The course of MS is highly diverse and unpredictable. With around 2.5 million worldwide and 120,000 people affected in Germany alone, billions of dollars are spent in health care costs. Women are affected twice as much by MS as men and persons of Northern European descent appear to be at a higher risk for MS (Brust, 2007; Hauser SL, 2008). MS typically occurs in adults aged 20 to 45 years; occasionally, it may also be present in childhood or late middle age (Brust, 2007). The cause of MS still remains unknown, but the current knowledge points to the involvement of combination of genetic susceptibility and a non-genetic trigger, such as virus, changes in metabolism or environmental factors. When that is put together it results in this autoimmune disorder that leads to recurrent immune attacks on the CNS (Brust, 2007).

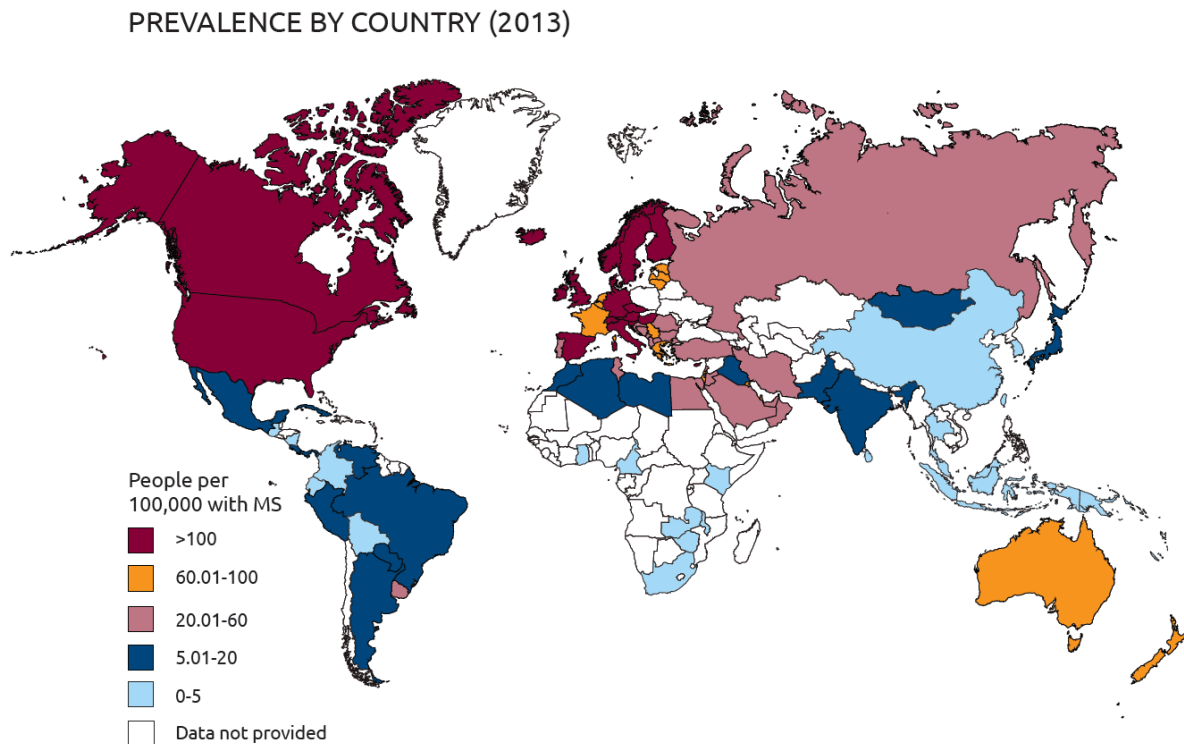


Figure 1 World distribution of multiple sclerosis: greater prevalence in higher northern and southern latitudes. (Source: WHO MS Atlas)

1.1.1 Etiology of MS

The primary cause of damage in MS is the inflammation of central nervous system. Previous studies suggested that genetic, environmental and infectious agents can be some of the factors influencing the development of MS (Loma & Heyman, 2011). Studies with families and twin have shown a 40-fold increase in susceptibility amongst first-degree relatives of MS patients, which suggests a genetic basis for a risk to develop MS (Loma & Heyman, 2011). Environmental factors, such as exposure to infectious agents as well as sunlight exposure/vitamin D can be accounted for risk of MS. The risk persists even when a person migrates from one risk area to another before the age of 15 years (Milo & Kahana, 2010). The infectious agents known to be possibly involved are human herpes virus type 6, Epstein Barr virus and mycoplasma pneumonia (Fujinami, von Herrath, Christen, & Whitton, 2006).

1.1.2 MS symptoms and pathology

The symptoms of MS are varied and differ from patient to patient, but some patterns are usually the same and can be defined (Compston & Coles, 2008). The most commonly affected sites, which show significant symptoms are the optic nerves, the cerebrum and the spinal cord. Patients can be manifested with a distinct number of symptoms including changes in vision (unilateral visual loss, diplopia), weakness, discoordination, distortions or changes in bowel and bladder function. There are other array of symptoms as well which have less diagnostic value; these include cognitive change, fatigue and mood disturbances. So many varied symptoms and progression of this disease may eventually lead to severe disability (Loma & Heyman, 2011).

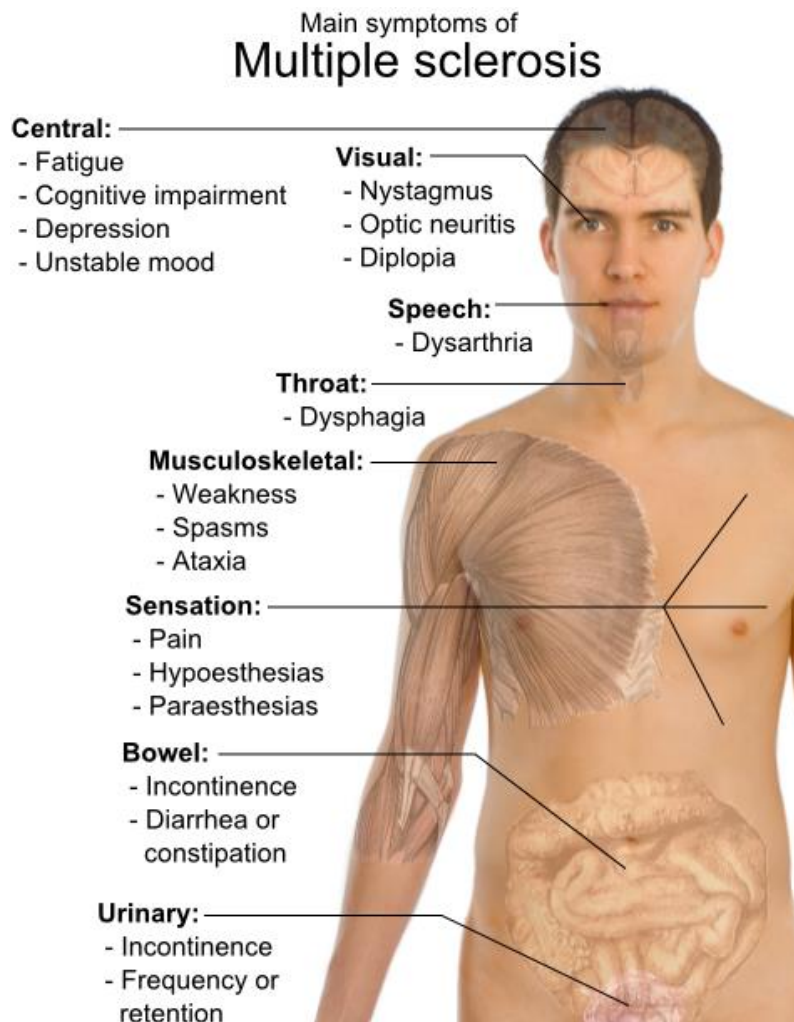


Figure 2: Major symptoms of multiple sclerosis. (Image by J.Oksenberg/UCSF)

The conventional view of explaining the sequence of events that occur in MS start with activation of myelin reactive T-cells which migrate from the periphery into the CNS. This leads to inflammation and development of focal demyelinating lesions, which is the main pathological feature for relapses. The progressive phase of MS consists of axonal degeneration with neuronal loss. Previous pathological studies have shown that throughout the normal appearing white matter, axonal degeneration occurs diffusely (Mahad, Trapp, & Lassmann, 2015). Conduction block is the major cause of the negative symptoms during relapses that range from paralysis, blindness to numbness. This is caused largely by inflammation and demyelination and possibly by defects in synaptic transmission. In remission the recovery from symptoms is mainly due to the restoration of axonal function. This restoration is either because of remyelination, the settlement of inflammation or the restoration of conduction to axons. These impairments persist in the demyelinated state which in turn contributes to weakness and sensory problems (K. J. Smith & McDonald, 1999).

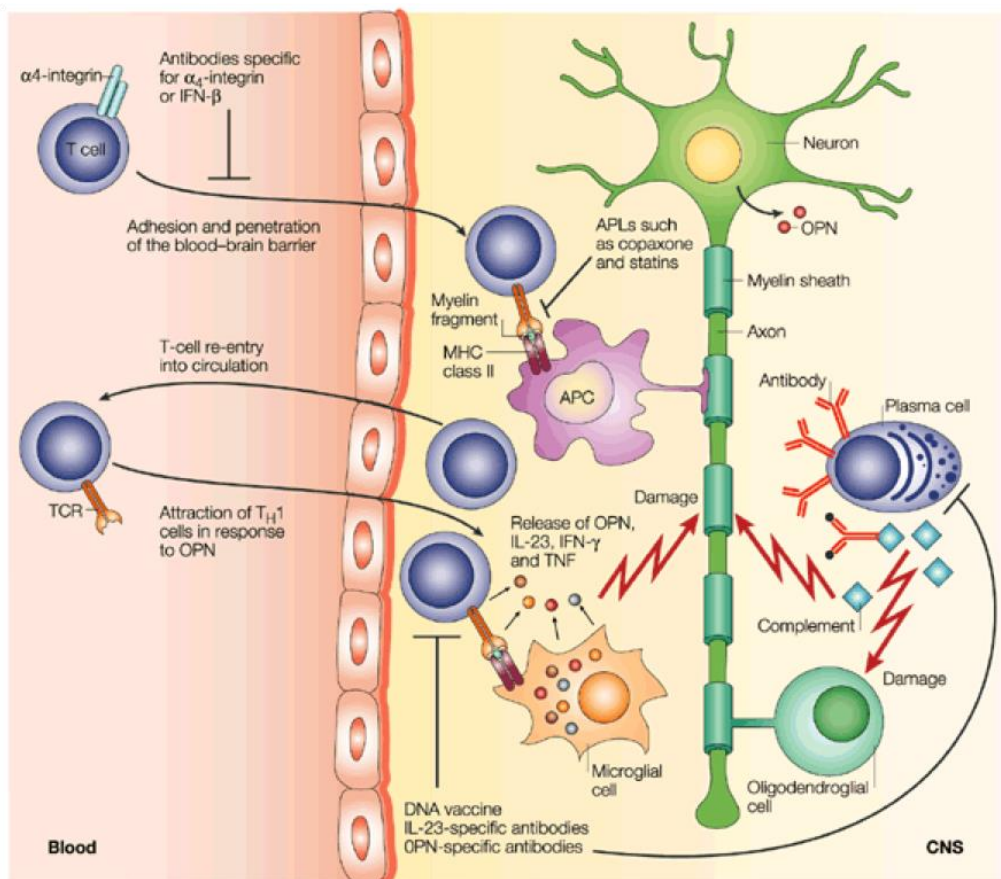


Figure 3: The inflammation phase of multiple sclerosis. Transcriptional analysis of targets in multiple sclerosis (Steinman & Zamvil, 2003)

MS is primarily an inflammatory disease of the CNS in which auto-aggressive T-cells cross the blood-brain barrier (BBB) causing demyelination and axonal loss resulting in progressive disability (Ortiz et al., 2014). The inflammatory process is started by autoimmune T-cells reaction that targets myelin antigens, which can be initiated through molecular mimicry mechanisms (Karussis, 2014). There are numerous other cell types and cell subsets that are also involved, like T helper 17 (Th17) cells (McFarland & Martin, 2007). Pro-inflammatory cytokines like IL-17, IL-6 are secreted by these T-cells (Th17) and are regulated by IL-23 (Langrish et al., 2005; Steinman, 2007). A transition from physiological surveillance to a pathological immune response occurs when these inflammatory cells and other cell types become deregulated, which is when the disease occurs (Compston & Coles, 2008; Dolei et al., 2014)

There are studies from thsions of MS patients confirming an overwhelming presence of CD4⁺ cells secreting IL-17 in active lesions. In MS lesions though, both CD4⁺ and CD8⁺ cells express IL-17 (Tzartos et al., 2008).

Chemokine receptor CCR6 expressed on Th17 cells interacts with CCL20/MIP-3 α expressed on endothelium, it facilitates transport through the choroid plexus into the CSF and perivascular space (Reboldi et al., 2009). GM-CSF might also be produced by Th17 cells, this can be promoted by resident antigen presenting cells (APCs) secreting IL-23. This initiates a positive feedback loop as the same APCs are stimulated by GM-CSF (Codarri et al., 2011; Dolei et al., 2014; El-Behi et al., 2011). Also, by disrupting the endothelial tight junctions the Th17 cells may further increase permeability of the BBB due to the secretion of IL-17 and IL-22. This allows interactions with endothelium, which allows further attraction of CD4⁺ subsets as well as other immune cells. Consequently a pathological sequence is initiated; consisting of inflammation, infiltrates and damage to neurons and glia cells (Dolei et al., 2014; Tzartos et al., 2008).

Myelin destruction is the essential component of the plaques within the CNS. The MS plaques are not simply an inflammatory demyelinating entity in isolation; rather lesions are composed of wide variety of immunological and pathological entities. There is a close relation of cellular and molecular components, time of damage and repair systems to myelin loss and axonal injury. Thus, it is important to understand the various features of plaque development as they provide a mechanism to understand the pathogenic mechanisms underlying MS.

MS plaques are classified based on the stages and the time for progression of inflammatory destruction. There are acute, chronic acute and chronic silent lesions. Studies have shown that these lesions occur along a continuous timeline, they eventually scar and harden the areas within the CNS. Acute plaques have non-defined myelin loss, infiltration of immune cells and parenchymal edema. The immune cell influx involves lymphocytes and monocytes. There are studies that reveal oligodendrocyte apoptosis, but the degree of damage inside an active lesion can vary (Henderson et al., 2009, Greenfield et al., 2008). Glial scarring and regions of hypocellularity with loss of myelin characterize the chronic plaques. It has been noticed that histologically the lesion borders are more distinct and differentiated in chronic plaques. Chronic plaques can be of two distinct forms: chronic active lesion and chronic silent lesion. The borders of chronic active plaques are populated with activated microglia, macrophages and astrocytes (Greenfield et al., 2008). Chronic silent lesions are at a loss of inflammatory traits along the borders of chronic active lesions. The presence of oligodendrocyte progenitors and remyelination are uncommon features (Wilson et al., 2006).

1.1.3 MS diagnosis

Multiple sclerosis is diagnosed by using both clinical and paraclinical laboratory assessments (Schumacher et al., 2006, Poser et al., 1983). The diagnostic criteria's emphasizes the need to demonstrate dissemination of lesions in space (DIS) and time (DIT). Though the diagnosis can be made on clinical grounds alone, magnetic resonance imaging (MRI) of the central nervous system (CNS) can be greatly supportive to supplement or even replace some clinical criteria, (Paty et al., 1988, Polman et al., 2005). This was most recently emphasized by the McDonald Criteria of the International Panel on the Diagnosis of MS (McDonald et al., 2001, Polman et al., 2005).

Clinical presentation	Additional data needed for MS diagnosis
≥ 2 attacks; objective clinical evidence of ≥ 2 lesions or objective clinical evidence of 1 lesion with reasonable	None

historical evidence of a prior attack	
≥ 2 attacks; objective clinical evidence of 1 lesion	Dissemination in space, demonstrated by: ≥ 1 T2 lesion in at least 2 of 4 MS-typical regions of the CNS (periventricular, juxtacortical, infratentorial or spinal cord); or Await a further clinical attack implicating a different CNS site.
1 attack; objective clinical evidence of ≥ 2 lesions	Dissemination in time, demonstrated by: Simultaneous presence of asymptomatic gadolinium-enhancing and nonenhancing lesions at any time; or A new T2 and/or gadolinium-enhancing lesion(s) on follow-up MRI, irrespective of its timing with reference to a baseline scan; or Await a second clinical attack.
1 attack; objective clinical evidence of 1 lesion (clinically isolated syndrome)	Dissemination in space and time, demonstrated by: For DIS: ≥ 1 T2 lesion in at least 2 of 4 MS-typical regions of the CNS (periventricular, juxtacortical, infratentorial or spinal cord); or Await a second clinical attack implicating a different CNS site; and For DIT: Simultaneous presence of asymptomatic gadolinium-enhancing and nonenhancing lesions at any time; or A new T2 and/or gadolinium-enhancing lesion(s) on follow-up MRI, irrespective of its timing with reference to a baseline scan; or Await a second clinical attack.
Insidious neurological progression suggestive of MS (PPMS)	1 year of disease progression (retrospectively or prospectively determined) plus 2 of 3 of the following criteria: <ol style="list-style-type: none"> 1. Evidence for DIS in the brain based on ≥ 1 T2 lesions in the MS-characteristic (periventricular, juxtacortical or infratentorial) regions 2. Evidence for DIS in the spinal cord based on ≥ 2 T2 lesions in the cord 3. Positive CSF (isoelectric focusing evidence of oligoclonal bands and/or elevated IgG index)

Table 1: The 2010 McDonald criteria for diagnosis of MS. Revisions to MS diagnosis, (Polman et al., 2011)

Using the McDonald Criteria results in the earlier diagnosis of MS, it helps in a highly specific and sensitive diagnosis, which helps in better counseling of patients and earlier treatment. MRI is the most sensitive test to detect and demonstrate MS lesions. It supports the diagnosis, estimates the lesion load and disease activity, measures brain atrophy and axonal loss (Milo & Miller, 2014).

1.1.4 Subtypes of MS

The vast variability of the clinical course of MS raised the need for a common language to describe the clinical courses and pathology of multiple sclerosis. The National MS Society in 1996 addressed in defining four distinct clinical subtypes of MS (Hauser SL, 2008).

- **Relapsing–remitting MS (RRMS)**

RRMS is the most common form of MS and accounts for affecting about 85% of MS patients. It is marked by worsening of symptoms followed by periods of remission, when symptoms improve or disappear. In the periods between attacks the patient has no worsening of neurological function.

- **Secondary progressive MS (SPMS)**

This type may develop in some patients with relapsing–remitting disease. Progressive and gradual neurological deterioration without acute attacks are the characteristics of disease course.

- **Primary progressive MS (PPMS)**

This type affects approximately 10% of MS patients. Symptoms gradually worsen from the beginning. The disease course is characterized by the absence of relapses or remissions. This form of MS is more resistant to the drugs typically used to treat the disease.

- **Progressive-relapsing MS**

A rare form of MS which affects fewer than 5% of patients. From the start there is steady functional decline, with symptoms worsening as the disease progresses. There are no periods of remission (Goldenberg, 2012).

1.1.5 MS treatment

There are no FDA-approved, curative therapies for MS currently available, although, various immunomodulatory agents reducing disease effects are available. These disease-modifying agents help reducing the duration of acute exacerbations and decrease their frequency. The FDA has approved several medications for relapsing–remitting MS,

which have been shown to reduce the number of relapses and new lesions formation. Four beta interferons (**Avonex**, **Betaseron**, **Extavia** and **Rebif**) and one polypeptide mixture (**Glatiramer acetate**) are preferred as first-line treatments for MS. Second-line of therapies includes **Natalizumab** and **Mitoxantrone** (Novantrone).

The four beta interferon drugs—**Avonex** (Biogen Idec), **Rebif** (Merck), **Betaferon** (Bayer) and **Extavia** (Novartis)—are naturally occurring cytokines secreted by immune cells. Interferon beta-1a and beta-1b perform regulatory functions and their anti-inflammatory properties are beneficial (Brust, 2007). The incidence of relapses are reduced by beta interferons by approximately one-third (Goldenberg, 2012).

Glatiramer acetate (Copaxone, Teva) is a synthesized copolymer polypeptide mixture constituting of L-glutamic acid, L-lysine, L-alanine and L-tyrosine. This drug was originally designed to mimic myelin basic protein (Brust, 2007). Studies have shown that subcutaneous injection of glatiramer acetate (20 mg/day) reduces the rate of attacks in patients.

Fingolimod (Gilenya, Novartis) is the first disease-modifying drug which is administered orally. It reduces attacks and delays the progression of disability in patients with relapsing forms of MS (Brust, 2007). Fingolimod is a sphingosine-1-phosphate (S1P) receptor modulator. Fingolimod isolates naïve T cells, Th17 cells and central memory T cells, within the lymphoid tissues. These lymphocyte subsets are important for inducing the neurological damage in MS; their isolation in lymphoid tissues is thus expected to have beneficial effects in MS patients.

Dimethyl fumarate (DMF) is a newly approved oral DMT which is taken twice-daily for relapsing MS. It is hydrolyzed to monomethyl fumarate on ingestion, which is eliminated through respiration and has little hepatic or renal excretion. Its mechanism of action has not been completely elucidated. Although it is known to activate the transcriptional pathway of nuclear-related factor 2, which reduces oxidative cell stress, as well as modulates nuclear factor kB, which could have anti-inflammatory effects (Linker et al., 2011, Albrecht et al., 2012).

Teriflunomide is an active metabolite of the parent drug, leflunomide. Leflunomide is used in the treatment of rheumatoid arthritis (RA) since 1998 (Osiri et al., 2003). The precise mechanisms by which teriflunomide exerts its beneficial effects in MS are not

completely understood. Teriflunomide inhibits dihydroorotate-dehydrogenase (DHODH), a key mitochondrial enzyme required for rapid proliferation of cells such as T lymphocytes and B lymphocytes. It, therefore, diminishes the inflammatory response to auto-antigens.

Alemtuzumab is a humanized monoclonal antibody directed against CD52, a 12-amino acid cell surface protein of unknown function (Hale, 2001, Xia et al., 1993, Xia et al., 1991) that is expressed at high levels on T cells and B cells and at lower levels on monocytes, macrophages and eosinophils with small effects on natural killer cells, neutrophils and hematological stem cells. Cells of the innate immune system are unaffected. One course of intravenous treatment depletes T, B and natural killer cell types, especially CD4+ T cells. Although B cells repopulate within 5 to 6 months, T cells deplete for more than 1 year. Treatment is repeated at 1 year and may be extended annually thereafter.

Daclizumab is a humanized mAb of the human IgG1 isotype that binds specifically on the α -subunit (CD25) of the interleukin-2 receptor (IL-2R). Due to its mitogenic effect on T cells it was the first interleukin molecule to be identified and characterized as ‘T-cell growth factor’ (Smith et al., 1980). IL-2 is produced mainly by activated T cells, activated dendritic cells and monocytes/macrophages also produce it but to a lesser degree. Daclizumab, was initially designed to block virally transformed T-cell proliferation in human T lymphotropic virus I (HTLV-I) induced adult T-cell leukemia (Waldmann et al., 1985, Lehky et al., 1998). It was shown that daclizumab showed positive results when combined with interferon beta-1a (Wynn et al., 2010).

Natalizumab (Tysabri, Biogen Idec/Elan) is a recombinant humanized immunoglobulin (IgG₄) monoclonal antibody. It is administered intravenously once a month, it then works on reducing the attack rate (Riley CS., 2010). Natalizumab is a α 4-integrin antagonist, it interferes with the migration of immune cells into the central nervous system. It binds to the α 4 subunit of the α 4 β 1-integrin and prevents leukocyte adhesion to endothelial vascular cell adhesion molecule-1 (VCAM-1). It thus stops the penetration of leukocytes into the blood brain barrier.

Patients with relapsing–remitting MS, experience attacks with exacerbated neurological functioning, which is later followed with periods of partial or complete recovery

(remission). To relieve symptoms a combination of drugs, along with physical therapies, speech therapies; exercise; rest; and healthful nutrition are required (Goldenberg., 2012).

1.2 Animal models of multiple sclerosis

1.2.1 Overview

About 85% of patients with MS initially have relapses. This disease phase is termed as relapsing-remitting MS. In about half of the patients, this is followed by secondary progressive MS, during which the neurological functions keep on worsening but the attacks have a fewer frequency (Gold et al., 2006). The single animal model of MS, experimental autoimmune encephalomyelitis (EAE) suggests that the disease is an autoimmune T-cell mediated disease. The origins of EAE date back to the 1920s, when Koritschoner and Schweinburg induced spinal cord inflammation in rabbits by inoculation with human spinal cord (Koritschoner RS., 1925). EAE since then was stimulated in many different species, this included rodents and primates. These studies made it evident that EAE could replicate and reproduce most of the clinical, neuropathological and immunological aspects of multiple sclerosis (Hohlfeld & Wekerle, 2001). Most of our current knowledge regarding principal mechanisms of brain inflammation has been gathered from studies on EAE and without this knowledge the understanding of the pathogenesis of multiple sclerosis and development of new therapies would not have been feasible.

1.2.2 Experimental autoimmune encephalomyelitis (EAE)

Experimental autoimmune encephalomyelitis (EAE) is a T cell-mediated autoimmune disease symbolized by CD4+ T cell and mononuclear cell inflammation. This subsequently leads to primary demyelination of axonal tracks in the central nervous system, which further results in progressive hind-limb paralysis. EAE has been shown to be a useful model for the study of the pathogenesis and immune regulation of CD4+ Th1/Th17-mediated tissue damage (Miller et al., 2007). The pathophysiology of EAE is based on the reaction of the immune system against brain-specific antigens. This reaction results in neurological and pathological features comparable to those observed in MS patients. These reactions involve inducing inflammation and destruction of the antigen carrying structures. Three different approaches for EAE can be distinguished as: Actively-induced EAE (aEAE; active immunization), passively transferred EAE (pEAE; transfer of encephalitogenic cells from an immunized animal) and more

recently spontaneous EAE mouse models (sEAE) which allow the study of autoimmune mechanisms without exogenous manipulation. aEAE however remains the easiest inducible model which yields fast and robust results in mice. This model is considered as the "gold standard" of neuroimmunological animal models by many researchers in the field (Stromnes & Goverman., 2006).

For aEAE induction, the animal is immunized with a subcutaneous injection of an emulsion which consists of the chosen antigen and complete Freund's adjuvant (CFA) accompanied by an intraperitoneal injection of pertussis toxin on the day of immunization and two days later (booster dose). This consequently leads to the activation of myelin-specific T lymphocytes in the periphery and these migrate into the CNS across the blood-brain-barrier. Once they enter the CNS, these T-cells are reactivated by local and infiltrating antigen-presenting cells. This results in subsequent inflammatory cascades, involvement of other cells like monocytes or macrophages and eventually in demyelination and axonal cell death (Fletcher et al., 2010). Depending upon the immunization protocol, combination of mouse strain (*e.g.* C57BL/6, SJL/J, Biozzi) and the chosen antigen (*e.g.* myelin oligodendrocyte glycoprotein (MOG), myelin basic protein (MBP), myelin proteolipid protein (PLP)), the disease course can take an acute, chronic progressive or relapsing remitting disease course.

Model	Similarities to human disease	Differences from human disease	Further comments
Lewis rat Active EAE (CNS myelin, MBP, MOG, PLP)	T-cell inflammation and weak antibody response	Monophasic, little demyelination	Reliable model, commonly used for therapy studies. With guinea-pig MBP little demyelination
Adoptive-transfer EAE (MBP, S-100, MOG, GFAP)	Marked T-cell inflammation. Topography of lesions	Monophasic, little demyelination	Homogeneous course, rapid onset. Differential recruitment of T cells/macrophages depending on autoantigen
Active EAE or AT-EAE + co-transfer of anti-MOG antibodies	T-cell inflammation and demyelination	Only transient demyelination	Basic evidence for role of antibodies in demyelination
Congenit Lewis, DA, BN strains Active EAE (recombinant MOG aa 1–125)	Relapsing–remitting disorders, may completely mimic histopathology of multiple sclerosis and subtypes	No spontaneous disease	Chronic disease course, affection of the optic nerve, also axonal damage similar to multiple sclerosis
Murine EAE (SJL, C57BL/6, PL/J, Biozzi ABH) Active EAE (MBP, MOG, PLP and peptides)	Relapsing–remitting (SJL, Biozzi) and chronic–progressive (C57BL/6) disease courses with	No spontaneous disease	Pertussis (toxin) required for many strains, whilst it is often not needed for SJL and some Biozzi EAE models. Higher variability

	demyelination and axonal damage		of disease incidence and course, often cytotoxic demyelination in C57BL/6. With rat MBP inflammatory vasculitis with little demyelination
Murine EAE in transgenic mice or knockout mice (mostly C57BL/6 background)	Specifically addresses role of defined immune molecules/neurotrophic cytokines/ neuroanatomical tracts	Most results obtained with artificial permanent transgenic or knockouts	Extensive backcrossing (>10 times) on C57BL/6 background required. Future work with conditional (cre/loxP) or inducible (e.g. Tet-on) mutants

Table 2: Commonly used rodent EAE models (Gold et al., 2006)

1.3 P38 and MK2 pathway

Cellular behaviour responds to extracellular stimuli by mediating through intracellular signaling pathways such as the mitogen-activated protein (MAP) kinase pathways (Rouse et al., 1994). MAP kinases are members of discrete signaling cascades and serve as centerpieces in response to a variety of extracellular stimuli. The MAP kinase family has four distinct subgroups that have been described: (1) extracellular signal-regulated kinases (ERKs), (2) c-Jun N-terminal or stress-activated protein kinases (JNK/SAPK), (3) ERK/big MAP kinase 1 (BMK1) and (4) the p38 group of protein kinases.

The p38 MAP kinase pathway is known to be rapidly tyrosine phosphorylated by heat shock, ultraviolet (UV) light, bacterial lipopolysaccharide (LPS) or the proinflammatory cytokines like IL-1 or TNF- α (Rouse et al., 1994, Freshney et al., 1994, Han et al., 1994). Activation of the p38 pathway results in phosphorylation of transcription and initiation factors (Raingeaud et al., 1996, X Wang, 1998). The pathway also is responsible for affecting cell division, apoptosis, invasiveness of cultured cells and the inflammatory response (Xia et al., 1995, Takenaka et al., 1998, Lee, 1994, Simon et al., 1998). The functional role of the mammalian p38 MAP kinase cascade has been studied using mutants of the upstream regulators of the cascade, such as MAP kinase kinase 3/6 (MKK3/6) (Takenaka et al., 1998; Z. Xia et al., 1995) or by using SB203580, a specific inhibitor of the α , β -isoforms of p38 MAP kinase (Lee, 1994; Lee et al., 1993; Simon et al., 1998; Takenaka et al., 1998).

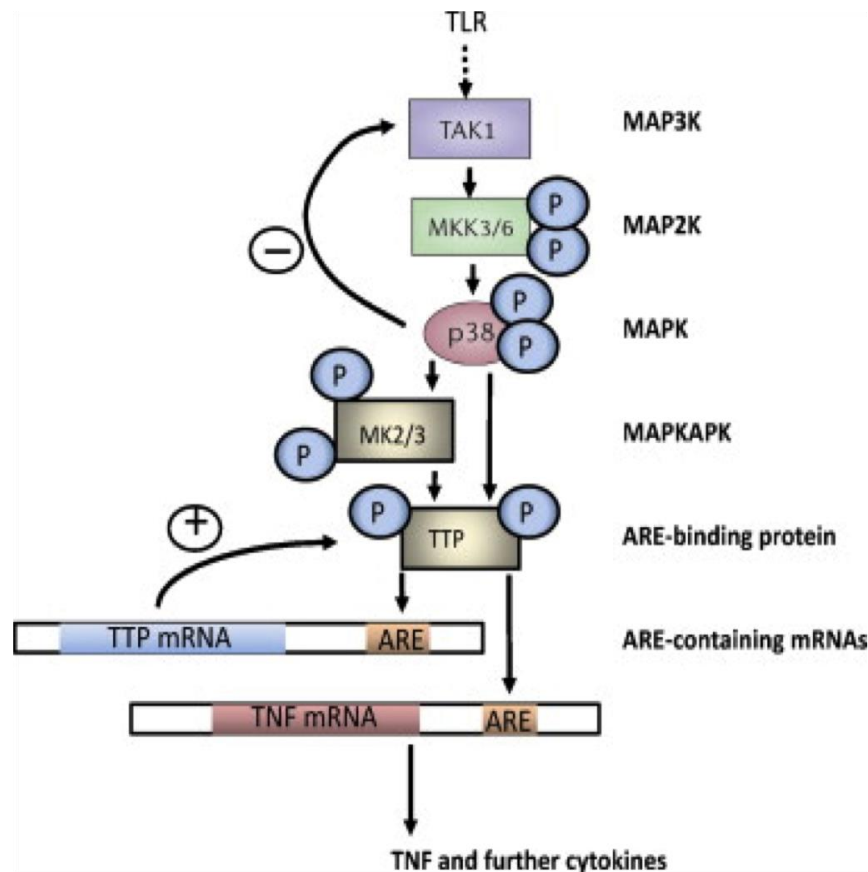


Figure 4: MK2 signaling pathway (Ronkina et al., 2010)

MAP kinase-activated protein kinase 2 (MAPKAPK2 or MK2) was the first identified p38 α substrate (Freshney et al., 1994; Rouse et al., 1994). This substrate, along with MK3 its closely related family member, both activate various substrates including small heat shock protein 27 (HSP27) (Stokoe et al., 1992), lymphocyte-specific protein 1 (LSP1) (Huang et al., 1997), cAMP response element-binding protein (CREB) (Tan et al., 1996), transcription factor ATF1, SRF and tyrosine hydroxylase (Heidenreich et al., 1999; Thomas et al., 1997). More recently, MK2 has been found to phosphorylate tristetraprolin (TTP), a protein that is known to destabilize mRNA (Mahtani et al., 2001).

1.3.1 MK2 and Inflammation

The central role of the p38 MAPK pathway responsible for activation of various downstream kinases and transcription factors limits the use of the p38 inhibitor as an anti-inflammatory therapy. Moreover, most of the p38 inhibitors have failed in clinical settings due to unacceptable safety profiles. Therefore, targeting downstream substrates

of p38 MAPK could be a better approach for treating various inflammatory diseases. MK2 is one of the several downstream substrates of p38 which has been shown to regulate post-transcriptional regulation of TNF- α and IFN- γ (Clark, Dean, & Saklatvala, 2003). MK2 acts on limited downstream substrates and therefore is a more specific target. Moreover, the potential side effects associated with p38 MAPK could be minimized by selectively targeting MK2.

Targeted disruption of MK2 reduces TNF- α production and lipopolysaccharide (LPS)-induced liver damage. In similarity to p38, MK2 also phosphorylates proteins that are found both in the nucleus (cAMP-response element binding protein (CREB)) and cytoplasm (HSP25/27 and LSP-1). The production of TNF- α and activation of inflammatory mediators that initiate leukocyte recruitment and activation are the main biological roles of MK2. The activation of the downstream target MK2 mainly mediates the inhibitory effect of p38 MAPK on TNF- α synthesis. The catalytically active MK2 could rescue the impaired inflammatory response in MK2-deficient animals that could not be achieved by the catalytically inactive enzyme (Kotlyarov et al., 2002), suggesting its important role in release of various cytokines and chemokines. In MK2-deficient mice, a significant reduction in NO production in response to LPS stimulation has been shown which provided evidence of the involvement of MK2 in NO release. NO on stimulation with LPS macrophages express iNOS and also participates in the inflammatory responses of macrophages (Lehner et al., 2002).

1.3.2 MK2 glial cells and myelination

Oligodendrocyte (OLG) differentiation and myelination is affected by p38 mitogen-activated protein kinase (MAPK) (Fragoso et al., 2007; Haines et al., 2008). When oligodendrocyte progenitors are treated with p38 inhibitors, their differentiation and myelination of dorsal root ganglion neurons is reduced. When p38 was silenced using siRNA, it decreases staining levels of myelin-associated glycoprotein (MAG) and galactosyl-ceramide (GaIC) in OLG membrane sheets (Fragoso et al., 2007). It is easy to conclude from these results that p38 α is essential for OLG differentiation.

There are a number of kinases through which p38 MAPK signals, including MK2 which is the most studied kinase (Gaestel, 2006; Ronkina et al., 2008). p38 MAPK phosphorylates MK2 on multiple amino acid residues, which result in its activation

(Ben-Levy et al., 1995). In early stages of OLG development, levels of phosphorylated MK2 were high but the levels decrease slightly with differentiation. MK2 is involved in OLG lineage progression since a pharmacological inhibitor (CMPD1) and siRNA to MK2 decreased myelin-lipids and proteins while increasing several factors that prevent differentiation. CMPD1 decreased several myelin-specific proteins, like MAG and MBP (Gaestel., 2006). Treatment of OPCs with MK2 inhibitor CMPD1 decreased myelin proteins in OLG membrane sheets. MK2 siRNA decreased MAG expression. The mRNA levels of myelin-specific markers were reduced after using CMPD1 while increasing the factors, which inhibit OLG differentiation. This implicates the role of MK2 in the regulation of OLG differentiation at the transcriptional level.

It was observed that pMK2 levels were increased in early-stage OLGs, which suggested a role for activated MK2 in OLG differentiation, which could affect cell cycle control, migration and cytoskeletal remodeling as reported in other systems (Ronkina et al., 2008).

The effect of the inhibitor was more pronounced when applied at the OPC stage, which helps concluding that MK2 activity is important for early stages of differentiation. The levels of transcription factor Myt1, which is involved in OLG lineage progression, had the most dramatic effects of CMPD1 inhibition (Nielsen et al., 2004). The reduction in Myt1 levels by almost 90% suggested that MK2 is involved in an early stage in progression of OPCs to a differentiated state. Furthermore, we found that MK2 signaling regulated mRNA levels of various transcriptional repressors in oligodendrocytes.

Similar to what has been observed with p38 α staining, pMK2 was found to be diffusely distributed in cytoplasm and nucleus of OPCs, but became more intensely localized to the nucleus as the cells matured (Haines et al., 2008). Activated MK2 can influence p38 compartmentalization through regulation of a MK2 nuclear export signal (Engel, Kotlyarov & Gaestel, 1998; Kotlyarov et al., 2002). Depending on their subcellular localization during differentiation, MK2 and p38 may play different roles in oligodendrocytes. Studies done by Haines et al., (2010) found that p38 α and MK2 form co-immunoprecipitable complexes in OPCs.

1.3.3 MK2 and EAE

The role of the MK2 has been investigated in various disease models before. All studies which had used MK2^{-/-} mice, the knockout proved to be more beneficial and mice showed reduced disease symptoms in e.g. spinal cord injury, Parkinson's disease and cerebral ischemia (Ghasemlou et al., 2010; Gorska et al., 2007; T. Thomas, Timmer, et al., 2008; Xinkang Wang et al., 2002). The role of p38 the upstream kinase of MK2 has been previously examined in EAE. The development and progression of both chronic and relapsing-remitting EAE has been shown to require the activation of p38 and its inhibition reduces the disease signs. To be precise, the disease severity is modulated by the p38 activity by regulating T cells activity (Noubade et al., 2011). In addition, it was found that inhibition of the p38 reduces the pathogenesis of EAE by decreasing the IL-17 production (Namiki et al., 2012).

As opposed to that, Tietz et al., (2014) found that a lack of the downstream kinase MK2 was not an advantage in MOG₃₅₋₅₅-induced EAE. In this study it was shown that elimination of MK2 in mice is beneficial in EAE, although pro-inflammatory cytokines were reduced. During the course of EAE, TNF- α was not detectable in the serum of MK2^{-/-} mice, implying that MK2^{-/-} mice may resemble the disease course of TNF- α knockout mice. The onset of MOG₃₅₋₅₅-induced EAE was not affected by MK2 knockout as in the case of TNF- α -deficiency, but led to prolonged disease activity correlating with more mononuclear cells infiltrated into the CNS (Liu et al., 1998; Probert et al., 2000).

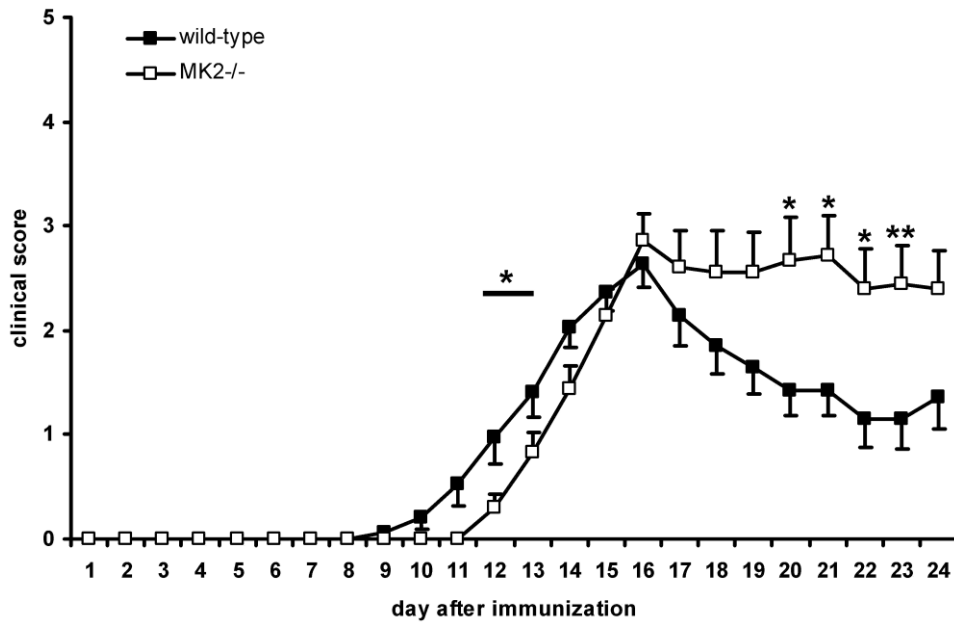


Figure 5: MK2 deficiency leads to severity and prolongation of EAE (Tietz et al., 2014)

In summary, the previous study done in our lab underlines the significance of MK2 in the regulation of CNS inflammatory disease, multiple sclerosis and its animal model, EAE. The initial hypothesis was rejected in the study as MK2 deficiency resulted in a more severe disease course and was associated with more cellular CNS inflammation.

2 Objectives

The p38/MK2 pathway is known to regulate inflammatory reactions and pathological processes. The pathway controls many downstream transcription factors that regulate many cellular functions. Therefore, we hypothesized that the deletion of MK2 in C57BL/6J mice would lead to a mild course of EAE accompanied by low inflammation and neurodegeneration.

The aim of this study was to characterize the role of MK2 in experimental autoimmune encephalomyelitis, the most common animal model of multiple sclerosis.

1. To investigate the role of MK2 in disease severity in acute and chronic experimental autoimmune encephalomyelitis.
2. To characterize the morphology, histology and distribution of immune cells in spinal cord lesions of MOG₃₅₋₅₅-EAE.
3. To study the expression and regulation patterns of the MK2 knockout downstream signalling pathway in MK2^{-/-} mice.
4. To study the pharmacological effects of GA in MK2^{-/-} C17.2 cells.

3 Materials and Methods

3.1 MATERIALS

3.1.1 Animals

3.1.1.1 Mice provider

Mice line	Supplier	Animal facility
MK2/MK3 ^{+/+}	MH Hannover	JLU, Central Animal facility, Frankfurter strasse, Giessen, Germany.
C57BL/6J		

3.1.1.2 Mice Diet

Diet Name	Provider
Trauben zucker	Müller's Mühle Gmbh, Gelsenkirchen, Germany
DietGel Boost	ClearH2O [®] Westbrook, ME
DietGel Recovery	ClearH2O [®] Westbrook, ME

3.1.2 Cell lines

Cell Line	Provider
C17.2	Neurologie Klinikum, MS Research group, Gießen
JURKAT	Neurologie Klinikum, MS Research group, Gießen

3.1.3 Primary antibodies

Name	Host	Reactivity	Mol. Weight	Method	Article Nr	Manufacturer
Anti-pStat1	Rabbit	H, M, R	84/91 kDa	WB	9171s	Cell Signaling Tech, MA, USA
Anti-Stat1	Rabbit	H, M, R, MK	84/91 kDa	WB	9172	Cell Signaling Tech, MA, USA

Anti-CNPase	Mouse	H, M, R	46/48 kDa	WB	ab6319	Abcam, UK
Anti-MBP	Mouse	H, M, R, G	33 kDa	WB	ab62631	Abcam, UK
Anti-PLP	Rabbit	H, M	26/30 kDa	WB	ab28486	Abcam, UK
Anti-pERK p-44/42	Rabbit	H M R Hm Mk	44, 42	WB	4370s	Cell Signaling Tech, MA, USA
Anti-Erk 1/2	Rabbit	H, M, R, MK	42/44 kDa	WB	9102	Cell Signaling Tech, MA, USA
Anti-Akt	Rabbit	H, M, R, MK	60 kDa	WB	9272	Cell Signaling Tech, MA, USA
Anti-pAkt (Ser473)	Rabbit	H, M, R, MK	60 kDa	WB	4060s	Cell Signaling Tech, MA, USA
Anti-GAPDH	Mouse	Ca, H, M, R	38 kDa	WB	MAB374	Chemicon/ Millipore, CA; USA
Anti-Trk B (794):sc12	Rabbit	H, M, R	145 kDa	WB	sc-12	Santa Cruz Biotech, CA, USA
Anti-BDNF	Rabbit	H, M, R	17, 13 kD	WB	sc-546	Santa Cruz Biotech, CA, USA
Mac 3 Clone M3/84	Rat	M	staining	IHC	553322	Pharmingen, USA
B220 clone RA3-6B2	Rat	H, M	staining	IHC	557390	Pharmingen, USA
CD3, clone CD3-12	Rat	M	staining	IHC	MCA 1477	Serotec, UK

MBP	Rabbit	M, R	staining	IHC	62301	Dako, Germany
MAPKAPK2	Rabbit	H, M, R, Mk	47, 49 kDa	WB	3042	Cell Signaling Tech, MA, USA
pMAPKAPK2(Thr334)	Rabbit	H, M, R, Mk	49kDa	WB	3007	Cell Signaling Tech, MA, USA
P38 MAPK	Rabbit	H, M, R, Mk	43 kDa	WB	9212	Cell Signaling Tech, MA, USA
Phospho-p38 MAPK	Rabbit	H, M, R, Mk	43 kDa	WB	9211	Cell Signaling Tech, MA, USA
NF-kB p65	Rabbit	H, M, R, Mk	65 kDa	WB	4764	Cell Signaling Tech, MA, USA
Phospho-NF-kB p65	Rabbit	H, M, R, Mk, Hm	65 kDa	WB	3033	Cell Signaling Tech, MA, USA
IkB α	Rabbit	H, M, R, Mk, Hm	39 kDa	WB	4812	Cell Signaling Tech, MA, USA
Phospho-IkB α (ser32)	Rabbit	H, M, R, Mk	40 kDa	WB	2859	Cell Signaling Tech, MA, USA

3.1.4 Secondary antibodies

Antibody	Host	Article Nr	Manufacturer
Anti-Rabbit-HRP	Goat	sc-2004	Santa Cruz Biotech, CA, USA
Anti-Mouse-HRP	Donkey	sc-2318	Santa Cruz Biotech, CA, USA

3.1.5 Kits

Kit	Manufacturer	Article Nr	Method
BCA Protein Assay Kit	Pierce® Thermo Scientific, IL, USA	23225	Protein quantification
Cell Proliferation reagent WST-1	Roche Applied Science, Mannheim, Germany	11644807001	Proliferation assay
DirectPCR Lysis Reagent (Tail)	Peqlab, Erlangen, Germany	31-121-T	DNA isolation
iTaq™ Universal SYBR® Green qPCR Master Mix	Bio-Rad, CA, USA	172-5124	PCR
QuantiTect® Reverse Transcription Kit	Qiagen GmbH, Hilden, Germany	205310	Reverse Transcription
SuperSignal® West Pico Chemiluminescent substrate	Thermo Scientific, IL, USA	34077	Western Blot
Viromer® BLUE	Lipocalyx GmbH, Halle, Germany		Transfection
Lipofectamine® RNAiMAX Transfection Reagent	Thermo Scientific, IL, USA	13778075	Transfection
HotStarTaq DNA Polymerase (250 U)	Qiagen GmbH, Hilden, Germany	203203	PCR

3.1.6 Genotyping Primers

Primers were designed using NCBI primer designing tool and all primers were purchased from Eurofins Genomics, Ebersberg, Germany.

Gene (Primer)	Primer name	Sequence
MK2	MK2 ^{-/-} Tneorc	CTGTTGTGCCAGTCATAGCCG
	MK2 ^{+/+} MK2 200rc	CCCTCTCTACCTCTTTCTGTGAATGCC

	MK2 ^{+/+} TMK2 dl	CATGCCATGATGAGGTGCCTCTGC
MK3	MK3 WT Forward	GCCAATGTCCCGCATTATCTCTGC
	MK3 WT Reverse	CAGGGAGCACTCACAGAGCAGTGGGC

3.1.7 Primers used for analysis

Primer	5' → 3' Sequence
TNF- α	Forward CGGTCCCAAAGGGATGAGAAGT
	Reverse ACGACGTGGGCTACAGGCTT
IL-1 β	Forward TACCTGTGGCCTTGGGCCTCAA
	Reverse GCTTGGGATCCACACTCTCCAGCT
IL-6	Forward CTCTGCAAGAGACTTCCA
	Reverse AGTCTCCTCTCCGGACTT
IL-12	Forward AGACCACAGATGACATGGTGA
	Reverse ACGACGTGGGCTACAGGCTT
iNOS	Forward TTGGAGGCCTTGTGTCAGCCCT
	Reverse AAGGCAGCGGGCACATGCAA
BDNF	Forward AAGGGCCAGGTCTGTTAAGC
	Reverse GGTAAGAGAGCCAGCCACTG
TrkB	Forward TGACGCAGTCGCAGATGCTG
	Reverse TTCCTGTACATGATGCTCTCTGG
GAPDH	Forward GGATGGGTCCTCATGCTCAC
	Reverse TGGTGCTGCAAGTCAGAGCAG
TGF- β	Forward CTCCTGCTGCTTTCTCCCTC
	Reverse GTGGGGTCTCCCAAGGAAAG
SEMA3A	Forward GGATGGGTCCTCATGCTCAC
	Reverse TGGTGCTGCAAGTCAGAGCAG
Lingo1	Forward TCATCAGGTGAGCGAGAGGA
	Reverse CAGTACCAGCAGGAGGATGG
PLP	Forward GAGCAAAGTCAGCCGCAAAA

	Reverse CAAGCCCATGTCTTTGGCAC
MBP	Forward TCCATCGGGCGCTTCTTTAG
	Reverse TCTCGTGTGTGAGTCCTTGC

3.1.8 Ladders

Marker	Manufacturer
PageRuler™ Plus Prestained Protein Ladder	Fermentas, Invitrogen, Carlsbad, USA
Fluorescent Low Range DNA Ladder	Jena Bioscience, Jena, Germany
Mid Range DNA Ladder	Jena Bioscience, Jena, Germany

3.1.9 Chemicals

Compound	Manufacturer
10x PBS for cell culture (DPBS)	Lonza, Köln, Germany
2-Mercaptoethanol	Sigma-Aldrich, Steinheim, Germany
2-Propanol	Sigma-Aldrich, Steinheim, Germany
3% Hydrogen peroxide	Carl Roth, Karlsruhe, Germany
Acetic acid	Merck, Darmstadt, Germany
Agarose	Bioline GmbH, Luckenwalde, Germany
Ammonium Persulphate (APS)	Carl Roth, Karlsruhe, Germany
Bovine Serum Albumin (BSA)	Merck, Darmstadt, Germany
Bromophenol Blue	Neolab, Heidelberg, Germany
Citric acid	Merck, Darmstadt, Germany
Complete Freund's adjuvant	Sigma, Steinheim, Germany
Distilled water (Ecostrain®)	Braun, Melsungen, Germany
Dimethylsulfoxide (DMSO)	Carl Roth, Karlsruhe, Germany
Disodium-hydrogen-phosphate	Merck, Darmstadt, Germany
DNase	Qiagen, Hilden, Germany
EDTA	Carl Roth, Karlsruhe, Germany
Eosin	Merck, Darmstadt, Germany
Eosin	Carl Roth, Karlsruhe, Germany

Ethanol 100%	Sigma-Aldrich, Steinheim, Germany
FBS	PAA Laboratories, Pasching, Austria
Glycerol	Carl Roth, Karlsruhe, Germany
Glycine	Merck, Darmstadt, Germany
Glycerin	Carl Roth, Karlsruhe, Germany
Hematoxylin	Carl Roth, Karlsruhe, Germany
Isopropanol	Merck, Darmstadt, Germany
Ketamine	Inersa Arzneimittel GmbH, Freiberg, Germany
Luxol-Fast-Blue	Sigma-Aldrich, Steinheim, Germany
Magnesiumsulfate (MgSO ₄)	Sigma Aldrich, Tachfkirchen, Germany
Methanol	Merck, Darmstadt, Germany
MOG ₃₅₋₅₅	Charité Berlin, Berlin, Germany
<i>Mycobacterium tuberculosis</i>	Difco Microbiology, Michigan, USA
NP40	US Biologicals, MA, Germany
Paraformaldehyde (PFA)	Sigma Aldrich, Taufkirchen, Germany
Pertussis Toxin	Calbiochem, Darmstadt, Germany
Poly-L-Lysine	Sigma-Aldrich, Steinheim, Germany
Potassium chloride (KCL)	Merck, Darmstadt, Germany
Potassiumdihydrogenphosphate	Merck, Darmstadt, Germany
Protease Inhibitor cocktail	Roche, Manheim, Germany
Proteinase K	Sigma-Aldrich, Missouri, USA
RNase free water	Millipore corporation, MA, USA
Rotiphorese Gel (30% acrylamide mix)	Carl Roth, Karlsruhe, Germany
Sodium chloride (NaCl)	Carl Roth, Karlsruhe, Germany
Sodium-dihydrogen-phosphate	Merck, Darmstadt, Germany
Sodium hydrogen carbonate (NaHCO ₃)	Merck, Darmstadt, Germany
Sodiumdodecylsulfate (SDS)	Neolab, Heidelberg, Germany
Sodiumazid (NaN ₃)	Merck, Darmstadt, Germany
Sunflower oil	Sigma-Aldrich, Steinheim, Germany
Tamoxifen	Sigma-Aldrich, Steinheim, Germany

TEMED	Carl Roth, Karlsruhe, Germany
Tris HCl	Carl Roth, Karlsruhe, Germany
Tris. acetat-EDTA buffer (TAE) 10x	Carl Roth, Karlsruhe, Germany
Trishdroxymethyl aminomethan (Tris)	Carl Roth, Karlsruhe, Germany
Tryphanblue	Carl Roth, Karlsruhe, Germany
Trypsin (2.5g/l)	Gibco, Invitrogen, Carlsbad, USA
Tween 20	Merck, Darmstadt, Germany
Xylazin 2%	CEVA Tiergesundheit GmbH, Düsseldorf, Germany

3.1.10 Laboratory consumables

Consumables	Manufacturer
Cellstar® 6 Well and 24 well Cell Culture Plate	GreinerBioOne, Frickenhausen, Germany
Cellstar® Plastikpipettes (5 ml, 10 ml)	GreinerBioOne, Frickenhausen, Germany
Cellstar® U-shape with Lid, TC-Plate, 96 well, sterile	GreinerBioOne, Frickenhausen, Germany
Cellstar® Flat bottom with Lid, TC-Plate, 96 well, sterile	GreinerBioOne, Frickenhausen, Germany
Cellstar® 75 cm ² Cell cultur flasks	GreinerBioOne, Frickenhausen, Germany
Cellstar® 125 cm ² Cell cultur flasks	GreinerBioOne, Frickenhausen, Germany
Cell scrapper	GreinerBioOne, Frickenhausen, Germany
Cryobox 136x136x130 mm	Ratiolab GmbH, Dreieich, Germany
Cryo Tube™ vials (1,8 mL; 4,5 mL)	Sarstedt AG & Co, Nümbrecht, Germany
Falcon tubes (15ml, 50ml)	Becton Dickinson, Heidelberg, Germany
Glass Pasteur pipettes 150 mm	Brand, Wertheim, Germany
Ministart single use filter (0,2 µm, 0,45 µm)	Sartorius Stedim Biotech GmbH, Göttingen, Germany
Nitra-Tex® powder free gloves	B. Braun Melsungen AG, Germany
Parafilm	Pechiney Plastic packaging, Menasha, WI

Pipette tips without filter (10 µL, 100 µL, 1000 µL)	Sarstedt AG & Co, Nümbrecht, Germany
Eppendorf tubes 1,5 mL, 2mL	Eppendorf Vertrieb Deutschland GmbH, Wesseling-Berzdorf, Germany
Eppendorf tubes 1,5 mL, 2mL (PCR clean-pyrogen & DNase free)	Nerbe Plus GmbH, Winsen (Luhe), Germany
Sterile PCR- clean pyrogen & DNase free with filter (10, 100, 200, 1000µl)	Nerbe Plus GmbH, Winsen (Luhe), Germany
Tissue culture dishes steril 35,0 /10mm	GreinerBioOne, Frickenhausen, Germany
UV-Spectroscopic cuvettes (RNA quantification)	BioRad, München, Germany
Falcon® Plastic pipettes 10ml, 5ml	Becton Dickinson, Heidelberg, Germany
Glasswares (different sorts)	Fisherbrand; IDL; Schott&Gen; Simax
Syringe 25ml for BSA	B. Braun Melsungen AG, Germany
Nitrocellulose membrane	GE Healthcare, Amersham™ Hybond ECL, Buckinghamshire, UK
PCR Tube, cap-strips	Applied Biosystems, Darmstadt, Germany

3.1.11 Laboratory instruments

Instrument	Manufacturer
Arpege 75, Liquid nitrogen tank	Air Liquide Medical GmbH, Düsseldorf, Germany
Axioplan 2 Fluorescence Microscope	Carl Zeiss, Jena, Germany
BEP 2000 Advance (ELISA-Reader)	Dade Behring Marburg GmbH, Marburg, Germany
Centrifuge type 2-6 Easia shaker Medgenix diagnostics	Sigma-Aldrich Chemie GmbH, Taufkirchen, Germany
Centrifuge Universal 32 R	Hettich GmbH, Kirchleggen, Germany
ELISA-Reader Multiscan EX	Thermo electron corporation, Langenselbold, Germany

Western blotting system	BioRad, München, Germany
Fusion FX7 chemiluminescence system	Peqlab Biotechnologie GmbH, Erlangen, Germany
Hettich centrifuge (cooling)	Hettich GmbH, Kirchlingen, Germany
Light Microscope for cell culture	Carl Zeiss Microscopy GmbH, Oberkochen Germany
Magnetic stirrer	IKA® Werke GmbH, Staufen, Germany
Nalgene™ Cryo 1°C Freezing container	Nalgene®, Germany
Nanophotometer	Implen GmbH, München, Germany
Neubauer improved cell chamber	Brand, Wertheim, Germany
Neubauer improved Haemocytometer	Brand, Wertheim, Germany
Nuaire™ Biological Safety Cabinets Class II type A/B3 (Sterilbank)	INTEGRA Biosciences GmbH, Fernwald, Germany
pH-Meter	Mettler Toledo GmbH, Giessen, Germany
Pipette boy	INTEGRA Biosciences GmbH, Fernwald, Germany
Power pack	Peqlab Biotechnologie GmbH, Erlangen, Germany
Refrigerators and freezers	Different companies
Rotamax 120 (Shaker)	Heidolph Instruments GmbH & Co. KG, Schwabach, Germany
Sanyo Incu-safe incubator for cell culture	Ewald Innovationstechnik GmbH, Bad Nenndorf, Germany
SmartSpec™ Plus Spectrophotometer	BioRad, München, Germany
StepOne® Real-Time PCR system	Applied Biosystems, Darmstadt, Germany
Surgical instruments	Various companies
Table top centrifuge EBA 20	Hettich GmbH, Kirchlingen, Germany
Table top centrifuge micro 120	Hettich GmbH, Kirchlingen, Germany
TissueRuptor	Qiagen Instruments, Hombrechtikon, Switzerland
Trans-Blot® SD Semi-dry transfer cell	BIO RAD, München, Germany
Trans-Blot® SD Semi-dry transfer cell	BioRad, München, Germany

Vortexer vortex-Genie2	Heidolph Instruments GmbH & Co. KG, Schwabach, Germany
Water bath	Memmert GmbH + Co.KG, Germany
Weighing balance	Sartorius Stedim Biotech GmbH, Göttingen, Germany

3.1.12 Buffers

Buffer	Components	Volume
1X SDS-PAGE Running Buffer	Rotiphorese [®] 10X Running Buffer H ₂ O	100 ml 900 ml
10x PBS (1 Liter) pH 7.4	137 mM NaCl 2 mM KH ₂ PO ₄ 2.7 mM KCl 10 mM Na ₂ HPO ₄ H ₂ O	80 g 2.4 g 2 g 14.4 g 1000 ml
10x TBS (1 Liter) pH 7.2 to 7.6	Tris NaCl H ₂ O	24.2 g 87.7 g 1000 ml
1x TBS-Tween (TBST) (1 Liter)	1x TBS 0.1% Tween [®] 20	1000 ml 1 ml
Lysis Buffer (250ml) pH 7.4	NaCl Tris EDTA Glycerol NP40 NaN ₃	2.19 g 0.61 g 0.07 g 25 ml 2.5 ml 0.025 g
6x SDS-PAGE Loading Buffer	60 mM Tris-HCl (pH 6.8) 2% SDS 0.01% Bromophenol blue 10% Glycerol ddH ₂ O	36 ml 60 ml 60 mg 60 ml 144 ml

	β -Mercaptoethanol	65 μ l/ml
SDS-PAGE Transfer buffer (1 Liter)	10x Running buffer Methanol ddH ₂ O	100 ml 200 ml 700 ml
Blocking buffer (5% BSA) Bovine Serum Albumin	BSA fraction V TBST	5 g 100 ml
10x Trypsin EDTA	10x Trypsin ddH ₂ O	5 ml 45 ml
10% Ammonium Persulfate (APS)	APS ddH ₂ O	1 g 10 ml
10% Sodiumdodecylsulfate (SDS)	SDS ddH ₂ O	1 g 10 ml

3.1.13 Softwares

Fusion Bio1D software (Peqlab, Erlangen, Germany)

Microsoft Office Professional Plus 2010 (Microsoft corporation, USA)

Image J software (Image J 1.47d, National Institute of Health, USA)

StepOne RealTime PCR Software v2.1 (Applied Biosystems, Darmstadt, Germany)

GraphPad Prism Software Version 7.01 (GraphPad Software, Inc. CA, USA).

3.2 Methods

3.2.1 Mice

C57BL/6J OlaHsd, MAPKAPK2^{+/-} and MAPKAPK3^{+/-} (MK2/MK3^{+/-}) mice were supplied from the MH Hannover (AG Prof. Dr. Gästel). These mice were crossed to yield the mice MAPKAPK2^{-/-} (known as MK2^{-/-}). Mice were bred and grown in JLU-central animal facility, Frankfurter Strasse 110, Giessen, Germany. All animal experiments were carried out in JLU central animal facility and analyzed in the

Neurochemisches Labor, Department of Neurology, Giessen, Germany. Animal studies were performed according to the guidelines of FELASA and local authority of animal ethical committee. Animal experiments were approved by the local state authorities of Hessen, Giessen, Germany (GI 20/23-Nr. 31/2008) and Institutional Animal Care and Use Committee at Justus Liebig University. All efforts were made to minimize pain and suffering.

3.2.1.1 Preparation of mice genomic DNA

The genotype was controlled by PCR (DirectPCR-Tail, Peqlab, Erlangen, Germany) using MK2 Wild type, MK2 Knockout and MK3 Wild type locus. Presence of MK2 gene was confirmed using PCR with SYBR green and then running the agarose gel to identify the bands. The second PCR was done to control MK3 WT gene using HotStar Taq polymerase QIAGEN and running another agarose gel with DNA binding dye to identify the bands. 1mm portion of the tail from each mice were lysed to obtain DNA lysates in 200µl of Direct PCR tail reagent with 0.3mg/ml proteinase K for overnight at 55 °C to digest the tissues and then for 45 minutes at 85 °C to deactivate Proteinase K. The tail lysates were centrifuged for 20 seconds to settle down the debris. 1 µl of this tail lysate which contain the genomic DNA was used for genotyping PCR.

3.2.1.2 Genotyping and identification of locus

Genomic DNA from all mice (1 µl) was used in SYBR Green PCR and HotStar Taq Polymerase QIAGEN; the primers for MK2 and MK3 locus were used.

MK2 master mix per probe	10 µl SYBR Green master mix
	6 µl H ₂ O
	1 µl TMK2 dl
	1 µl Tneorc
	1 µl MK2 200rc
	1 µl genomic DNA

3.2.1.3 *Band detection in the agarose gel for MK2 PCR*

For the MK2 PCR both WT and Knockout bands were detected in the same gel as opposed to the MK3 gel which is explained later. 3 different primers were used; TMK2 dl and MK2 200rc detected the WT bands (200bp), TMK2 dl and Tneorc detected the KO bands (560bp). Amplified PCR product was run in 1.5% agarose gel electrophoresis at 120v for 45 min (BioRad electrophoresis) and bands were identified using Fusion Fx7 chemiluminescence system (PEQLAB, Erlangen, Germany).

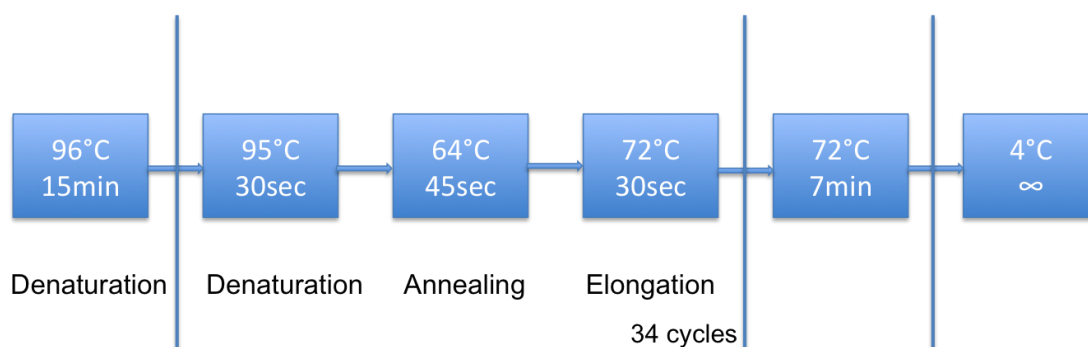
MK3 master mix probe:	10 µl SYBR Green master mix
	6 µl H ₂ O
	1 µl MK3 WT Fw
	1 µl MK3 WT Rev
	1 µl genomic DNA
MK3 KO master mix per probe	2.5 µl PCR Buffer 10X (pH=8.7)
	1 µl Q-solution 5X
	0.2µl Hot Star-Taq-Polymerase5 U/µL
	14.8 µl H ₂ O
	1 µl MK3 WT Fw
	1 µl MK2 Tneorc
	0.5 µl dNTP 10.0 mM
	0.5 µl MgCl 25 mM
	1 µl genomic DNA

3.2.1.4 Band detection in the agarose gel for MK3 PCR

There are two separate PCR reactions for detection of MK3 wild type and knockout alleles. In one of the PCR reactions two primers were used (MK3 WT FwP, MK3 WT RevP) which detected the WT bands (879). Amplified PCR product was run in 1.5% agarose gel electrophoresis at 120v for 45 min (BioRad electrophoresis) and bands were identified using Fusion Fx7 chemiluminescence system (PEQLAB, Erlangen, Germany). For the detection of the MK3 knockout bands (1239bp) the PCR reaction was done using the QIAGEN HotStar TAQ DNA polymerase (reaction mixture specified above). So, for the detection of bands in the gel we use a DNA dye (GelGreen™ Nucleic Acid Gel Stain, Biotium, Hayward, CA) 8µl for 100ml of agarose gel. Amplified PCR product was run in 1.5% agarose gel with 8µl of DNA dye; electrophoresis at 120v for 50 min (BioRad electrophoresis) and bands were identified using Fusion Fx7 chemiluminescence system (PEQLAB, Erlangen, Germany).

3.2.1.5 PCR thermal profile for genotyping

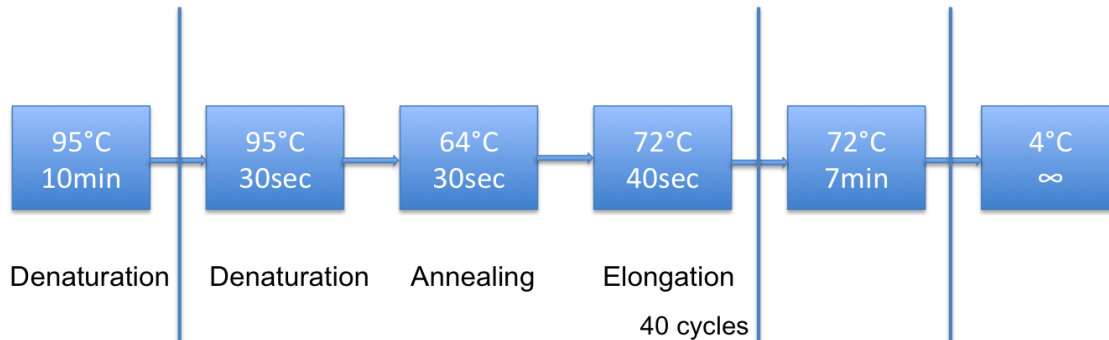
MK2 Locus:



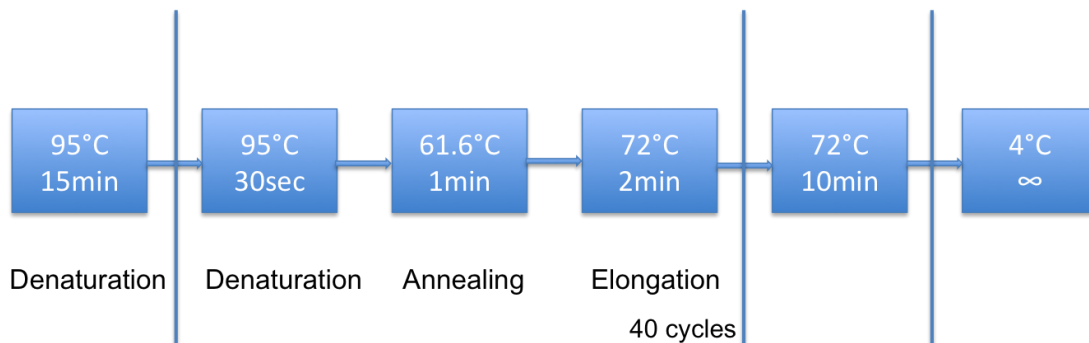
MK3 Locus:

There are separate PCR reactions for detection for MK3 wild type and knock out alleles.

MK3 WT PCR



MK3 KO PCR



3.2.1.6 Anesthesia in mice

All animals were anesthetized with isoflurane prior to treatment. For this purpose, a paper towel was impregnated with 5% isoflurane and placed in a glass container with a perforated metal bottom. While injecting the mice with MOG-emulsion for EAE induction, 1.5-2% of isoflurane was given with the help of an anesthesia machine.

3.2.1.7 Induction of MOG₃₅₋₅₅-induced EAE and clinical scoring

Mice were anesthetized using isoflurane as explained above and then EAE was induced. EAE induction was done in 10-12 weeks old female C57BL/6J01aHsd and B6 Mapkapk2^{tm1Mg1}. On day 0 both WT and MK2^{-/-} mice were injected intraperitoneally with 300ng of pertussis toxin in 100 µl PBS (Cannula size: 0.4 x 12 mm; Gr. 27). Subcutaneous injection of 300 µg myelin oligodendrocyte glycoprotein peptide (MOG₃₅₋₅₅; MEVGWYRSPFSRVVHLYRNGK; Charité Hospital, Berlin, Germany)

emulsified in complete Freund's adjuvant (Sigma, Steinheim, Germany) containing 10 mg/ml *Mycobacterium tuberculosis* (Difco, Michigan, USA) were injected in 2 upper flanks and 2 lower flanks (Cannula size: 0.55 x 25 mm; Gr 17). 48 hrs later (day 2) a booster dose of pertussis toxin was given intraperitoneally as described above.

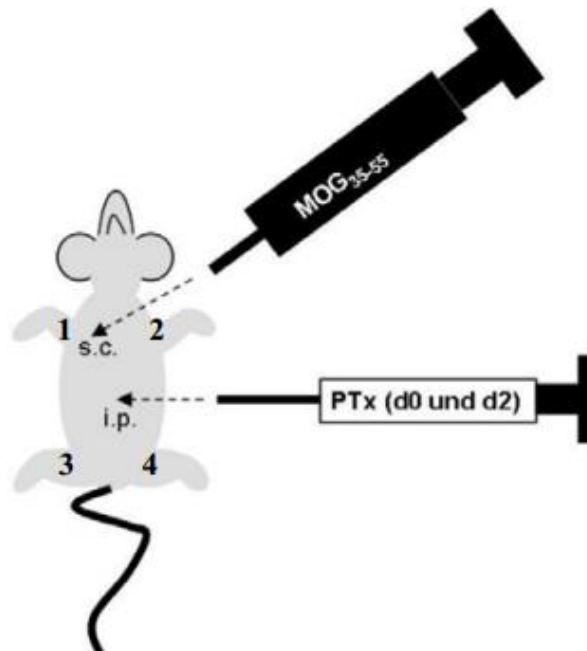


Figure 6: Induction of MOG₃₅₋₅₅-induced EAE

3.2.1.8 Determining the extent of EAE:

The immunized animals are observed for clinical signs daily until the end of the experiment. Mice were euthanized on day 16 p.i. (acute phase) and day 60 p.i. (chronic phase) for analysis. The extent of the neurological symptoms is quantified according to the following scale:

0	no discernible signs
0.5	partial tail paralysis
1	complete tail paralysis
1.5	slight hind limb paralysis
2	moderate hind leg paralysis

2.5	severe hind limb paralysis
3	Complete hind limb paralysis
3.5	Complete hind limb paralysis and paralysis of the front legs

3.2.1.9 Score sheet:

The following score sheet was maintained in the animal facility according to the local authority recommendation to minimize the pain and suffering in mice. All the factors were checked, which control the wellbeing of animals. These include body weight, bladder functions, observing the grooming of mice etc. There were decided scores given for everything. Mice were euthanized and removed from the experiment when they reaches the score of 45 with clinical score alone or with these factors combined.

1. Körpergewicht	Score
Bezogen auf Ausgangsgewicht [x] Bezogen auf Gewicht der Kontrollgruppe []	
Unbeeinflusst oder Anstieg	0
Reduktion > 20%	10
Reduktion > 25%	20
2. Allgemeinzustand	
Fell glatt, glänzend und anliegend, Augen glänzend, Körperöffnungen sauber	0
Fell matt, Augen trüb	5
Fell stumpf, Augen eingesunken trüb, verklebte oder feuchte Körperöffnungen	10
Fell gesträubt, Tier fühlt sich kalt an, Augen geschlossen, Krämpfe, Atemgeräusche, bläuliche Schleimhäute	20
3. Spontanverhalten	
aufmerksam, neugierig, Aufrichten, flinke Bewegungen	0
ungewöhnliches Verhalten, eingeschränkte oder reduzierte Bewegung oder Überaktivität, reduziertes Explorationsverhalten	5
Isolation, Apathie, ausgeprägte Sterotypie oder Hyperkinetik	10
Automutilation, Rektumvorfall	20
4. Versuchsspezifische Kriterien	
EAE Score 1 (Schwanzlähmung)	0

EAE Score 2 (Hinterlaufparese)	5
EAE Score 3 (Hinterlaufplegie)	10
EAE Score 3,5 (Hinterlaufplegie und Vorderlaufschwäche) ohne relevante Einschränkung der Mobilität	15
EAE Score 3,5 (Hinterlaufplegie und Vorderlaufschwäche) mit relevanter Einschränkung der Mobilität	20
Nekrose/Ulzeration an einer der 4 Injektionsstellen (CFA-Application)	5
Nekrose/Ulzeration an 2-3 Injektionsstellen (CFA-Application)	10
Nekrose/Ulzeration an 4 Injektionsstellen (CFA-Application)	20
Bewertung und Maßnahme	
Keine Belastung	
Geringgradige Belastung: 1 xtgl beobachten, bei Nekrose/Ulzeration an der Injektionsstelle (CFA-Applikation), mit Bepanthenalbe und ggf. antibiotische Salben behandeln. Wenn nach 3 Tagen kein Einsetzen der Wundheilung oder Verstärkung der Entzündungsreaktion, dann Abbruch.	Bis 9
Mittelgradige Belastung: 2 xtgl beobachten, Wasserflaschen mit langen Trinkhälsen (7 cm), Futterstelle auf dem Käfigboden und Ernährung mit DietGel Recovery, 15% Glucose neben normalem Trinkwasser anbieten, „Paper shavings“ (Cellulose) zur verbesserten Flüssigkeitsresorption und Verhinderung des sich Wundreibens, Versuchsleiter und Tierarzt informieren, Heating plate längerandauernd als 1 Woche gilt als hochgradige Belastung Bei Nekrosen: Wenn nach 3 Tagen kein Einsetzen der Wundheilung oder Verstärkung der Entzündungsreaktion, dann Abbruch.	10 - 19
Hochgradige Belastung: 2 x tgl beobachten, Versuchsleiter und Tierschutzbeauftragte informieren, Entscheidung: Tiere werden aus dem Versuch genommen und getötet.	20 und höher
Abbruchkriterien:	45 und höher
Gesamtscore:	höher
Einzel-score:	20

3.2.1.10 Euthanasia in mice

For euthanasia by CO₂, the animals were placed in a plastic container. 6 Litres of CO₂ per minute was introduced in this container for a successful euthanasia.

3.2.2 Molecular biology

3.2.2.1 Protein extraction and quantification

Mice were euthanized by CO₂ and different CNS tissues (spinal cord, brain stem, cortex, cerebellum, hippocampus, rest of the brain) were separated. Tissues were homogenized in lysis buffer (150 mM NaCl, 10% glycerol, 20 mM Tris HCl, 1% NP40, 1 mM EDTA, 0.01% sodium azide) with a tissue ruptor (Qiagen Instruments, Hombrechtikon, Switzerland). The lysates were centrifuged at 4°C for 45 minutes at 14000 rpm and supernatant was collected. The concentration of protein was estimated using BCA assay/Bradford assay as manufacturer instructions (Pierce® BCA Protein Assay Kit, Thermo Scientific, IL, USA). The original protein was diluted 1:10 and 25 µl of diluted protein were taken in triplicates in a 96 well flat bottom ELISA plate and 200 µl of Reaction Reagent (Pierce) was added and incubated for 30 minutes at 37 °C. The plate was measured in an ELISA reader at the nanometer range of 540 nm. Measured protein level was normalized to 2 µg/µl concentrations in the lysis buffer with 6X loading dye and stored at -20 °C for further use.

3.2.2.2 SDS-PAGE and western blot

Protein loading buffer 6x was added to 30 µl of protein sample (60 µg) and cooked for 6 minutes at 96 °C. Normalized protein was loaded and separated by 10% SDS-PAGE (Rotiphorese® Gel 30, 10x SDS-PAGE, Carl Roth GmbH, Karlsruhe, Germany), transferred (Trans Blot, semi dry transfer cell, BioRad) to a nitrocellulose membrane (GE Healthcare, Amersham™ Hybond ECL, Buckinghamshire, UK) and blocked with 5% BSA for 1.5 hours. Membranes were further incubated overnight at 4°C with the primary antibodies diluted in 1x TBST buffer and washed with TBST for 10 minutes for 3 times. Membranes were then incubated for 2 hours at 4°C with the secondary antibody diluted in 1x TBST followed by 3 times TBST wash for each 5-10 mins. The membranes were developed using Super Signal West Pico chemiluminescent substrate (Thermo, Pierce Biotechnology, Rockford, IL, USA) in Fusion Fx7 chemiluminescence system (PEQLAB, Erlangen, Germany). GAPDH was used as a loading control; proteins were analyzed by use of the Fusion Bio1D software (PEQLAB, Erlangen, Germany).

3.2.2.3 RNA isolation

The total RNA was isolated using the PEQLAB RNA isolation kit (VWR International GmbH, Erlangen, Germany). RNA lysis buffer T was added according to the weight of each tissue and the samples were homogenized with Tissue ruptor (Qiagen Instruments, Hombrechtikon, Switzerland). The lysates were transferred to DNA removing columns placed in a 2.0 ml collection tube and centrifuged at 14000 rpm for 1 min at room temperature. Equal volumes of 70% ethanol were added to the lysates and mixed thoroughly by vortexing. Lysates were added to the PerfectBind RNA columns in a new 2.0 ml collection tube and centrifuged at 14000 rpm for 1 min; the flow through was discarded. 500µl of Wash buffer I was added to PerfectBind RNA column and placed in a new 2.0ml collection tube, centrifuged at 14000rpm for 15 sec. The flow out was discarded and 600µl of Wash buffer II was added and centrifuged at 14000rpm for 15 sec. The centrifugation was repeated to dry the column without adding any more buffers. The column was placed in new PCR grade 1.5ml tube and 50-100µl of sterile dH₂O was added directly to the binding matrix. The column was centrifuged for 1 min at 5000g to elute RNA.

3.2.2.4 cDNA synthesis

cDNA synthesis was done using the QuantiTect[®] Reverse Transcription Kit (Qiagen GmbH, Hilden, Germany) from 1 µg/ml of total RNA. 1 µg/ml of total RNA was diluted in 20 µl of water, to this 3 µl genomic DNA wipeout buffer was added and incubated at 42 °C for 2 minutes. Then 4 µl 5x RT buffer, 1 µl RT Primer, 1 µl RT master mix was added followed by incubation at 42 °C for 30 minutes and at 95 °C for 3 minutes. The synthesized cDNA was stored at -20°C for further use.

3.2.2.5 Real time-PCR quantification

Relative quantification of gene expression in the spinal cord and spleen tissues were measured using iTaq[™] Universal SYBR[®] Green qPCR Master Mix (Bio-Rad, CA, USA) at 40 cycles at an annealing temperature according to specific various primers in the StepOne[®] Real-Time PCR system (Applied Biosystems, Darmstadt, Germany). Primers were designed by NCBI nucleotide primer designing tool and primers were synthesized in Eurofins-Genomics (Eurofins MWG Synthesis GmbH, Ebersberg, Germany). The quantification of target genes was done using the listed primers (Table

3.1.7) and the PCR reaction mixture of 10 µl Mastermix (iTaqTM Universal SYBR[®] Green), 1 µl forward primer and reverse primer, 7 µl H₂O and 1 µl of cDNA. GAPDH was used as the internal control gene and the comparative $\Delta\Delta CT$ method ($\Delta CT = \text{target gene} - \text{housekeeping gene}$; $\Delta\Delta CT = 2^{-\Delta CT}$) was used to evaluate the relative quantification of gene expression.

3.2.3 Histopathology and immunohistochemistry

3.2.3.1 Mice Perfusion

MK2^{-/-} mice and WT mice was anaesthetized by an intraperitoneal injection of ketamine (100 mg/kg body weight) and xylazin (20 mg/kg body weight). Transcardial perfusion with 4% paraformaldehyde was performed in mice at day 16 (acute phase) and day 60 (chronic phase) after EAE induction. The spinal cord and brain tissues were removed and embedded in paraffin blocks. Tissue processing starts by placing them in 70% ethanol for 1 hour, followed by 95% ethanol (95% ethanol/5% methanol) for 1 hour. Then they were transferred for the first time in absolute ethanol for 1 hour and for the second time in absolute ethanol for 1½ hours. This is followed by 2 more soakings in absolute ethanol for 2 hours each. The tissues are then transferred to the first clearing agent (Xylene) for 1 hour and a second soak in xylene for 1 hour again. First soak in the wax at 58°C for 1 hour and second soak in the wax at 58°C 1 hour. These tissues were sectioned into 1µm thick slices and were fixed onto glass slides for histopathology and immunohistochemistry.

3.2.3.2 Histology

Paraffin sections were evaluated for inflammatory infiltrates (hematoxylin and eosin stain), demyelination (Luxol fast blue/periodic acid-Schiff stain) and axonal density (Bielschowsky staining). Histological evaluation was done with a light microscope (Carl Zeiss, Germany).

3.2.3.3 Hematoxylin and Eosin staining (H & E)

Inflammation in the spinal cord in acute and chronic EAE was analyzed by H & E staining. Slides were placed in 60°C for the wax to melt overnight, the next day slides

were incubated in xylene for deparafinization followed by ethanol (100% ethanol, 96% ethanol and 70% ethanol; 2 mins each) hydration. Then slides were stained in Hematoxylin for 5 minutes, washed with water and then stained in eosin for 5 minutes. After this the slides were rinsed in 96% ethanol and 100% ethanol for dehydration. This was followed by 10 mins in first xylene and in second xylene; slides were mounted with mounting medium with a glass cover slip.

3.2.3.4 *Luxol fast blue/periodic acid-schiff stain (LFB / PAS)*

Demyelination in spinal cord following EAE was analyzed by LFB/PAS staining. Slides were placed in 60°C for the wax to melt overnight, next day the tissue sections were deparafinized with xylene and then hydrated in ethanol (100% ethanol, 96% ethanol and 70% ethanol; 2 minutes each) followed by overnight incubation in luxol fast blue stain at 56°C. The glass slide holder was sealed tightly as the stain tends to evaporate fast in such conditions. After a few rinses in dH₂O and 70% ethanol the slides were counter stained in crystal violet for 30-40 seconds. The slides were again shortly rinsed in dH₂O and dehydrated (96% ethanol and 100% ethanol). Sections were mounted with mounting medium in glass cover slip. The final % value for demyelination was calculated using equation shown below:

$$\text{Demyelinated area (\%)} = \frac{\text{Demyelinated area in white matter}}{\text{Total white matter area}} \times 100$$

3.2.3.5 *Bielschowsky (Silver staining)*

Axonal density in the spinal cord tissue was analyzed by Bielschowsky-silver staining. Deparafinized and hydrated (100% ethanol, 96% ethanol and 70% ethanol; 2 minutes each) sections were incubated in dark with 20% silver nitrate (AgNO₃) for 20 minutes. This is usually used as a stock solution (typically 20% w/v), which must be stored in a dark place. The reaction was stopped with a water wash. Then the sections were incubated for 2 minutes in 2% Na-Thiosulfate (Sigma Aldrich): 2 gm. of sodium thiosulfate in 100ml of distilled water. This was followed by a water wash. Sections were dehydrated in ethanol (96% ethanol and 100% ethanol) and mounted with mounting medium and cover glass.

3.2.3.6 Immunohistochemistry

For immunohistochemistry, sections were deparaffinized in xylene, hydrated, endogenous peroxidase was blocked for 10 minutes with 3% hydrogen peroxide and pretreated with citrate buffer (10 mM, pH 6) over 5 minutes for 3 times. Paraffin sections were incubated with 10% FCS and stained overnight for activated microglia-macrophage (Mac 3, clone M3/84, 1:200, Pharmingen, San Diego, CA, USA), activated B cells (B220, clone RA3-6B2, 1:200, Pharmingen, San Diego, CA, USA) and T cells (CD3, clone CD3-12, 1:150, Serotec, Oxford, UK). Respective secondary antibodies (Mac 3-goat anti-rat, 1:100, B220-goat anti-rat 1:200 and CD3 goat anti-rabbit-1:250) and avidin-biotin method was used and the signals were detected with DAB. Microscopic images were captured using a Zeiss light microscope (Germany) and analyzed using the ImageJ software.

3.2.4 Cell culture experiments

C17.2 cells were cultured in DMEM + 2 mM Glutamine + 10% FBS. Cells were cultured at 37 °C in 5% CO₂. Cell line was passaged by 1x PBS wash, the adherent cell line was followed by 1% Trypsin at 37 °C for 1 minute incubation.

3.2.4.1 MK2 inhibition and stimulants used for cell lines

C17.2 cells

Transfection in C17.2 cells was done using Lipocalyx Viromer. The Mouse MK2 siRNA was diluted in buffer F to 11µM concentration. 11µl of this diluted siRNA with 99µl of the diluted transfectant which gives a final concentration of 1.1µM siRNA in complex. This was incubated for 5-10 min at room temperature. 200µl of this complex was transferred to each well.

3.2.4.2 Cell proliferation assay

Cells were seeded in 96 well plates in a final volume of 100 µl/well (1x10⁵ cells/ml). Then the old medium was removed and the cells were incubated for 24 hours with fresh medium containing TNF-α (10 ng/ml), SB203580 (1 µg/ml), Glucosamine acetate (10µg/ml) and their combinations. The readings were taken at 0 hrs, 24 hrs and 48 hrs after incubation with these reagents. Then 10 µl of WST-1 reagent (Cell proliferation

reagent WST-1, Roche applied science, Indianapolis, IN) was added in each well and the assay was carried out as mentioned in the instructions provided by the manufacturer. Plates were shaken thoroughly for 1 minute on a shaker and incubated for 4 hours at standard cell culture conditions. The colour developed from the soluble formazan dye cleaved from the tetrazolium salt WST-1 was measured at an absorbance of 420-480 nm in an ELISA reader. To calculate proliferation, mean absorbance was calculated and background absorbance (medium alone) subtracted from each value. The percentage of specific proliferation was quantified using the following calculation: % Proliferation = (experimental release / spontaneous release) x 100.

3.2.4.3 Protein extraction

Culture medium was removed from the cells after they were 80% confluent then fresh medium was added with respective treatments for 2-3 hours. Cells were stimulated with 10 ng/ml TNF- α and or 10 μ l/ml GA with or without MK2 inhibition (1 μ g/ml SB203580) or MK2 transfection. Then medium was removed from the cells and washed with cold 1x PBS. Cells were scraped from the flask and centrifuged for 3500 rpm, 15 minutes at 4 °C. Supernatant was discarded and cell pellets were lysed with lysis buffer and incubated in ice for 30 minutes. Cell lysates were centrifuged (14000 rpm) at 4 °C for 30 minutes, supernatant were collected and stored at -20 °C until analysis.

3.2.4.4 Protein quantification and western blot

Protein quantification (BSA protein assay), SDS-PAGE and western blot procedure were followed as described in Section 3.2.2.1 and 3.2.2.2.

3.2.5 Statistics

All analyses were performed blinded to the genotype. All mice and samples were included into the analysis. Statistical analysis for differences between the genotypes in the clinical course, histological data, reverse transcription-PCR and protein data were performed using the Unpaired t-tests. Statistical significance was set at $P \leq 0.05$. Statistical analysis and preparation of graphs was performed using GraphPad Prism version 7.00 for Windows (GraphPad Software, San Diego, California, USA). Values are expressed as mean \pm standard error of mean. P values of * $P < 0.05$, ** $P < 0.005$, *** $P < 0.001$ were considered as significant.

4 RESULTS

4.1 Genotype and phenotype confirmation of MK2 deletion in C57BL/6J mice

MK2^{-/-} mice were generated by Kotlyarov et al (1999). To study the function of MK2 in mouse biological system, a mutation was introduced by homologous recombination in embryonic stem (ES) cells. A neomycin-resistance gene (*neo*) was inserted into the catalytic domain of MK2 i.e. exon encoding subdomains V and VI, thereby introducing stop codons in all reading frames. The mutant allele is expected to encode a truncated kinase that deletes amino acids 130–383, which are essential for the catalytic activity. These ES cells were used to generate mice that carry the MK2 mutation. The MK2^{-/-} mice did not display any obvious behavioral defects; they were viable, fertile and grew to normal size.

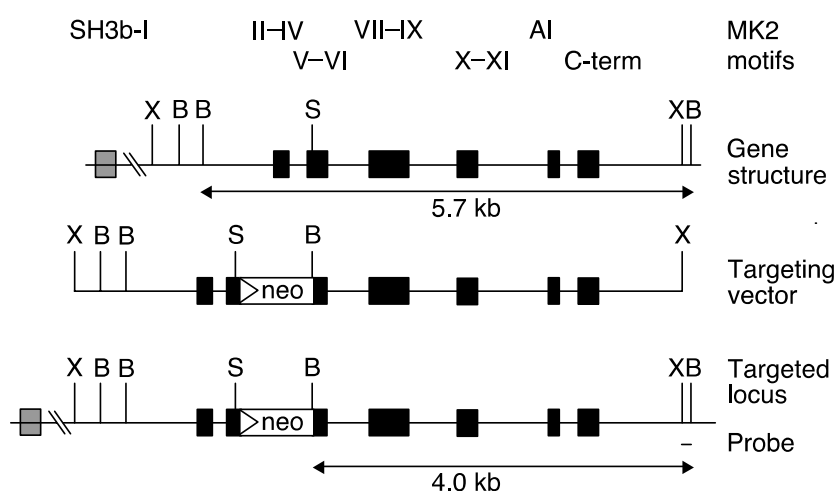


Figure 7: Strategy applied to mutate the MK2 gene and effect of the mutation on MK2 activity. Structure and partial restriction map of the MK2 gene, the targeting vector and the targeted locus. X, XbaI; B, BamHI; S, SacI) The MK2 sequence motifs encoded by different exons (shown by black boxes) are indicated (roman numerals, catalytic subdomains; SH3b- I, Src-homology 3 -binding motif; AI, autoinhibitory motif; C-term, carboxy terminus). The neo cassette, which contains in-frame translational termination codons, was inserted into the exon encoding subdomains V and VI; the mutant locus is expected to encode a truncated kinase that lacks sequences essential for enzymatic activity (Kotlyarov et al., 1999)

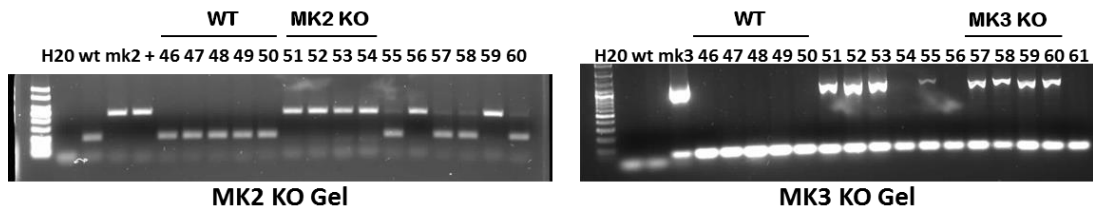


Figure 8: In the MK2 knockout gel (left panel) mice numbers 51, 52, 53, 54, 56, 59 are the mice with the MK2^{-/-} gene. The second gel (right panel) represents the MK3 KO gel where the mice 51, 52, 53, 57, 58, 59, 60 are with MK3^{-/-} gene. When put together we have mice 54 and 56, which are the MK2^{-/-} mice.

4.1.1 Total MK2 was decreased in the MK2^{-/-} mice

The level of total MK2 was analyzed in spinal cord lysates of control and MK2^{-/-} mice in EAE to confirm the knockout efficiency. Total MK2 expression were significantly reduced in MK2^{-/-} mice in both acute and chronic EAE (Figure 9).

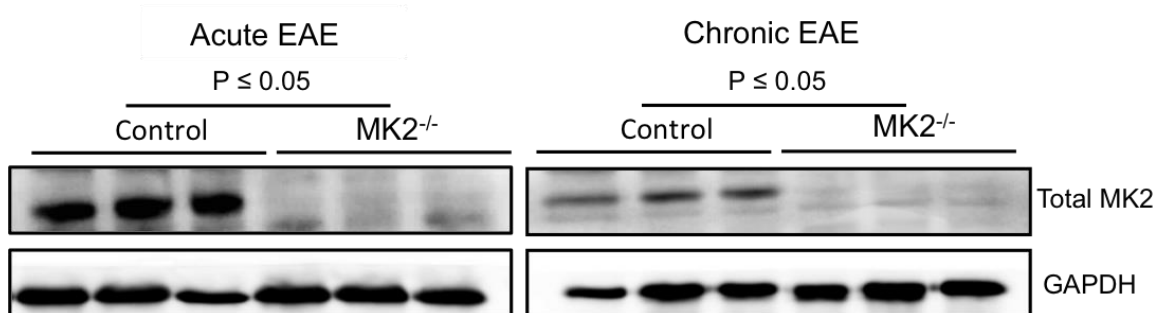


Figure 9: Total MK2 in acute (n=8) and chronic (n=5) EAE mice spinal cord. Total MK2 was significantly decreased in acute EAE (left panel) and chronic EAE (right panel) of the spinal cord. GAPDH act as the internal loading control. P values of * $P < 0.05$, ** $P < 0.005$, *** $P < 0.001$ were considered as significant.

4.2 EAE in MK2^{-/-} and control mice

4.2.1 Clinical scoring

EAE was induced in 10-12 weeks old MK2^{-/-} and control female mice with the MOG₃₅₋₅₅ peptide. Mice were scored daily for EAE clinical symptoms.

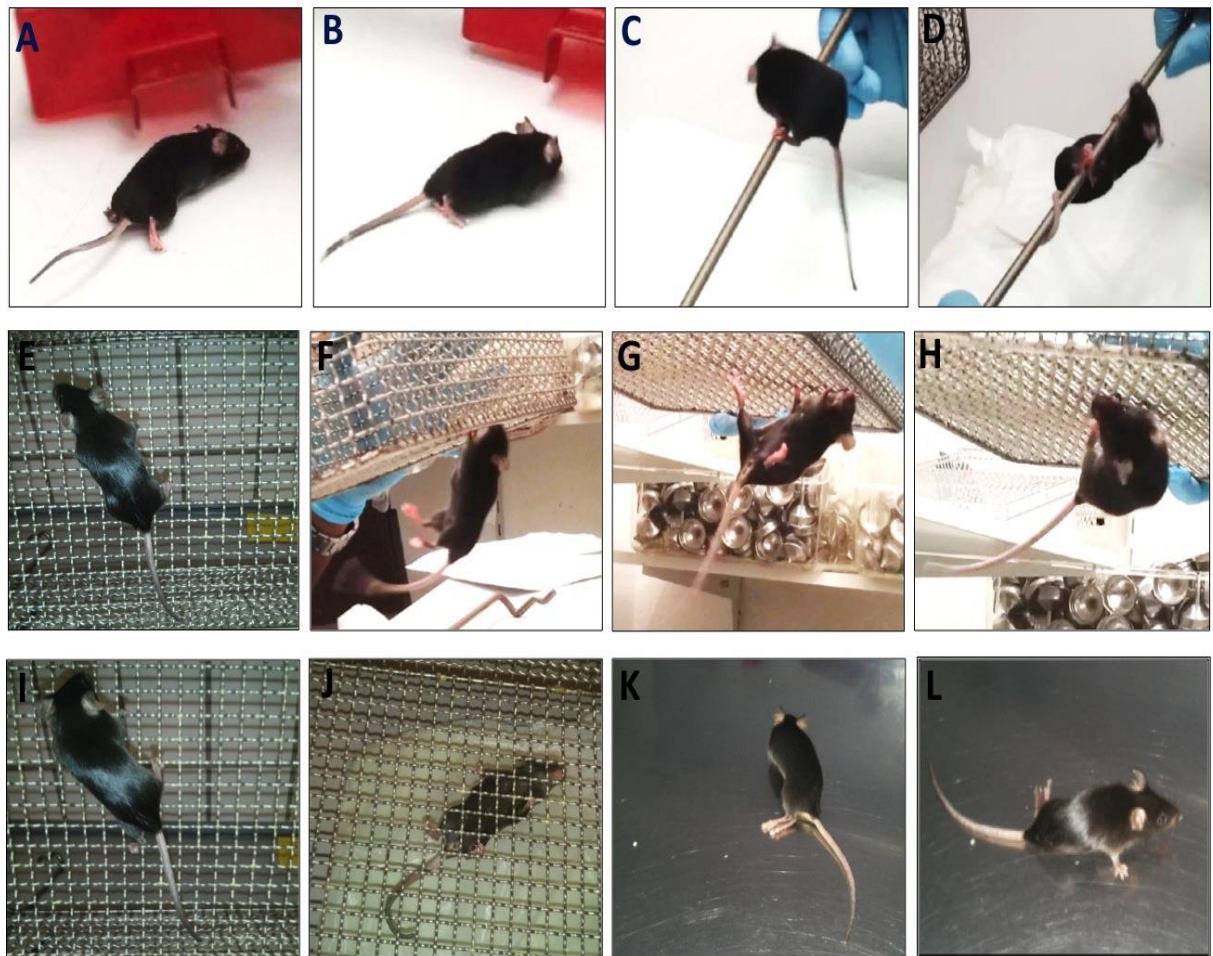


Figure 10: Clinical symptoms of MOG₃₅₋₅₅-induced EAE in MK2^{-/-} and control mice. A-J represent tail paralysis with mild hind limb weakness. K, L depicts the hind limb paralysis which hinders the walking and strength in mice thus shown on the plain surface.

4.3 Clinical symptoms of MK2^{-/-} mice

4.3.1.1 Chronic phase EAE

Mice with MK2 deletion (MK2^{-/-}) and controls were analyzed for their susceptibility to MOG₃₅₋₅₅ peptide EAE induction. EAE was induced in 12 ten-week-old female MK2^{-/-} mice and compared with 11 age- and sex-matched controls. There were no significant changes seen in the disease course between MK2^{-/-} mice and control mice (Figure 11). Table 3 shows the summary of the EAE score in control and MK2^{-/-} mice. The onset of clinical symptoms was from day 9-11 in control and MK2^{-/-} mice.

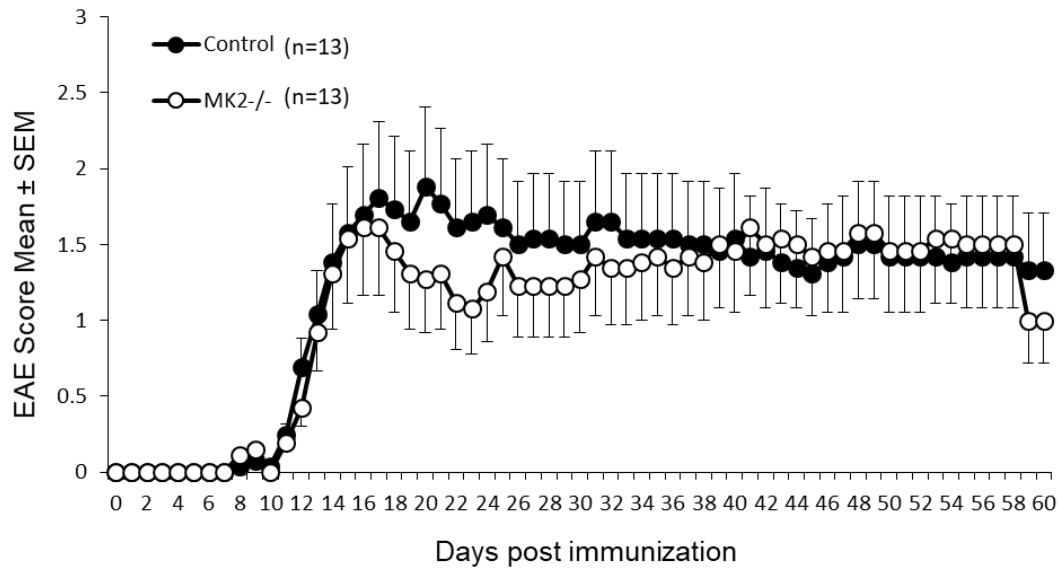


Figure 11: MOG₃₅₋₅₅-induced EAE in MK2^{-/-} mice and control mice. The data is from 1 chronic EAE experiment. The onset of clinical symptoms was from day 9 in controls in MK2^{-/-} mice. Milder disease course was found in MK2^{-/-} mice from day 10 onwards p.i.

4.3.1.2 Acute phase EAE

EAE was induced in 16 ten-week-old female control mice and compared with 14 age- and sex-matched MK2^{-/-} mice. The onset of clinical symptoms was from days 9-12 in controls and from days 9-11 in MK2^{-/-} mice. During the acute phase I experiment there were significant differences in the clinical symptoms of MK2^{-/-} mice and control mice. The MK2^{-/-} mice showed reduced clinical signs as compared to control mice (Table 3, $P \leq 0.001$). There were 3 experimental replicates done for acute phase. In the acute phase, second experiment there were 3 ten-week old female MK2^{-/-} mice compared with 5 age and sex-matched controls. There were significant differences seen in the clinical symptoms between the two groups, with MK2^{-/-} mice showing reduced symptoms as in the first acute EAE experiment ($P \leq 0.01$) (Table 3). In the third EAE experiment, 5 MK2^{-/-} mice were compared with 5 age and sex-matched controls. The last EAE experiment was not in similar lines as compared to the first two EAE experiments. There were no differences seen between the clinical symptoms of two groups of mice ($P = n.s$). All the three EAE scores were pooled into Figure 12.

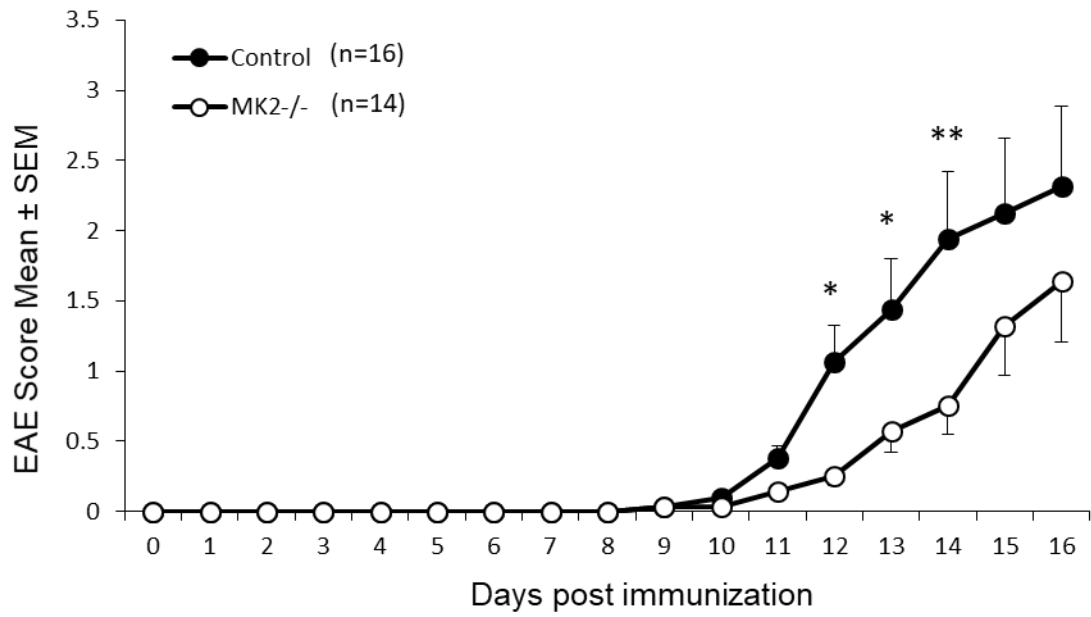


Figure 12: MOG₃₅₋₅₅-induced EAE in MK2^{-/-} mice and control mice. The data is pooled from 3 acute EAE experiment. The onset of clinical symptoms was from days 9-12 in controls and from days 9-11 in MK2^{-/-} mice. Significantly milder disease course was found in MK2^{-/-} mice, on day 12, 13 and 14 p.i.

Experiment	Mice	Number	Day of onset	Incidence	Score Max	P-value
Chronic EAE 1	Control	13	9	100%	3.5	n.s.
	MK2 ^{-/-}	13	9	100%	3.5	
Acute EAE 1	Control	6	12	100%	3	P ≤ 0.001
	MK2 ^{-/-}	6	10	100%	2	
Acute EAE 2	Control	5	9	100%	3.5	P ≤ 0.01
	MK2 ^{-/-}	3	9	66.67%	3	
Acute EAE 3	Control	5	11	100%	3	n.s.
	MK2 ^{-/-}	5	11	80%	3	

Table 3: Clinical characteristics of MOG₃₅₋₅₅-induced EAE in MK2^{-/-} mice

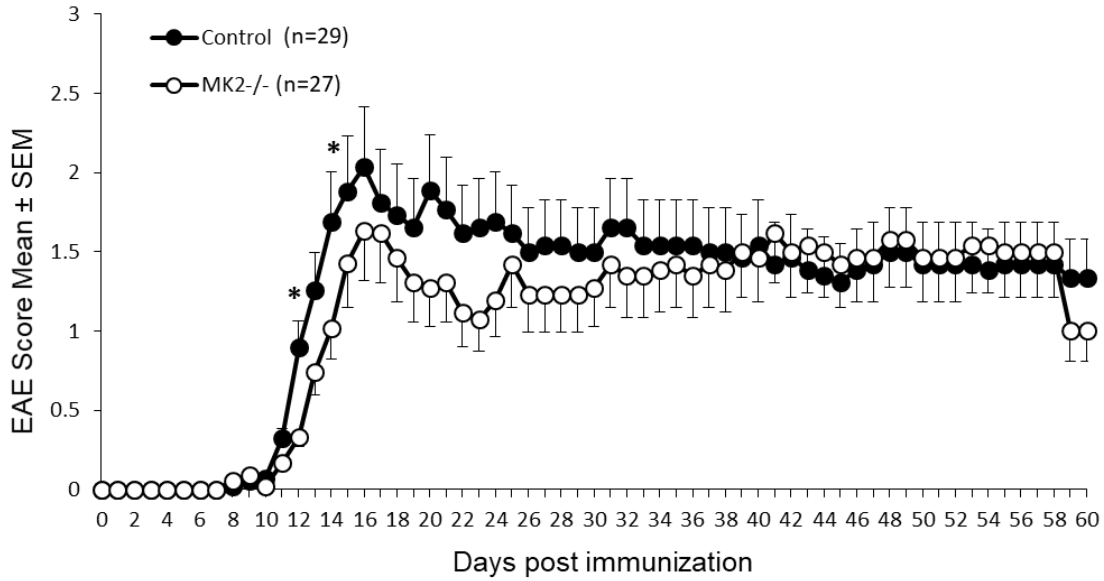


Figure 13: MOG₃₅₋₅₅-induced EAE in MK2^{-/-} mice and control mice. The data is pooled from 3 acute EAE and 1 chronic EAE experiment. The onset of clinical symptoms was from days 9-12 in controls and from days 9-11 in MK2^{-/-} mice. Milder disease course was found in MK2^{-/-} mice, on day 12 and 14 p.i.

As it is clear from the description above, the EAE model of MK2 was not stable. In the chronic phase no differences were seen, but in the acute phase statistical significant differences were seen. The second acute phase was in similar lines as the first acute phase. The last acute phase displayed no differences again.

The mice from the first and second EAE experiments were used for histology. The mice from the first and the third EAE experiments were used for protein and RNA analysis. It is important to point this out as the results seen in the histological, protein and mRNA analysis depends on the mice taken from the experiments.

4.3.2 Assessment of inflammation: Cell infiltration of T-cells, B-cells and macrophages

To further investigate underlying mechanisms, MK2^{-/-} mice were assessed for susceptibility to inflammation in the spinal cord white matter. Haematoxylin and eosin staining was used to evaluate inflammatory index. In the chronic phase no difference in inflammation was observed between MK2^{-/-} mice and controls (Figure 14D-F). Inflammatory index was reduced in MK2^{-/-} mice as compared to control mice ($P \leq 0.05$) (Figure 14A-C).

Immunohistochemical analysis were performed to further investigate the composition of infiltrates in spinal cord EAE lesions. Immunostaining for CD3(+), B220(+) and Mac3(+) cells were performed and quantified to analyze cellular infiltrate composition in spinal cord white matter lesions. The number of CD3(+) T cells was not affected by MK2 deletion in acute EAE (Figure 15A-C) and in chronic stage (Figure 15D-F). In the acute phase of EAE Mac3(+) cells were reduced in MK2^{-/-} mice (P = 0.039) (Figure 17A-C). In the chronic phase of EAE there was no significant difference seen in Mac3(+) cells and B220(+) cells in MK2^{-/-} mice (Figure 17D-F, Figure 16D-F).

Disease pathology	Acute EAE			Chronic EAE		
	Control	MK2 ^{-/-}	P-value	Control	MK2 ^{-/-}	P-value
Inflammatory index	8.838 ± 1.32	4.208 ± 0.81	P = 0.0181	6.56 ± 1.48	5.78 ± 1.88	P = 0.753
CD3 (+) T cells	1662 ± 264.7	1186 ± 263.9	P = 0.236	907.8 ± 111.1	745.6 ± 184.7	P ≤ 0.473
B220 (+) B cells	1049 ± 303.7	293.6 ± 57.9	P ≤ 0.056	533.2 ± 63.04	945.8 ± 180.6	P ≤ 0.063
Mac3 (+) Macrophages	1701 ± 150.5	1124 ± 207	P ≤ 0.039	721.3 ± 153.2	760.6 ± 97.81	P ≤ 0.834

Table 4: Immune cell infiltration in spinal cord of EAE mice. Blinded quantification of immune cell infiltration of T cells, B cells and macrophages in spinal cord of controls and MK2^{-/-} mice in acute and chronic EAE. Data are presented as mean ± SEM.

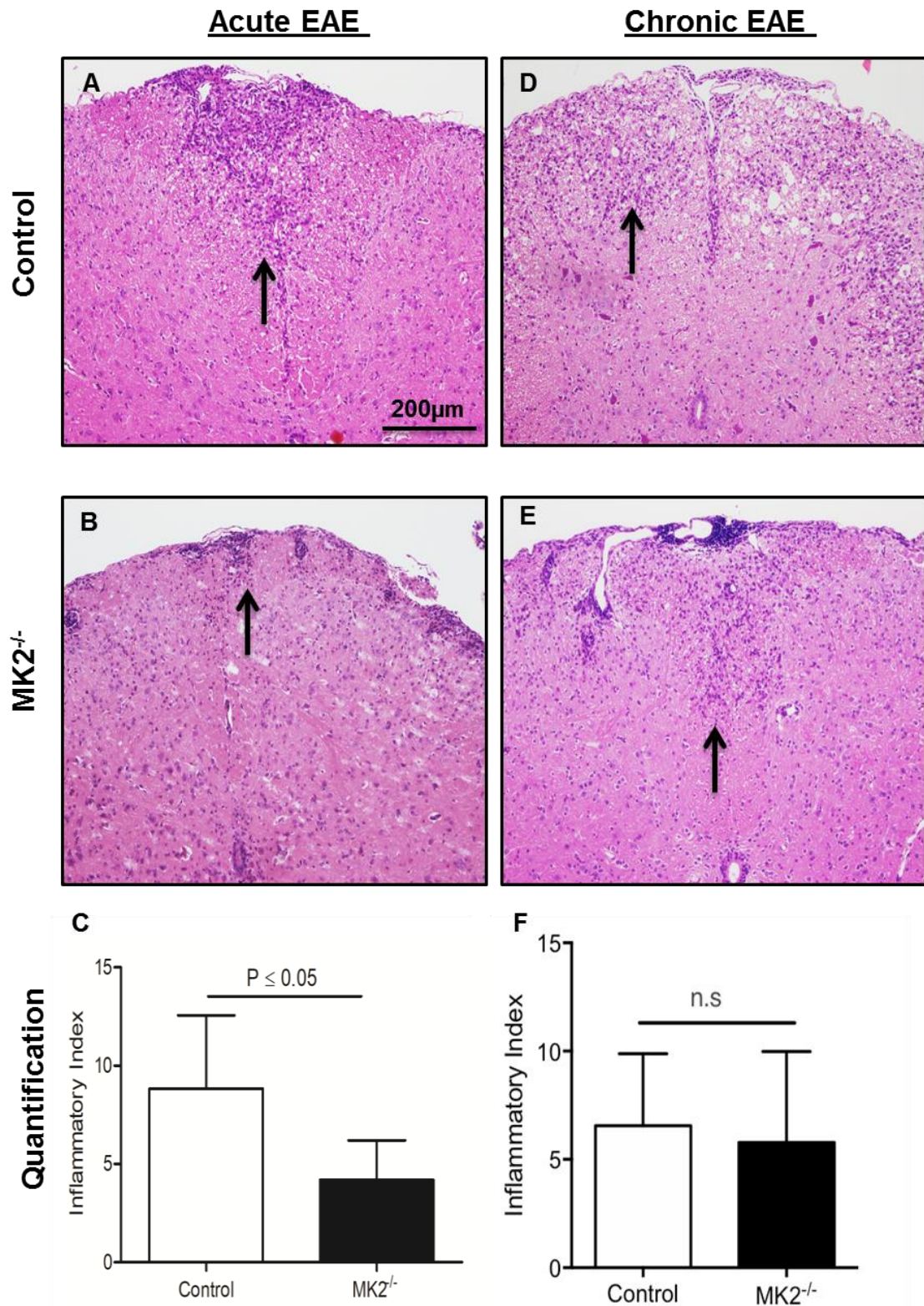


Figure 14: Histopathological analysis of acute (n=8) and chronic (n=5) EAE (H and E). Inflammatory index in the spinal cord sections of acute (A, B and C) and chronic (D, E and F) EAE in controls (A, D) and MK2^{-/-} mice (B, E). Representative images of spinal cord sections are shown. The inflammatory index (C and F) was lower in MK2^{-/-} mice compared to control. Bar: 200 μ m, Data are presented as mean \pm SEM.

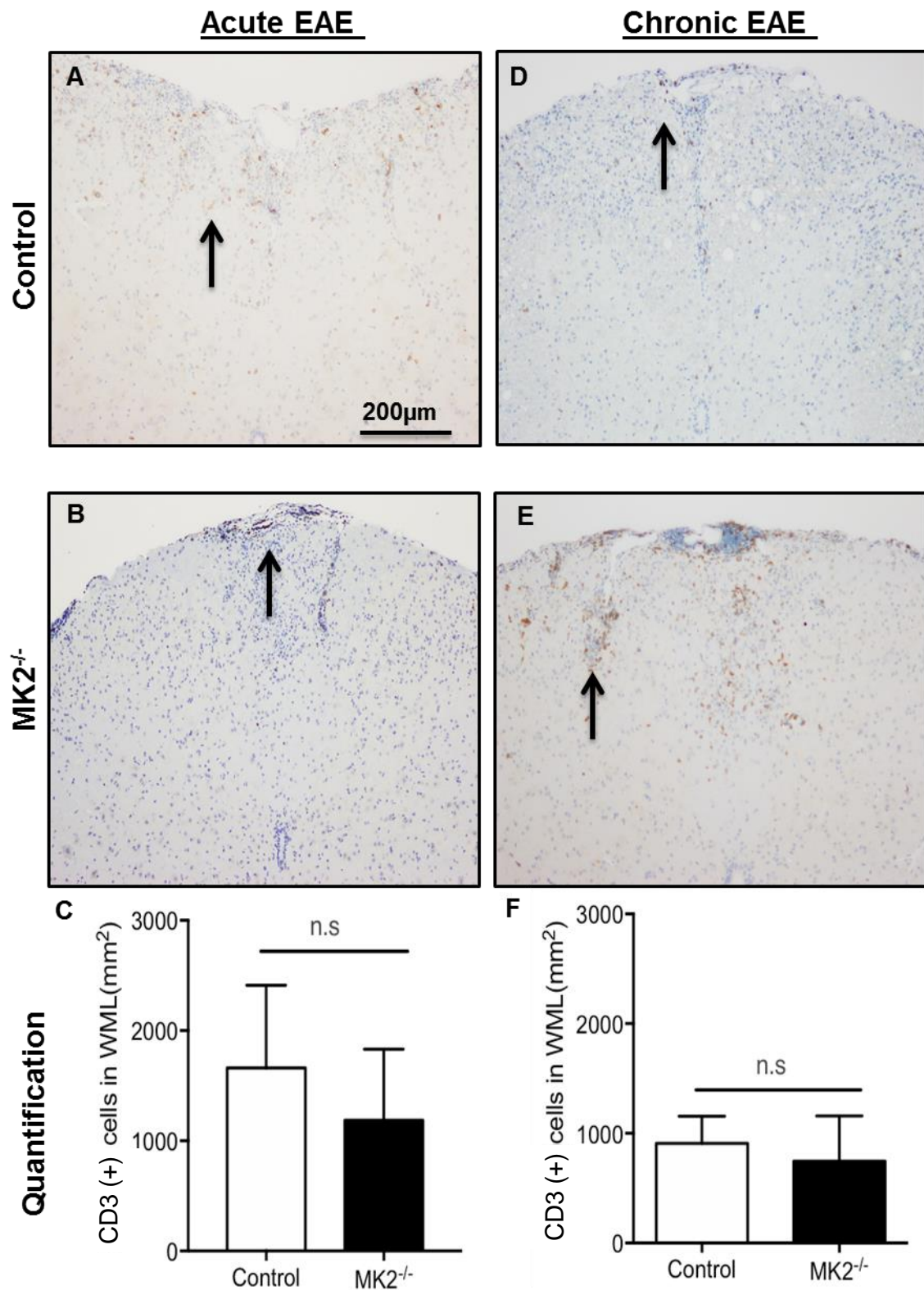


Figure 15: T cell infiltration in acute (n=8) and chronic (n=5) EAE spinal cord. CD3 (+) T cells in white matter lesions of spinal cord sections in acute (A, B and C) and chronic (D, E and F) EAE in controls (A, D) and MK2^{-/-} mice (B, E). The number of CD3 (+) T cells per mm² was not significantly different in MK2^{-/-} mice compared with controls. Bar: 200 µm, Data are presented as mean ± SEM

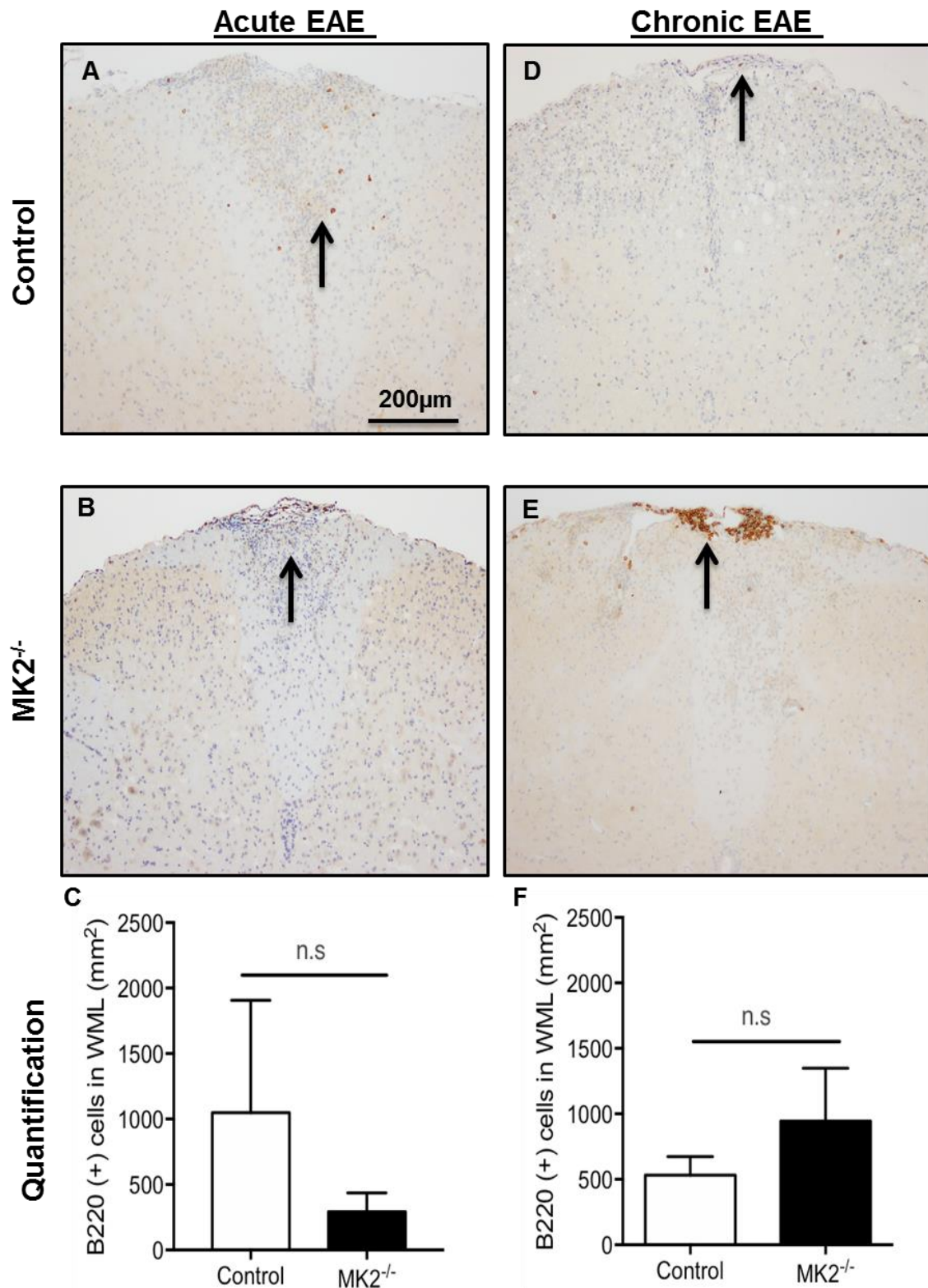


Figure 16: B cell infiltration in acute (n=8) and chronic (n=5) EAE spinal cord. B220 (+) B cells in white matter lesions of spinal cord sections in acute (A, B and C) and chronic (D, E and F) EAE in controls (A, D) and MK2^{-/-} mice (B, E). The number of B220 (+) B cells per mm² was less in MK2^{-/-} mice compared with controls in acute EAE (C), though not significant. Bar: 200 μm, Data are presented as mean ± SEM.

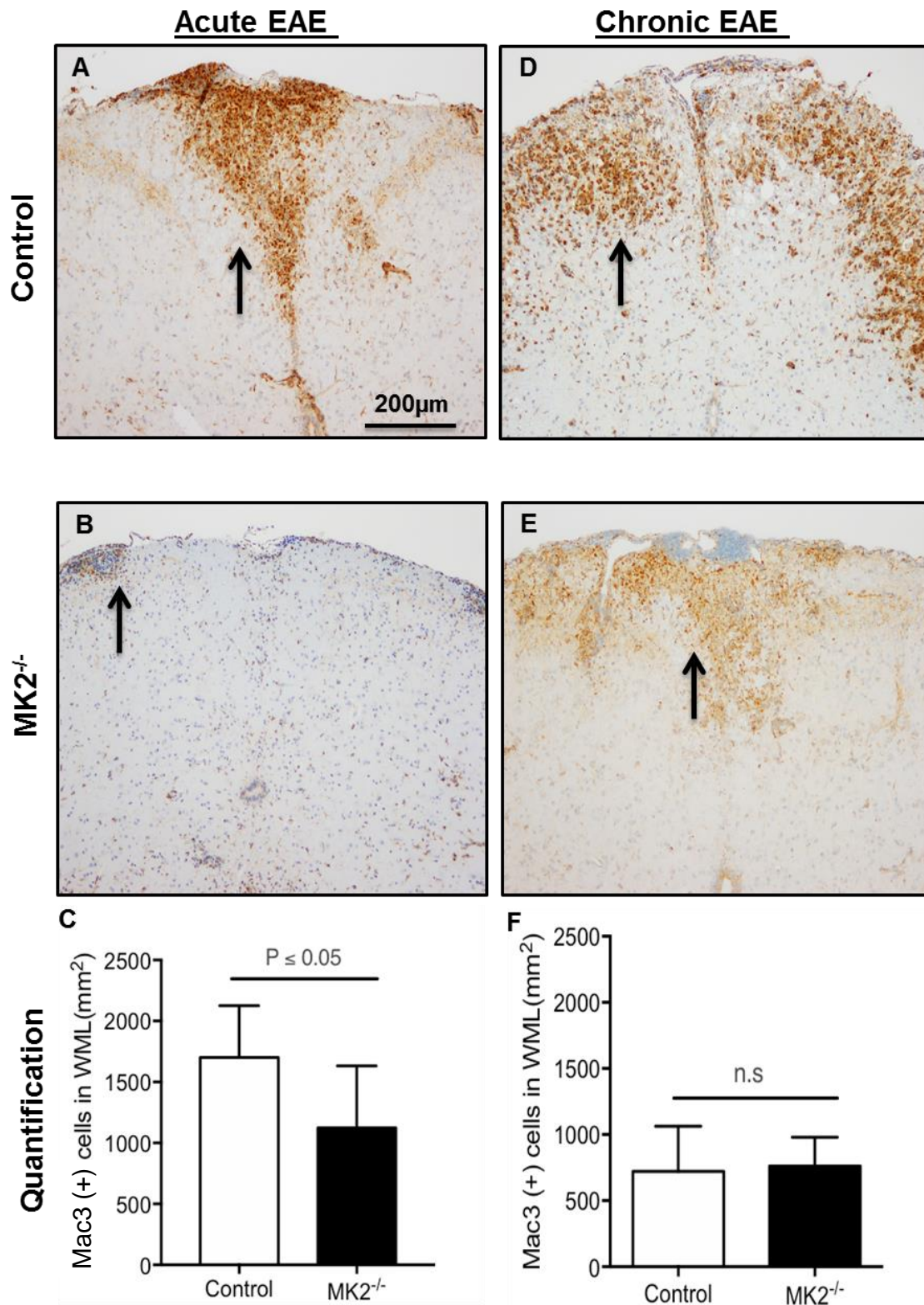


Figure 17: Macrophage infiltration in acute ($n=8$) and chronic ($n=5$) EAE spinal cord. Mac3 (+) Macrophages in white matter lesions of spinal cord sections in acute (A, B and C) and chronic (D, E and F) EAE in controls (A, D) and MK2^{-/-} mice (B, E). The number of Mac3 (+) macrophage per mm² was lower in MK2^{-/-} mice compared with controls in acute phase EAE (C). Bar: 200 μm, Data are presented as mean ± SEM.

4.3.3 Demyelination and axonal density in MK2^{-/-} mice

Luxol fast blue staining was done to evaluate demyelination. At acute phase, day 16 p.i., demyelination was significantly reduced in MK2^{-/-} mice as compared to controls ($P \leq 0.05$) (Figure 18A-C). In the chronic phase no significant differences in demyelination ($P = 0.171$) were observed between MK2^{-/-} mice and controls.

Axonal density was evaluated by Bielschowsky staining. In the chronic phase no difference in axonal density was observed between MK2^{-/-} mice and controls (Figure 19D-F). At day 16-time point, axonal density was higher in MK2^{-/-} mice than in controls ($P \leq 0.05$) (Figure 19A-C).

Pathology	Day 16		P-value	Day 60		P-value
	Control	MK2 ^{-/-}		Control	MK2 ^{-/-}	
Demyelination (%)	88.75 ± 4.40	56.42 ± 12.95	$P = 0.0211$	17.47 ± 3.31	11.86 ± 1.72	$P = 0.171$
Axonal density (%)	53.44 ± 3.08	68 ± 5.42	$P = 0.028$	35.94 ± 5.66	44.6 ± 5.13	$P = 0.289$

Table 5: Histopathological analysis of spinal cord from EAE mice. Blinded quantification of demyelination (LFB/PAS) and axonal density (silver staining) in spinal cord of controls and MK2^{-/-} mice in EAE. Data are presented as mean ± SEM.

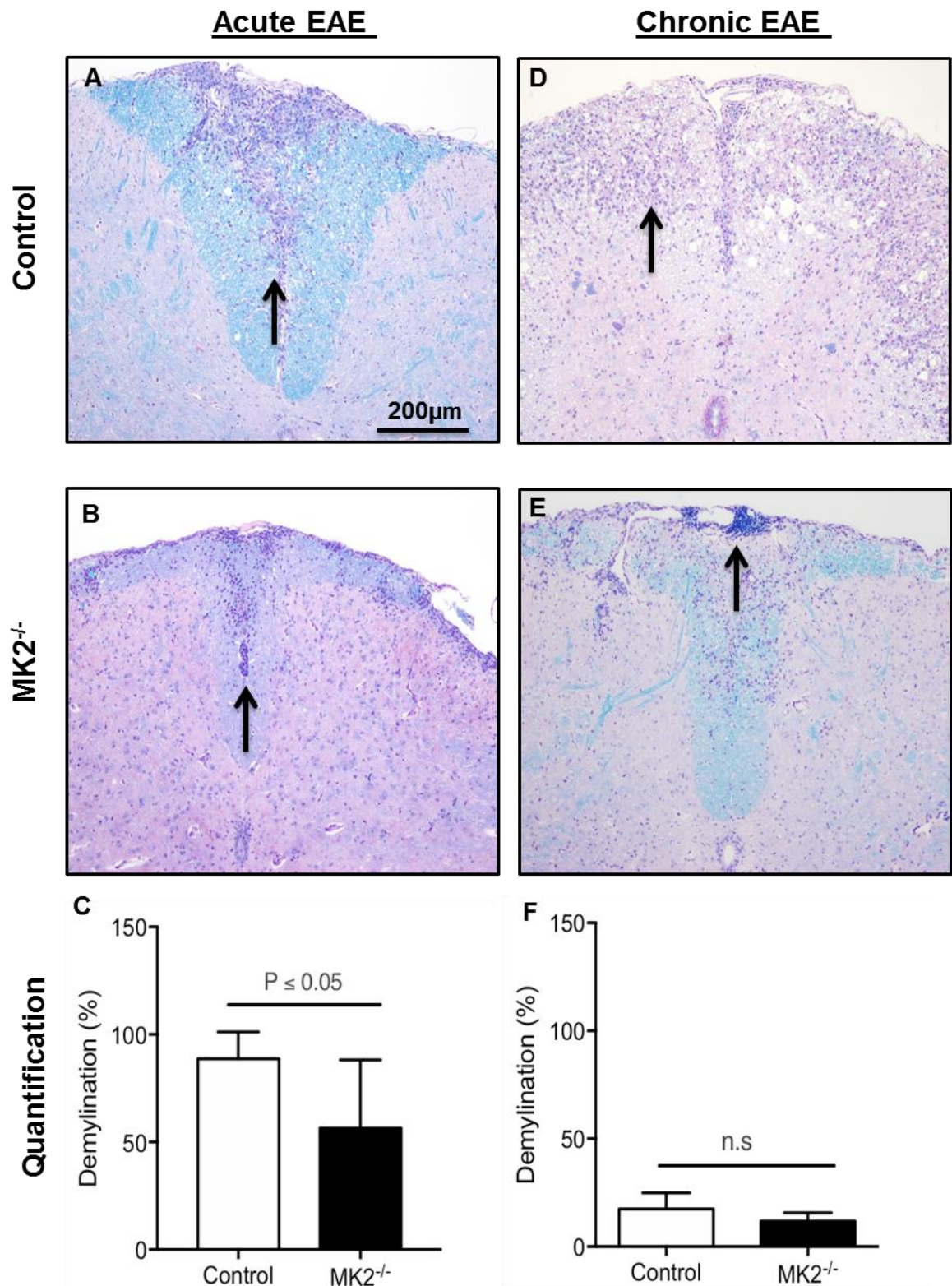


Figure 18: Histopathological analysis of acute (n=8) and chronic (n=5) EAE (LFB/PAS). Demyelination in the spinal cord sections of acute (A, B and C) and chronic (D, E and F) EAE in controls (A, D) and MK2^{-/-} mice (B, E). Representative images of spinal cord sections are shown. The percentage of demyelination (F) was lower in MK2^{-/-} mice compared to control in chronic EAE. Bar: 200 μ m, Data are presented as mean \pm SEM.

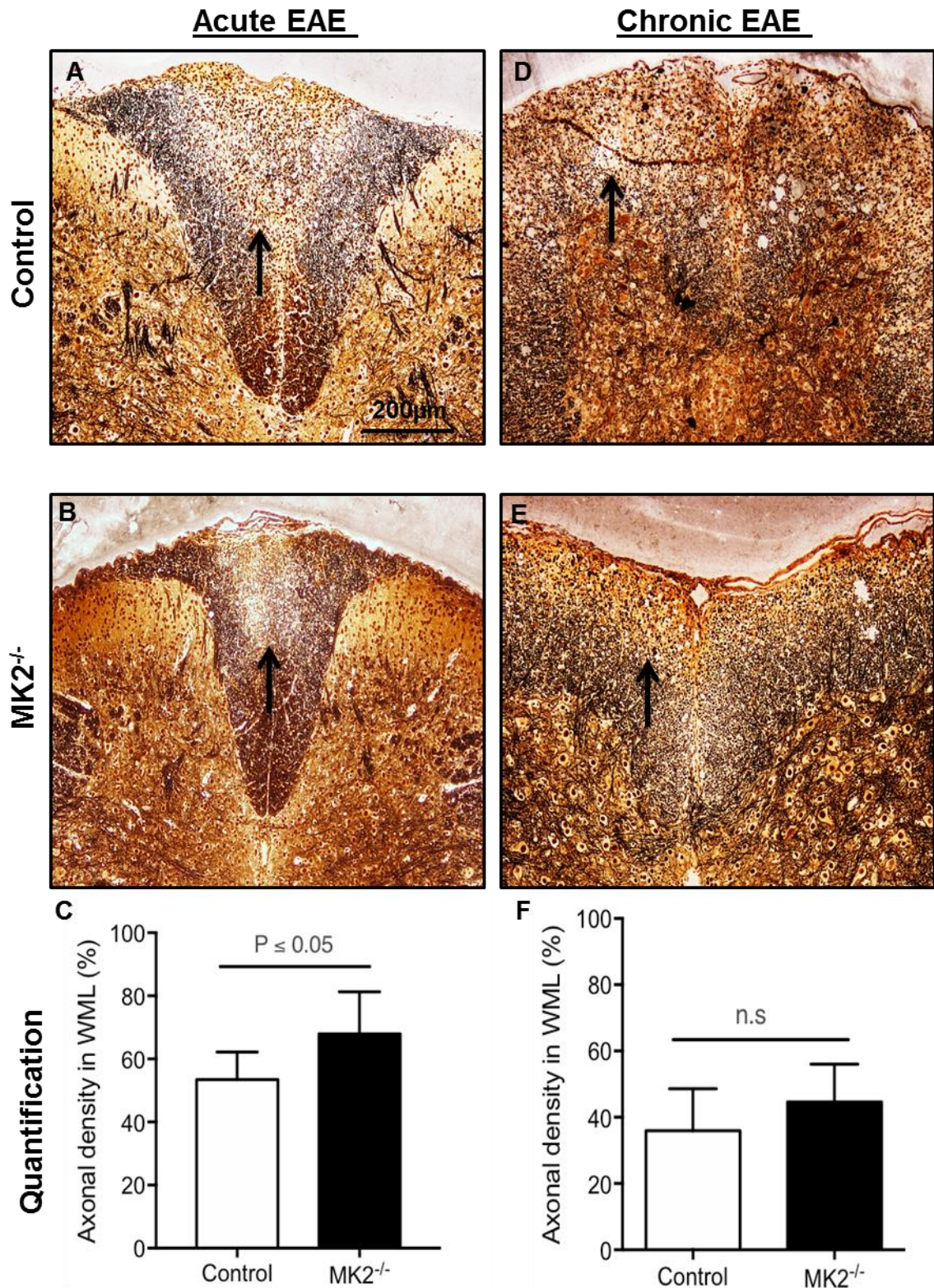
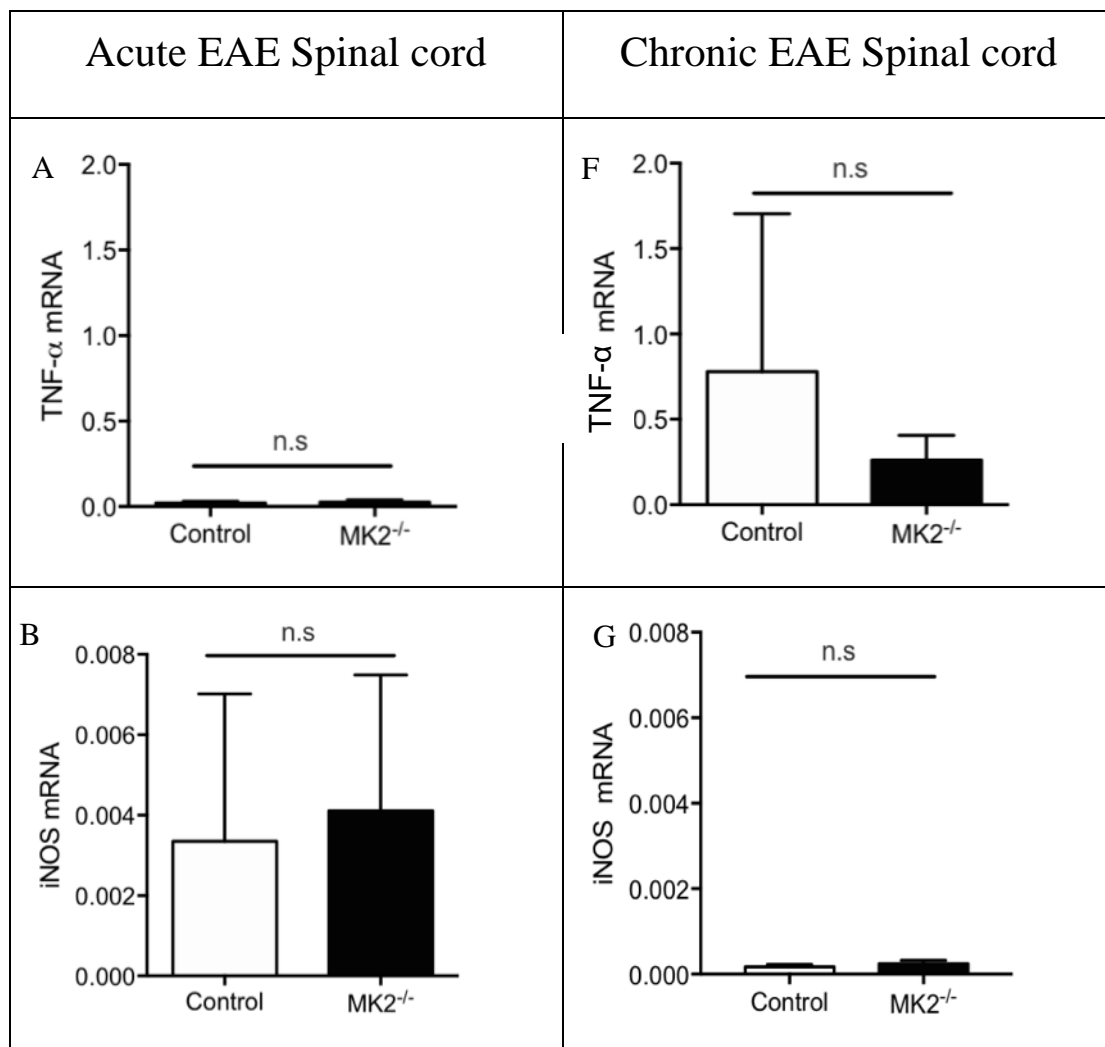


Figure 19: Histopathological analysis of acute (n=8) and chronic (n=5) EAE (Silver staining). Axonal density in the spinal cord sections of acute (A, B and C) and chronic (D, E and F) EAE in controls (A, D) and MK2^{-/-} mice (B, E). Representative images of spinal cord sections are shown. Percentage of axonal density (C and F) was higher in MK2^{-/-} mice compared to control. Bar: 200 μm, Data are presented as mean ± SEM.

4.3.4 Pattern of cytokines expression in MK2^{-/-} mice spinal cord

The role of cytokines as important regulatory elements in immune cell infiltration processes has been well established in EAE. To quantify the cytokine pattern, pro-inflammatory cytokine mRNA was analyzed in the spinal cord in the acute and chronic phase of EAE. The mice used for the mRNA analysis did not show a significant difference in the clinical scores between control vs MK2^{-/-} mice at day 16. In the acute phase MK2^{-/-} mice showed no change in the expression of TNF- α (P = 0.301), IL-17 (P = 0.650), iNOS (P = 0.673), IL-1 β (P = 0.876) and IL-6 (P = 0.310) compared with controls (Figure 20A-E). In the chronic phase no differences in pro-inflammatory cytokine expression for TNF- α (P = 0.254), IL-1 β (P = 0.084), IL-6 (P = 0.6905) and IL-17 (P = 0.213) were observed (Figure 20F-J).



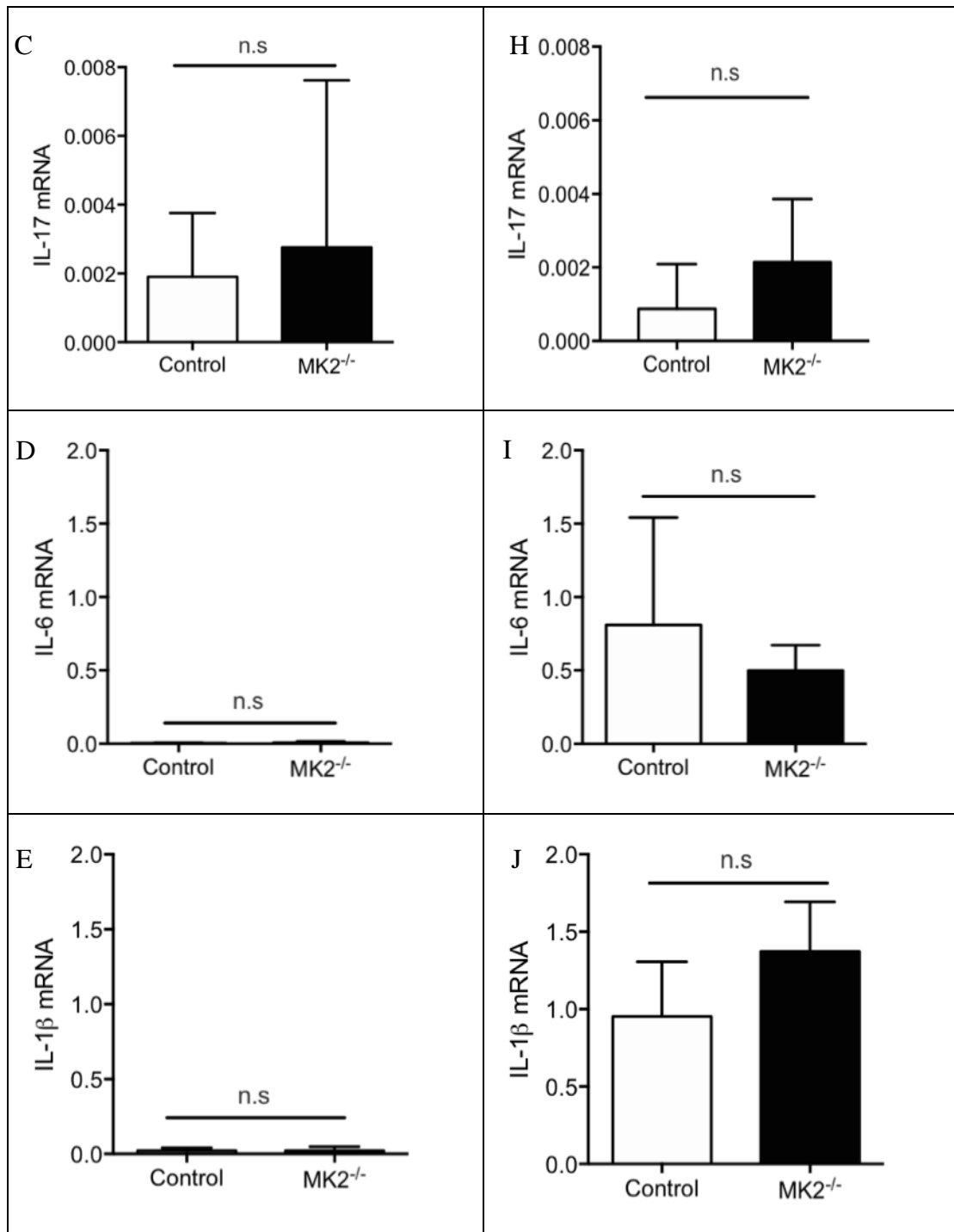
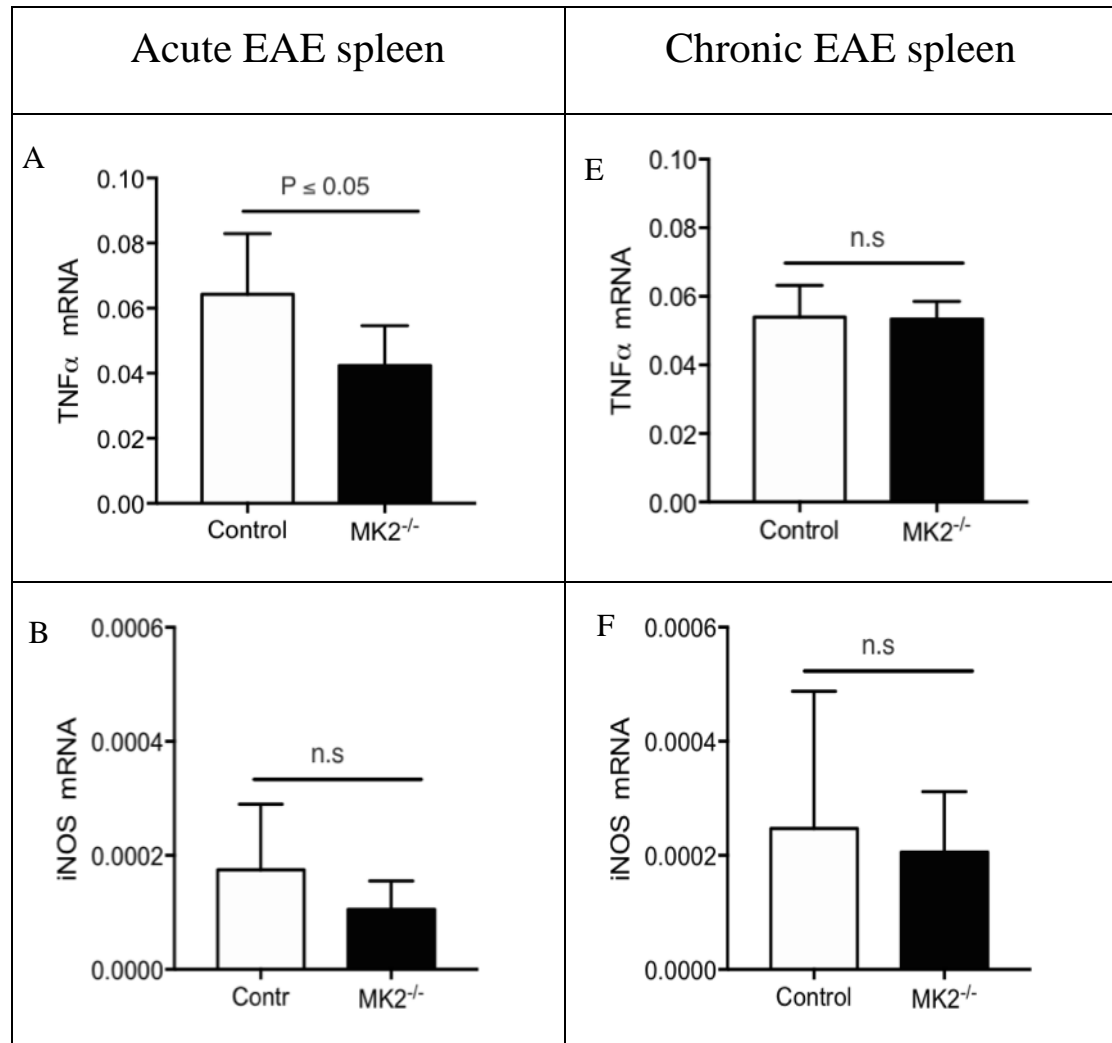


Figure 20: Gene expression of proinflammatory cytokine levels in the spinal cord of controls and MK2^{-/-} mice in acute (n=8) and chronic (n=5) EAE. Findings at the acute phase (A-E) and the chronic phase (F-J) are shown. Data are presented as mean ± SEM.

4.3.5 The cytokine expression in the spleen of MK2^{-/-} and wild type mice

Spleen from MK2^{-/-} and controls of acute and chronic EAE mice was isolated and used for RNA isolation. The cytokines IL-12, IL-6, IL-17 and TNF- α expression were measured. The levels of iNOS were also measured.

The proinflammatory cytokine TNF- α was significantly reduced in spleen of MK2^{-/-} on day 16 p.i. ($P = 0.0204$); (Figure 21A). IL-12 levels were not detectable in the spleen of MK2^{-/-} and control mice in the acute phase. In the chronic phase there were no significant changes in the cytokines detected in the spleen of control and MK2^{-/-} mice (Figure 21E-H); although there was a trend towards reduced levels of TNF- α ($P = 0.896$) and iNOS ($P = 0.734$) expression (Figure 21E, F).



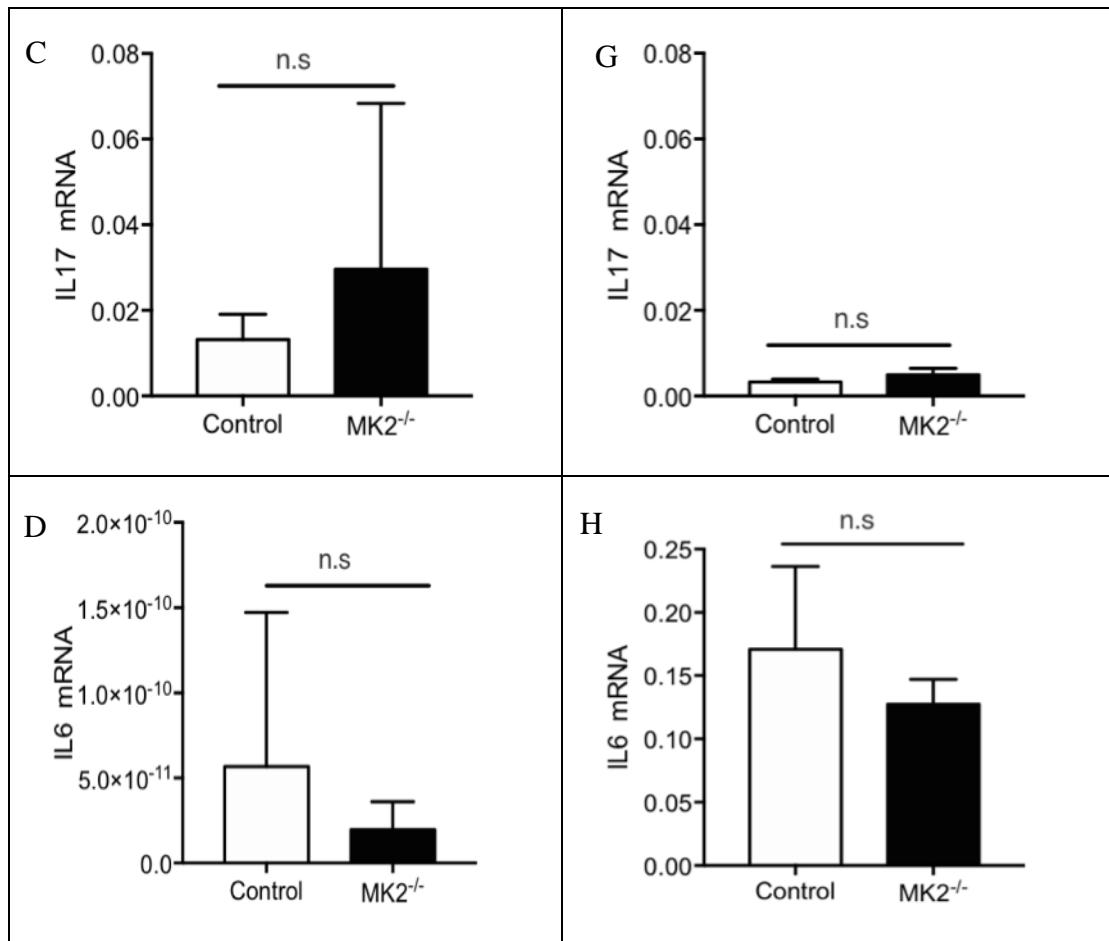


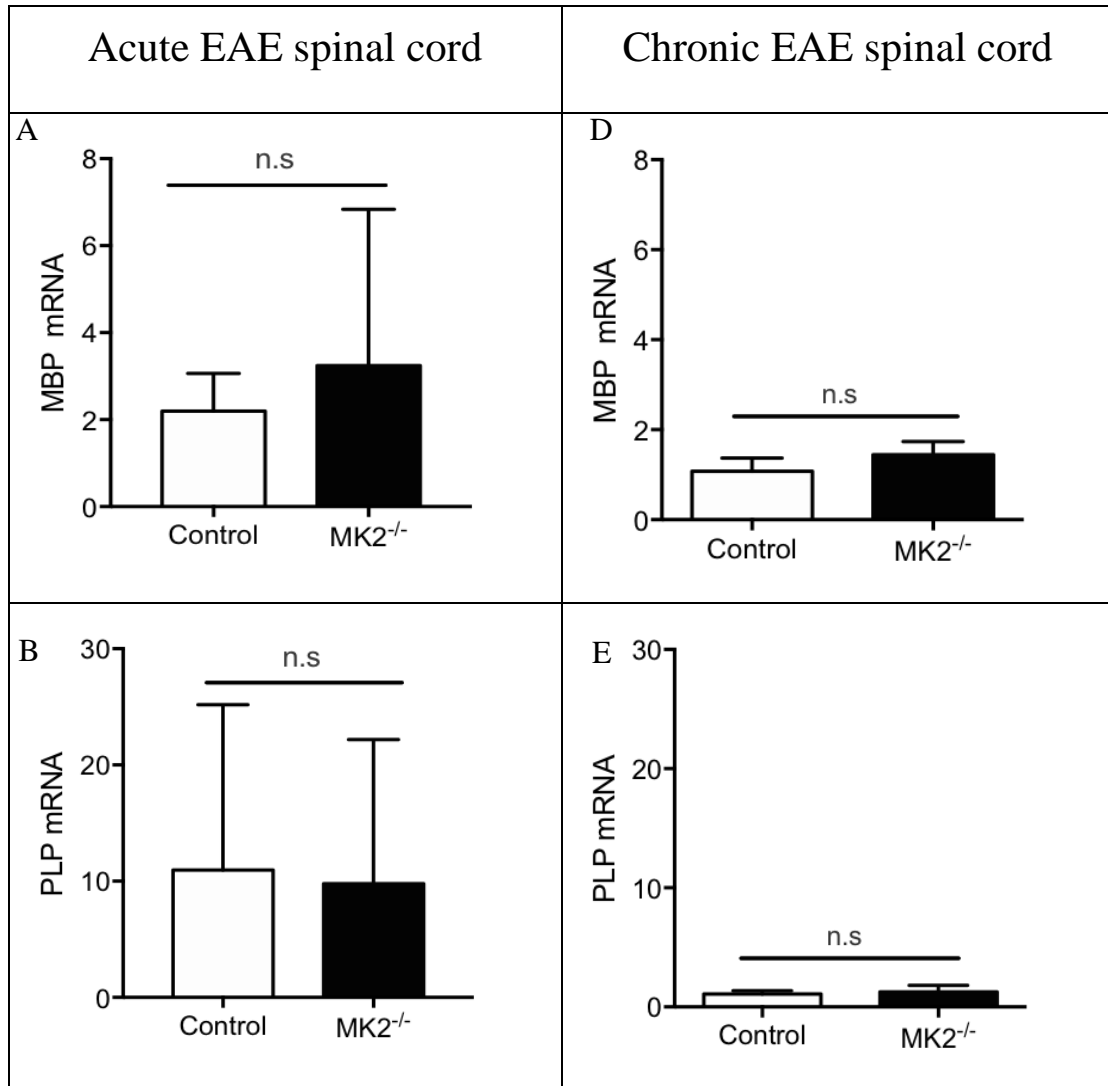
Figure 21: Gene expression of proinflammatory cytokine levels in the spleen of controls and MK2^{-/-} mice in acute ($n=8$) and chronic ($n=5$) EAE. Findings at the acute phase (A-D) and the chronic phase (E-H) are shown. Data are presented as mean \pm SEM.

4.3.6 Myelin protein expression in the spinal cord of MK2^{-/-} and wild type mice

To analyze the effect of MK2 deletion on myelin protein expression, we further studied the mRNA levels of MBP, PLP and CNPase in acute and chronic phase EAE. In the acute phase the mRNA levels of MBP, PLP and CNPase expression is not regulated in MK2^{-/-} mice compared to control (Figure 22A-C). Whereas CNPase expression in MK2^{-/-} mice was significantly increased in MOG induced chronic EAE spinal cord (day 60 p.i, $P = 0.0201$, Figure 22F), Myelin basic protein and PLP levels were not affected in chronic EAE spinal cord in protein (Figure 22B, C).

The levels of MBP were also analyzed in the spinal cord on protein level of both acute and chronic EAE. There were no significant differences seen in the acute and chronic EAE (Figure 23).

At tissue level the protein levels of MBP were analyzed by MBP staining in both acute (Figure 24A-C) and chronic phase (Figure 24D-F) of EAE. In the acute phase the difference in MBP levels were not significant ($P = 0.117$). In the chronic phase there was no change seen ($P = 0.204$) in the protein levels of myelin basic protein.



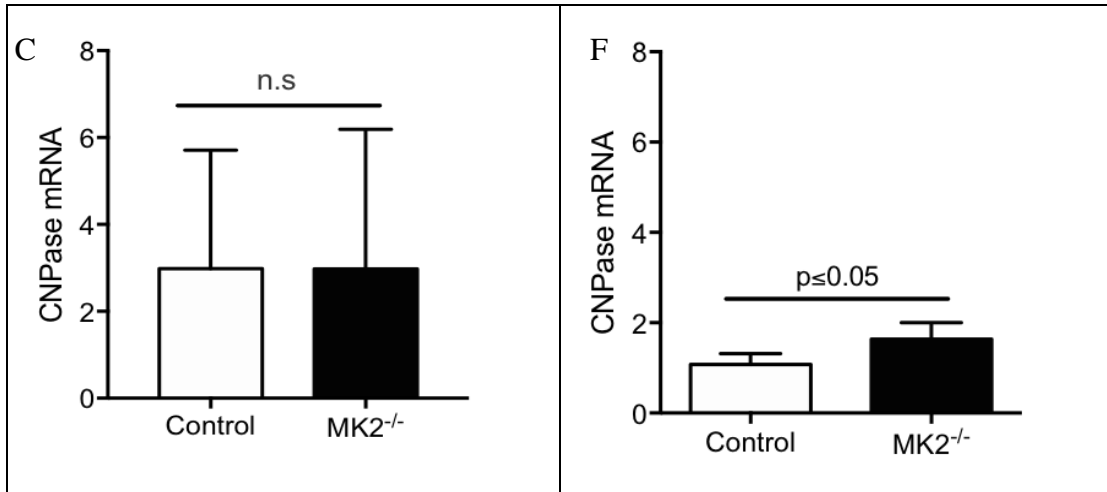


Figure 22: Gene expressions of the myelin proteins in the spinal cord of controls and MK2^{-/-} mice in acute (n=8) and chronic EAE (n=5). Findings at the acute phase (A-C) and the chronic phase (D-F) are shown. Data are presented as mean ± SEM.

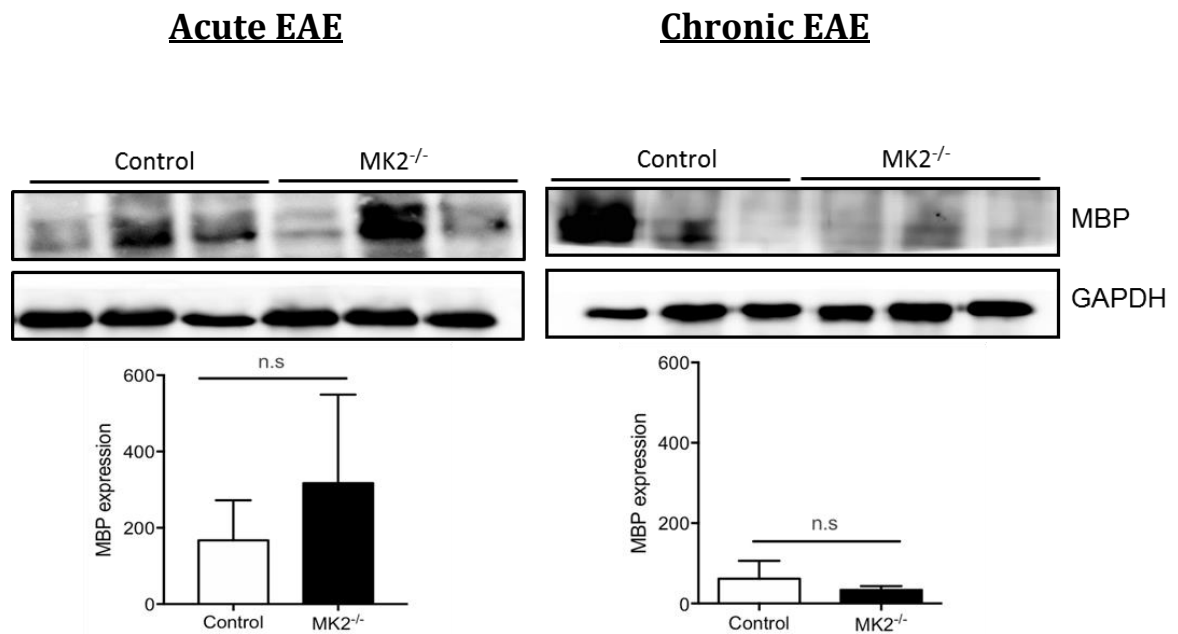


Figure 23: MBP expression in acute (n=8) and chronic (n=5) EAE mice spinal cord. GAPDH act as the internal loading control. Values are expressed as mean ± standard error of mean. n.s. = not significant.

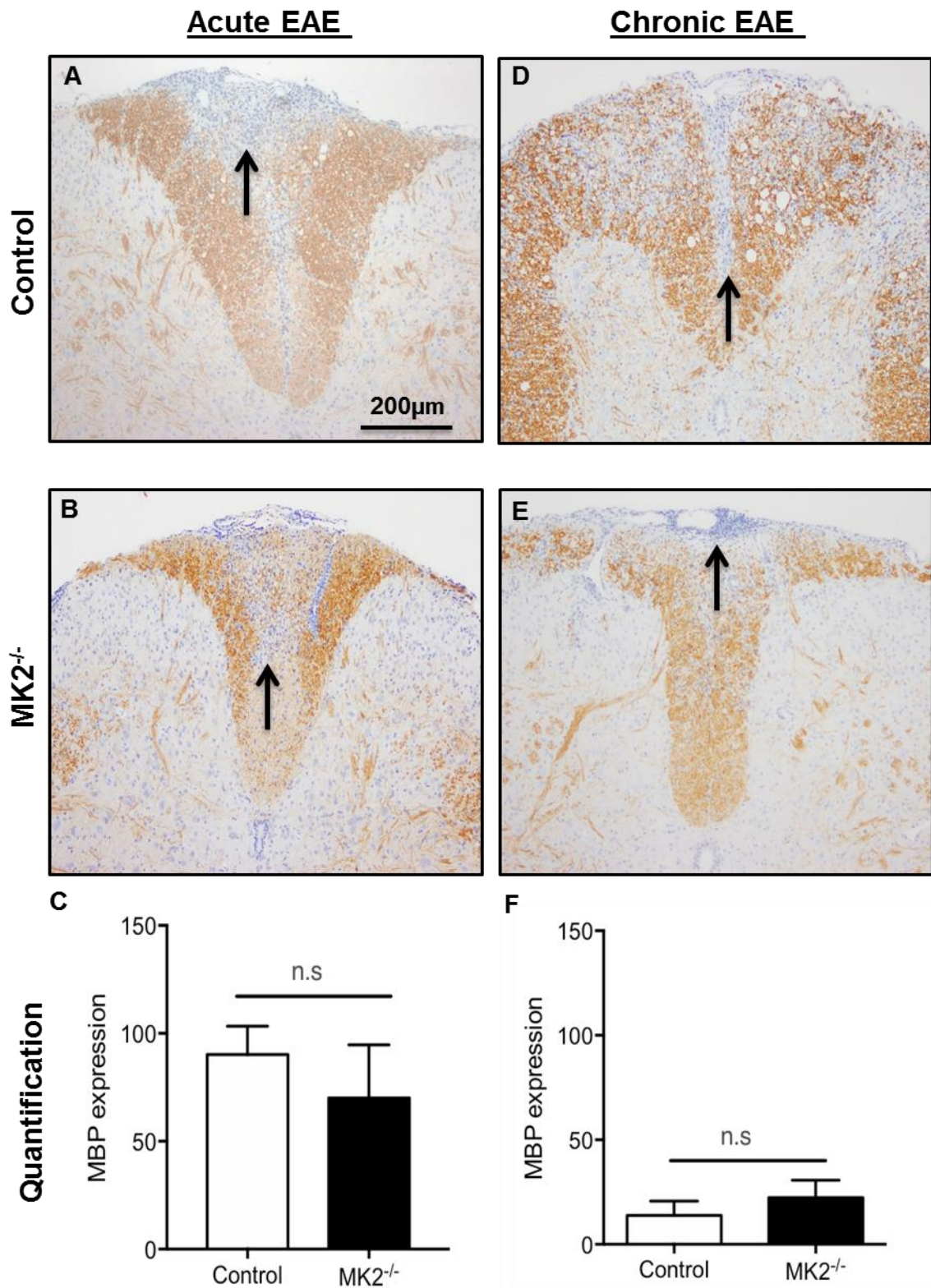
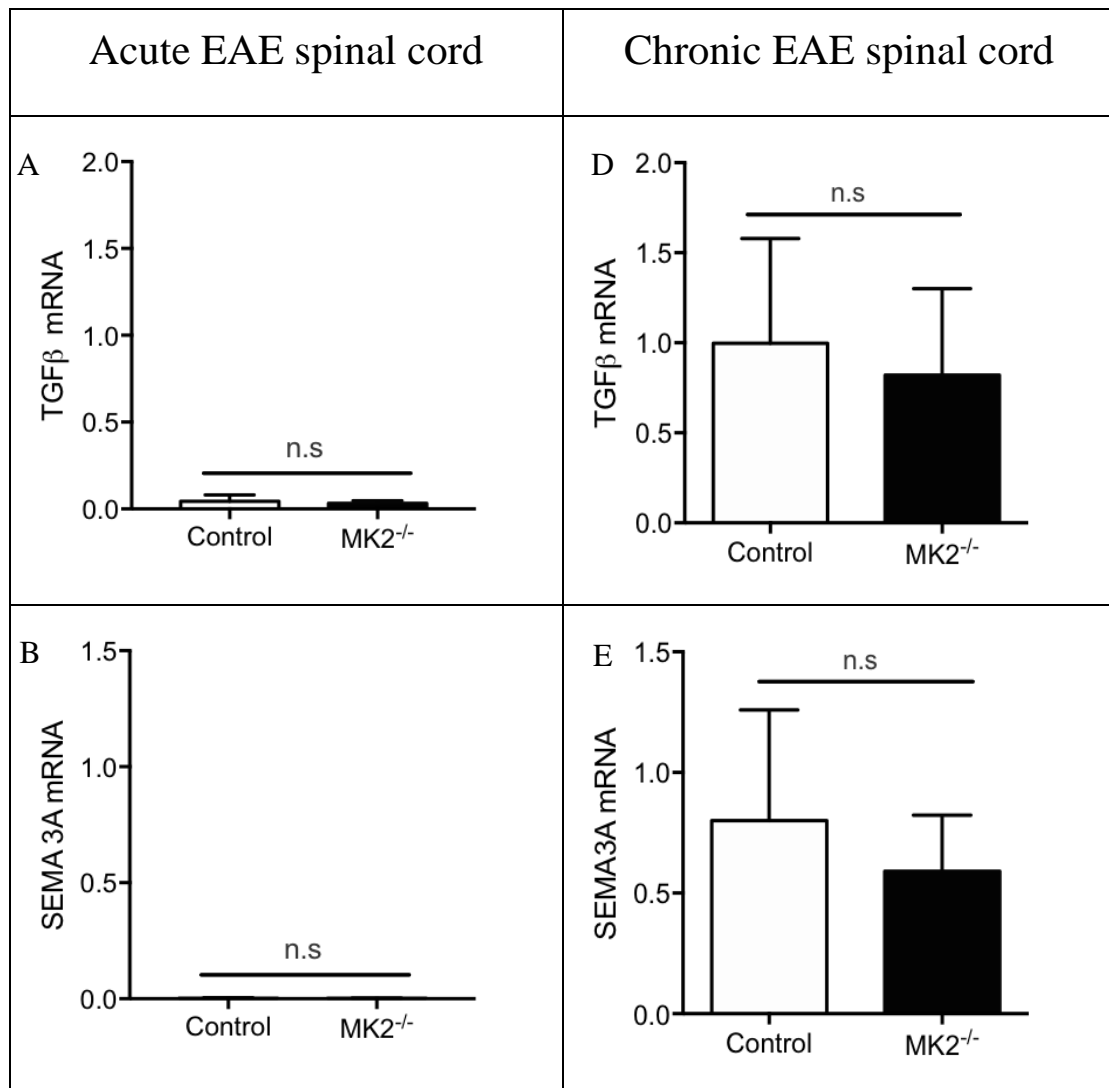


Figure 24: Histopathological analysis of acute (n=8) and chronic (n=5) EAE (MBP staining). MBP expression in the spinal cord sections of acute (A, B and C) and chronic (D, E and F) EAE in controls (A, D) and MK2^{-/-} mice (B, E). Representative images of spinal cord sections are shown. MBP expression (C and F) did not show significant differences between the two groups. Bar: 200 µm, Data are presented as mean ± SEM.

4.3.7 The remyelination markers were altered in MK2^{-/-} mice

To get a clear picture on all the myelination markers, we studied the inhibitors of remyelination in the spinal cord of acute and chronic phase EAE. The mRNA levels of TGF β , SEMA3A and LINGO-1 were not detectable in the acute phase of EAE in both control and MK2^{-/-} mice (Figure 25A-C). In the chronic phase, LINGO-1 was significantly increased in the MK2^{-/-} mice as compared to control mice ($P = 0.006$). There were no differences seen in the levels of TGF- β and SEMA-3A in MK2^{-/-} and control mice (Figure 25D, E).



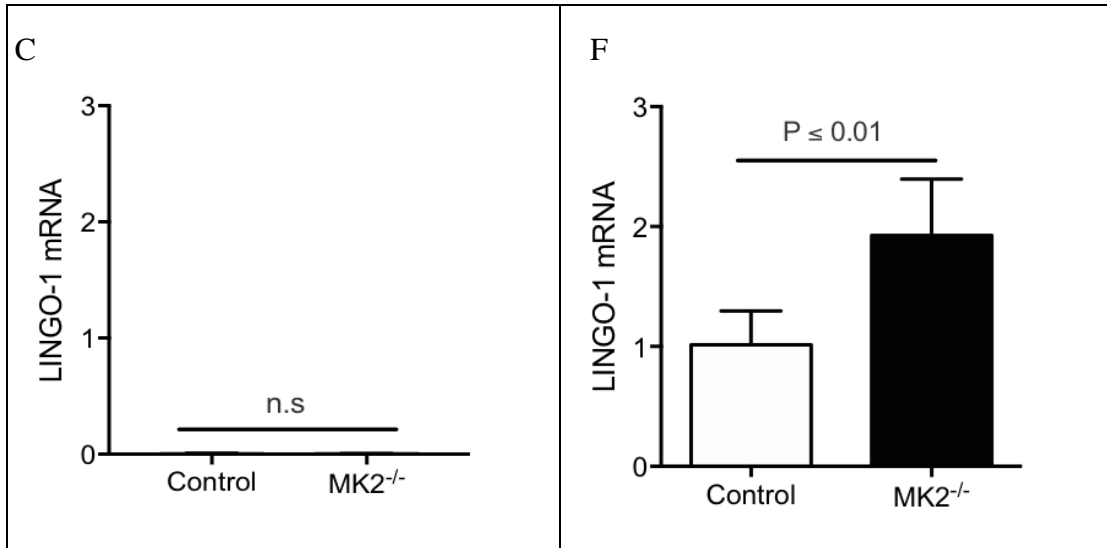


Figure 25: Gene expressions of the remyelination inhibitors *TGFβ*, *SEMA3A* and *Lingo-1* in the spinal cord of controls and *MK2^{-/-}* mice in acute (n=8) and chronic EAE (n=5). Findings in the acute phase (A-C) and the chronic phase (D-F) are shown. Data are presented as mean ± SEM

4.3.8 CREB phosphorylation was increased in the MK2^{-/-} mice

It was previously known that immature neurons of adult mice expressed phosphorylated CREB (Bender, Lauterborn, Gall, Cariaga, & Baram, 2001; Nakagawa et al., 2002). Recently activated CREB is reported to stimulate myelin basic protein (MBP) expression and to overcome inhibitors in myelin regeneration (Gao et al., 2004). CREB phosphorylation was analyzed at the protein level in spinal cord tissue of control and MK2^{-/-} mice. In the acute phase of EAE MK2^{-/-} mice showed increased levels of phosphorylated CREB ($P = 0.0224$) as compared to the control mice (Figure 26). There were no changes seen ($P = 0.0602$) in the levels of phosphorylated CREB in the chronic phase EAE (Figure 26).

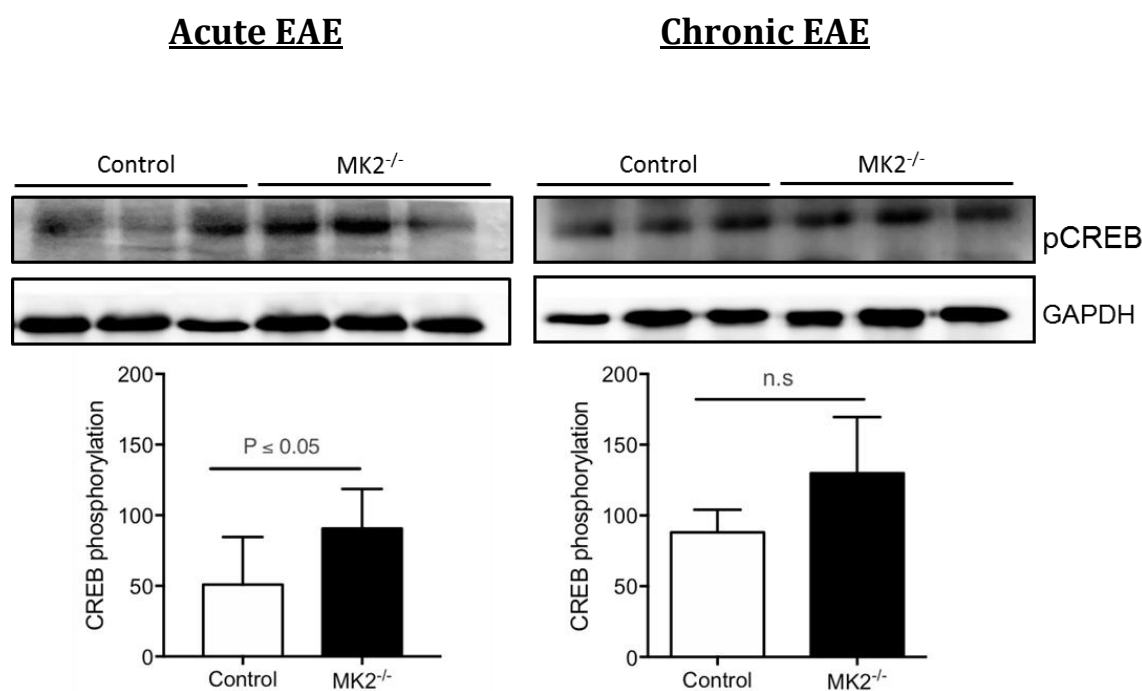


Figure 26: CREB phosphorylation in acute ($n=8$) and chronic ($n=5$) EAE mice spinal cord. GAPDH was used as the internal loading control. P values of * $P < 0.05$, ** $P < 0.005$, *** $P < 0.001$ were considered as significant. Values are expressed as mean \pm standard error of mean. n.s. = not significant.

4.3.9 NF- κ B phosphorylation is reduced in the MK2^{-/-} mice

NF- κ B pathway is known to be a proinflammatory signaling pathway. NF- κ B has a role in the expression of proinflammatory genes including cytokines and chemokines. Phosphorylation of NF- κ B was analyzed at protein level in acute and chronic EAE. In the acute phase, phosphorylated NF- κ B was significantly reduced ($P = 0.0463$) in the

MK2^{-/-} mice (Figure 27). There were no differences seen in the chronic phase for phosphorylated NF-κB (Figure 27).

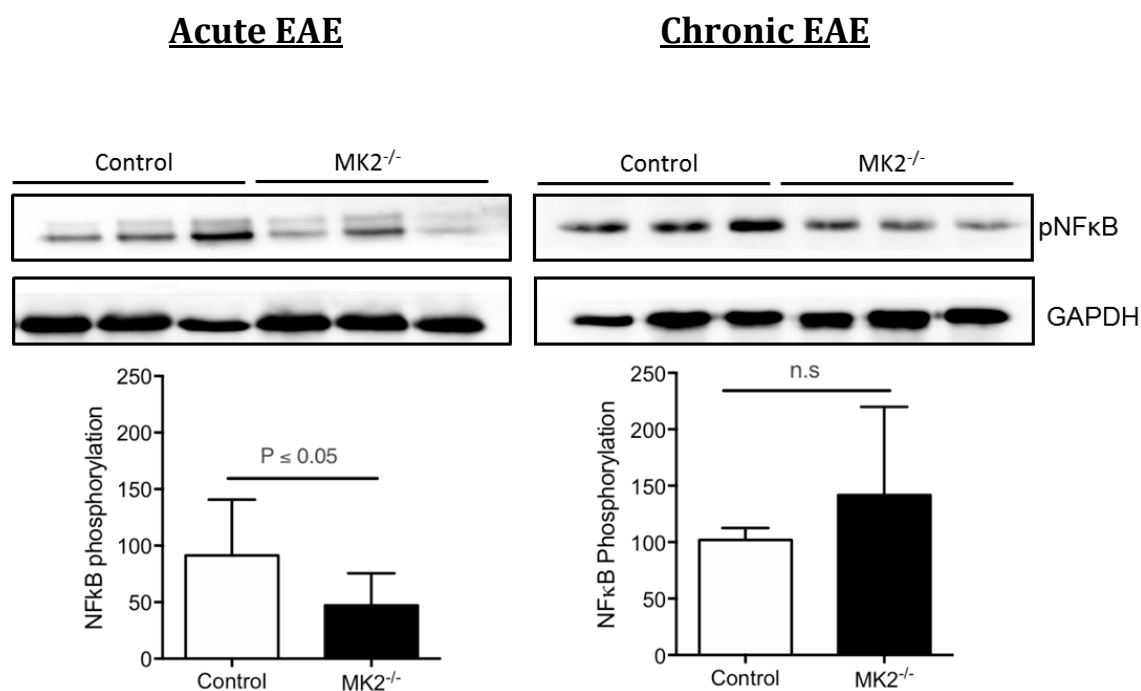


Figure 27: NF-κB phosphorylation in acute (n=8) and chronic (n=5) EAE mice spinal cord. GAPDH act as the internal loading control. P values of * P < 0.05, **P < 0.005, ***P < 0.001 were considered as significant. Values are expressed as mean ± standard error of mean. n.s. = not significant.

4.3.10 Levels of Akt and STAT-1 remained unchanged in the MK2^{-/-} mice

PI3K-Akt pathway is a signal transduction pathway that promotes survival and growth in response to extracellular signals. Spinal cord lysates from acute and chronic EAE were analyzed to see the levels of Akt and STAT-1. There were no differences seen in the levels of Akt phosphorylation and STAT-1 phosphorylation in acute phase (Figure 28 left panel).

In the chronic EAE the phosphorylation of Akt and STAT-1 showed no differences. The phosphorylation of STAT-1 was increased but not significantly (P = 0.096) (Figure 28).

Acute EAE

Chronic EAE

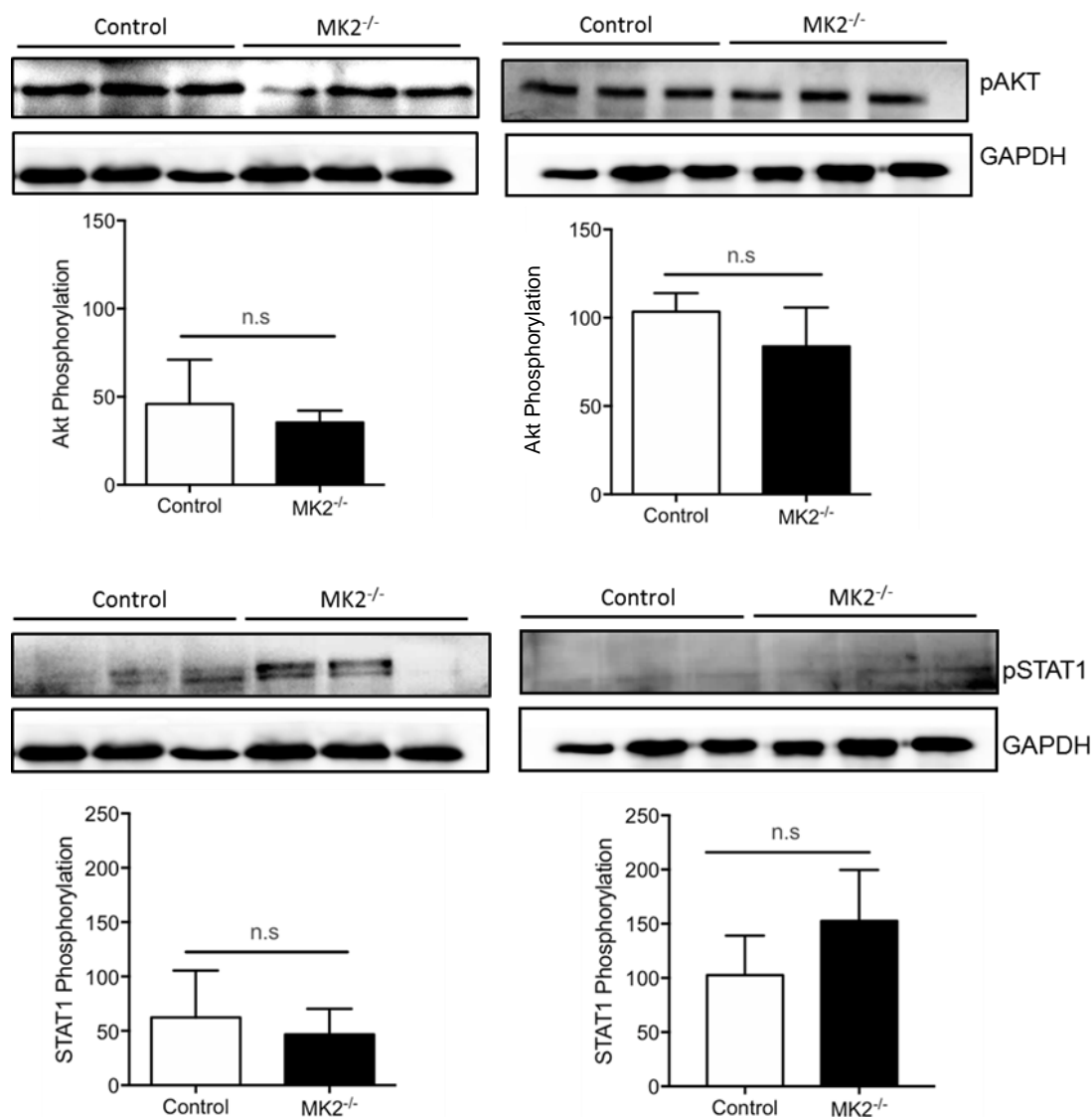


Figure 28: AKT and STAT1 phosphorylation in acute (n=8) and chronic (n=5) EAE mice spinal cord. GAPDH act as the internal loading control. P values of * $P < 0.05$, ** $P < 0.005$, *** $P < 0.001$ were considered as significant. Values are expressed as mean \pm standard error of mean. n.s. = not significant.

4.3.11 Analyzing the growth factor receptor Trk-B in MK2^{-/-} mice

To study the effect of MK2 ablation in mice, the receptor TrkB was studied at protein levels in the acute and chronic phase. In the acute phase TrkB receptor protein expression was similar between MK2^{-/-} mice and controls ($P = 0.950$). In the chronic phase TrkB receptor protein remained unchanged in MK2^{-/-} mice ($P = 0.112$) (Figure 29).

Acute EAE

Chronic EAE

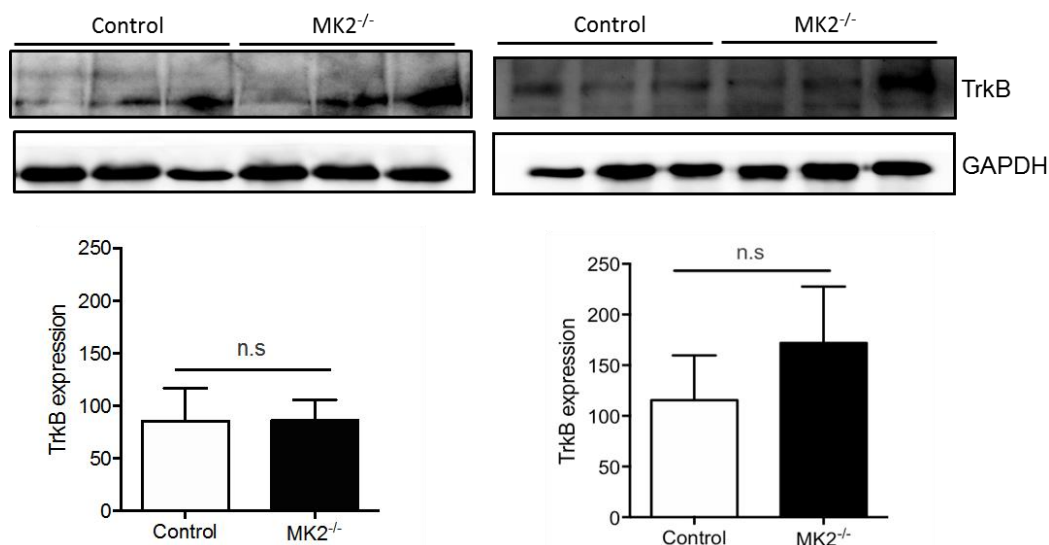


Figure 29: TrkB expression in acute (n=8) and chronic (n=5) EAE mice spinal cord. GAPDH act as the internal loading control. P values of * $P < 0.05$, ** $P < 0.005$, *** $P < 0.001$ were considered as significant. Values are expressed as mean \pm standard error of mean. n.s. = not significant.

4.4 In vitro experiments

4.4.1 MK2 is required for glatiramer acetate mediated C17.2 neuronal cell survival/proliferation

We hypothesized that MK2 the downstream regulator of p38 can be the potential interaction partner of GA involved in neuronal cell survival and proliferation.

C17.2 mouse neuronal cells and p38 inhibitor SB203580 were used in this study. MK2 gene was knocked down by siRNA transfection using FlexiTube siRNA Mm_MK2 (0.3 μ M) and VIROMER BLUE. Cells were incubated with SB203580 (2 μ g/ml) and stimulated with TNF- α (10 ng/ml) and/or GA (10 ng/ml). The MK2/TNF- α signaling molecules Akt/STAT3 were analyzed by western blot. Cell proliferation was analyzed for the same treatments using the WST assay.

MK2 knock down in C17.2 cells resulted in a down-regulation of Akt phosphorylation and there was no difference on STAT3 phosphorylation. The phosphorylation of Akt was increased by GA treatment alone, while there was no effect on STAT3 (Figure 30). The combined treatments of MK2 knock down and GA decreased the phosphorylation of Akt and STAT3. Cell proliferation of C17.2 was reduced by p38 inhibition while

GA treatment alone did not induce a difference in the proliferation of the cells (Figure 31).

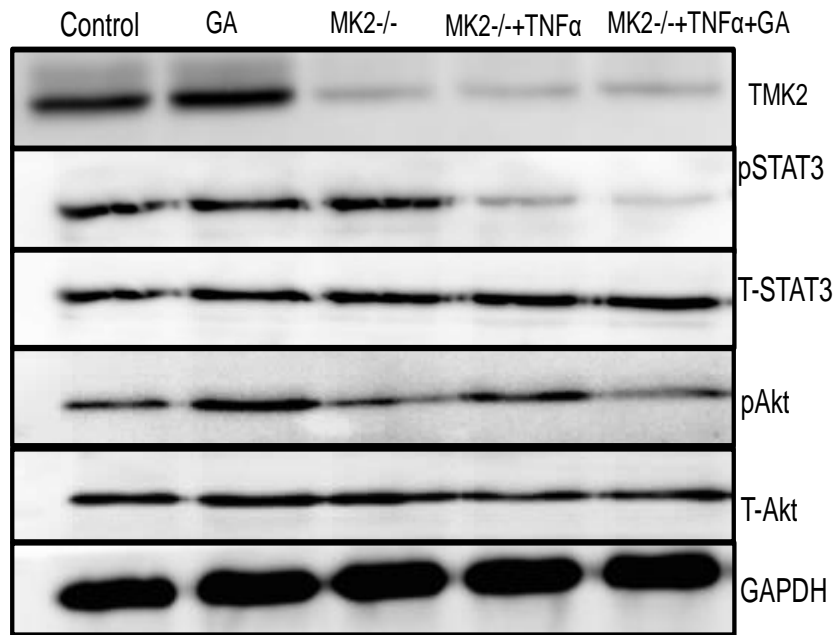


Figure 30: Akt phosphorylation decreases after MK2 inhibition. PSTAT3 is down regulated after GA treatment in MK2 knockdown C17.2 cells.

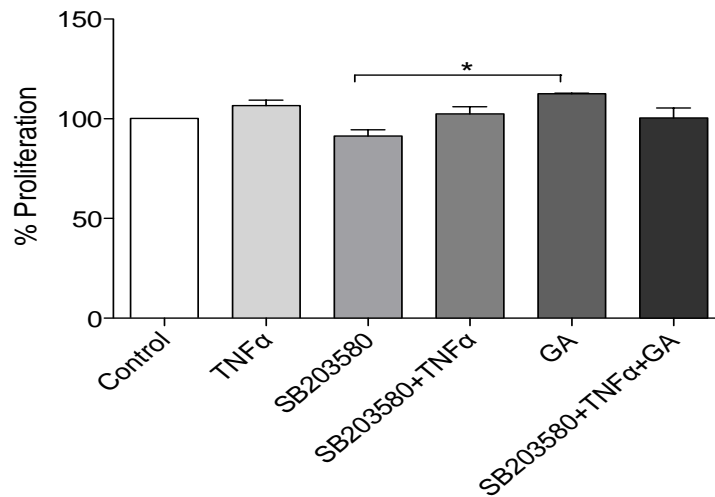


Figure 31: WST proliferation assay shows decreased proliferation after P38 inhibition as compared to Glatiramer acetate treatment.

5 DISCUSSION

In the present study the *in vivo* function of MK2 was characterized using a complete gene knockout in mice. Knowing that MK2 is essential for TNF- α biosynthesis we hypothesized that knocking out MK2 will lead to a milder disease course. We found that MK2 does not affect the disease course of EAE.

The pathological analysis of acute EAE showed decreased macrophage infiltration, myelin and axon degeneration in MK2^{-/-} mice. There were few differences seen in chronic EAE such as an increase of the inhibitor of remyelination Lingo-1 and an increase in the levels of CNPase mRNA levels.

5.1 MK2 knockout mice have a normal phenotype

The p38 MAPK pathway is known to be activated by heat shock, ultraviolet light, bacterial lipopolysaccharide (LPS) or pro-inflammatory cytokines like TNF- α or IL-1 β (Freshney et al., 1994; Han et al., 1994; Rouse et al., 1994). After the failure of p38 MAPK inhibitors in clinical trials, MK2 was unveiled as a potential target to regulate inflammatory cytokines mRNA stability and translation. It is possible to determine the physiological function of MK2 *in vivo* by introducing a targeted mutation into the mouse MK2 gene. MK2^{-/-} mice show increased stress resistance and survive LPS-induced endotoxic shock (Kotlyarov et al., 1999). MK2^{-/-} mice grew to normal size, were fertile and did not display any noticeable behavioral changes as compared to its C57BL/6J background control mice.

Mitogen-activated protein kinase (MAPK)-activated protein kinase 2 (MAPKAPK-2 or MK2) is a downstream substrate of the p38 MAPK responsible for the signaling pathways for inflammation, apoptosis and cell motility. In addition, MK2 is a prominent kinase that phosphorylates heat shock protein 27 (Hsp27), an intensively investigated biomarker of cancer progression (Gurgis, Ziaziaris & Munoz, 2014). In experimental asthma, MK2 knockout mice showed less airway inflammation because of reduced vascular permeability of the blood-lung-barrier (Gorska et al., 2007).

In the MPTP mouse model for Parkinson's disease, MK2-deficient mice show reduced neuroinflammation and less degeneration of dopaminergic neurons in the substantia nigra; particularly by reducing the production of the neurotoxic substances like TNF- α

and nitric oxide (Thomas et al., 2008). MK2- deficient mice exhibited a better Rotarod performance as compared with WT mice. The development of typical Parkinson's disease symptoms like tremor, slow movement, stiffness and poor balance were reduced in MK2- deficient mice.

In the KA-induced animal model of seizure disorder, the role of MK2 was investigated. After injection of KA, a reduced degeneration of neurons in the hippocampus of MK2 deficient mice was found when compared with wild type mice. As the role of MK2 in inflammation is well known, the observed neuroprotection was a secondary effect due to diminished inflammation in MK2-deficient mice (Thomas, Hitti et al., 2008).

5.2 EAE in MK2^{-/-} mice

MK2^{-/-} and C57BL/6J mice were analyzed for EAE symptoms. There was one chronic phase EAE study done till day 59 and then three acute phase EAE studies till day 16.

The first EAE study to be analyzed was conducted till day 59. There were no significant differences seen in the disease course between control and MK2^{-/-} mice. Next we analyzed the first acute EAE experiment. Here a significant difference was seen in the disease course between control and MK2^{-/-} mice from days 14-16 ($P \leq 0.001$). The second acute EAE study showed a significantly different disease course from days 12-16 ($P \leq 0.01$). The last acute EAE study, however, showed no significant difference between the disease course of control and MK2^{-/-} mice. The onset of clinical symptoms for all the EAE experiments was on similar days.

It is also known that there are many factors responsible for the variability in the EAE disease course. Some of the causes known for the variability between experiments are: Sex and age related differences, variability caused by environment and seasons, early weaning increase susceptibility to disease (Papenfuss et al., 2004; Teuscher et al., 2004); whereas gentling decreased susceptibility (Laban et al., 1995). In addition, sound stress increased disease susceptibility (Laban et al., 1994).

Sex and age does not matter in our case as all female mice were used, they were all aged between 10-12 weeks, and these were kept in a stable environment.

5.3 Decreased inflammation and infiltration of immune cells

In the acute phase of EAE, the impaired MK2 signaling led to reduced inflammation. Inflammatory infiltrates were present as both aggregated and in a more diffused form. In the acute phase, lymphocytes aggregated around the blood vessels in the spinal cord white matter in a typical sleeve-shape. Lymphocyte infiltration could still be seen during the chronic phase, but this was reduced to some extent compared with that at the acute stage. H&E staining also revealed that the normal brain and spinal cord structures were well preserved. There has been a study done with TNF KO mice, which exhibited a delayed disease induction. It was revealed by H&E staining of spinal cord sections that there was impaired accumulation of inflammatory cells in the CNS, which was the reason behind delayed disease onset. The CNS infiltrates isolated from TNF KO mice at this time point contained lower numbers of both CD4⁺ T cells and CD11b⁺ myeloid cells, compared with their WT counterparts (Kruglov, Lampropoulou, Fillatreau, & Nedospasov, 2011).

In the acute phase of EAE there was a marked reduction in the infiltration of macrophages in the spinal cord sections of MK2^{-/-} mice as compared to control mice. There were no significant changes observed in the chronic phase of EAE. In TNF KO mice the distribution of myeloid cells within the CNS had no apparent effect on the localization of inflammatory macrophages (Mac-3⁺ cells) in CNS tissue during EAE. These data altogether indicated that TNF- α is required for initial recruitment of inflammatory cells into the CNS and TNF- α does not affect the localization of cells later in the disease progression (Kruglov et al., 2011). According to Gold et al. 2006 macrophages is the dominant effector cell population in the acute phase of EAE. Activated macrophages produce a large number of detrimental soluble factors, which can induce functional blockade and/or structural damage. Few of these include nitric oxide, which is mostly in combination with reactive oxygen species (Redford et al., 1997). There was another study done by Nikic et al (2011) and they observed that this macrophage mediated reactive oxygen and nitrogen species (ROS and RNS) initiated axonal degeneration. Then a reduction in the degeneration of axons was noticed when these reactive oxygen and nitrogen species were neutralized. Other studies revealed a beneficial role of the presence of alternatively expressed macrophages, this lead to

reduced EAE severity. Comparative studies done by Berger et al., (1997) demonstrate that the major neuropathological symptoms and disease severity was correlated to the absolute number of activated macrophages recruited into the CNS parenchyma.

In animals actively immunized with MOG, there is a sequence of pathogenic T-cell and antibody-dependent effector mechanisms. As analyzed by immunohistochemistry done on spinal cord sections, there were no significant differences between T-cell infiltration between the two groups of MK2^{-/-} mice and control mice. Although, there was a marked reduction in T-cell infiltration between acute phase and chronic phase of EAE in control mice. MOG induced EAE, where MOG is a unique myelin autoantigen as it induces not only an encephalitogenic T-cell response but also a demyelinating response. Demyelinating anti-MOG antibodies reinforce disease severity and initiate wide-ranged demyelination in T-cell-mediated brain inflammation in models of EAE (Genain et al., 1995; Linington et al., 1988; Schluesener & Weiner, 1987).

B-cell infiltration was analyzed in MK2^{-/-} and control mice. B cells play an important role in antibody production, modulating immune response through the production of cytokines (Barr et al., 2012; Matsushita et al., 2008) and presentation of antigen to T cells (Chen & Jensen, 2008). The resulting “cognate” interactions between T and B cells specific for the same or physically linked antigen are fundamental to the development of most complex immune responses (Phan, Gray & Cyster, 2009; Ramiscal & Vinuesa, 2013). After the analysis no significant differences were seen in the B-cell infiltration of MK2^{-/-} and control mice.

5.4 Myelination and axonal density

Myelin-specific CD4⁺ T cells are the major components of the autoimmune response in EAE. These cells initiate a series of neuroinflammatory events leading to infiltrating immune cells (Domingues, Portugal, Socodato, & Relvas, 2016). This results in an attack on myelin-producing oligodendrocytes, which ultimately leads to demyelination followed by axonal damage (Bauer et al., 2009; Nicol et al., 2015). It is also known that when TNF- α was knocked out from the mice resulted in prolonged confinement of activated T cells in the secondary lymphoid organs, leading to severe disease symptoms (Kassiotis & Kollias, 2001).

Further analysis of myelin proteins revealed reduced demyelination by LFB-PAS staining in MK2^{-/-} mice in both acute and chronic phase. The results were pointing towards a reduction of total myelin proteins in MK2^{-/-} mice in both acute and chronic EAE. It has been earlier reported that in the CNS of MOG-induced EAE-rodents there is widespread demyelination (Storch et al., 1998) along with MOG-reactive T-cells (Iglesias et al., 2001). In mice lacking TNF- α only in T cells, EAE was induced and milder disease severity was seen in comparison to WT animals. Decreased demyelination was visualized by Luxol fast blue staining of spinal cord sections correlated with milder disease severity in T-TNF KO mice compared with WT animals (Kruglov et al., 2011). In TNF- α KO mice there was an overall delay in the onset of the disease but later the disease was severe and associated with widespread perivascular inflammation in the CNS, but primary demyelination appeared to be reduced overall (Körner et al., 1997).

Bielschowsky silver impregnation for axons revealed a huge loss of axons in the demyelinated areas, but axons were preserved in the myelinated areas. Since demyelination further leads to axonal damage, this resulted in almost identical lesions. It has been known before that in rodents with MOG-induced EAE, axonal damage is not only present in the active lesions of white matter, but also in the normal white and grey matter (Herrero-Herranz, Pardo, Gold & Linker, 2008; Kornek et al., 2000).

It has been reported that high prevalence of axonal damage in the CNS of EAE-rodents appears to involve direct damage induced by cytotoxic T-cells and myelin autoantibodies (Lassmann, 2010).

5.5 Cytokine levels

Cytokines are secreted signaling proteins that play an important role in regulating immune responses in EAE. Cytokines provide cell signals both in the immune system and CNS compartment, but interestingly, some have detrimental effects in the immune system while having beneficial effects in the CNS compartment. Cytokines were detected in spinal cord mRNA and spleen mRNA with the help of real-time PCR. There were no differences detected in the levels of TNF- α , iNOS, IL-17, IL-6 or IL-1b. The levels of TNF- α , IL-6, IL-1b were almost non-detectable in the acute phase of EAE,

while this was not true for the chronic phase of EAE. There have been other EAE studies, which show non-detectable levels of cytokines after induction. Recent studies where cytokine expression in antigen presenting cells in the CNS of mice with severe EAE was investigated by Wlodarczyk et al (2014). They had CD45^{high} CD11c⁺ cells express higher level of IL-1 β , IL-6 and IL-23. Whereas, in contrast to CD11c⁻ microglia, the expression of IL-6 and IL-23 in CD11c⁺ microglia was undetectable.

However, the levels of iNOS reduced dramatically between the acute and chronic phase of EAE. It has been reported that IL-17 may work in cooperation with other proinflammatory cytokines, such as IL1 and TNF- α , to activate iNOS transcription by astrocytes (Trajkovic et al., 2001). There have been other reports suggesting that IL1-induced astrocyte activation causes NO production and contributes to neuronal damage (Colombo et al., 2012).

There was an increase in the levels of IL-1 β in MK2^{-/-} mice when compared between the acute phase and chronic phase of EAE. IL-1 β is a protein produced by activated macrophages to mediate series of effects that range from proliferation to apoptosis. Due to this variant signaling, IL-1 β plays multiple pathogenic roles in EAE. The importance of IL-1 β is highlighted by the significant reduction in disease severity during EAE in IL-1 β receptor KO mice (Sutton, Brereton, Keogh, Mills, & Lavelle, 2006).

In spleen mRNA cytokines were also checked using RT-PCR. There was a significant reduction in the level of TNF- α in the acute phase of EAE, while the levels were almost similar in chronic EAE. TNF- α is a transmembrane or a soluble protein that can signal as a homotrimer while it is membrane bound (tmTNF- α) or in a soluble form once it is proteolytically cleaved by metalloprotease TNF- α converting enzyme (Beutler & Cerami, 1989). Activated macrophages and T cells are a major source of TNF- α , also several other cell types, including brain resident cells, are capable of producing it as well. TNF- α signaling mediates cell death through activating one or more of the three classic pathways: nuclear factor NF- κ B, mitogen activated protein kinase (MAPK) and caspases (Aggarwal et al., 2005; Darnay & Aggarwal, 1997). Other cytokines like iNOS, IL-17, IL-6 showed no significant changes. IL-12 was not detected in the spleen samples.

5.6 NF- κ B protein level

When talking about inflammation, key molecules also include transcription factors such as NF- κ B, apart from the inflammatory cytokines discussed above such as IL-1 β , IL-6 and TNF- α (Karin, 2006; Langowski et al., 2006; Voronov et al., 2003; Yu, Pardoll, & Jove, 2009). IL-1, IL-6, TNF- α and the related receptor activator of NF- κ B ligand (RANKL) have long been known to affect multiple steps in the dissemination and inflammation cascade (Giavazzi et al., 1990; Luo et al., 2007; Mantovani, Allavena, Sica, & Balkwill, 2008). Recent reports have indicated that pathways leading to NF- κ B activation and NO production in astrocytes contribute to MS pathology (Colombo et al., 2012; Colombo & Farina, 2012; Farina, Aloisi, & Meinl, 2007).

Protein levels in the spinal cord lysates showed significant reduction in the expression of NF- κ B protein in the acute phase of EAE. There were no differences seen in the chronic phase of EAE between control and MK2^{-/-} mice. In both cellular contexts, NF- κ B operates downstream after sensing of microbes or tissue damage by the toll-like receptor (TLR)-MyD88 pathway, the inflammatory cytokines TNF- α and IL-1 β and downstream of tissue damage that results in release of alarm signals. NF- κ B induces the expression of inflammatory cytokines, adhesion molecules, key enzymes in the prostaglandin synthase pathway, like (COX2) and nitric oxide (NO) synthase.

It has been shown in several disease models that the NF- κ B pathway plays a role in astrocytes by sustaining scar formation, neuroinflammation and neurodegeneration (Brambilla et al., 2009; Raasch et al., 2011); thus, its blockade is beneficial and limits tissue damage. Similar in the lines we have reports which say that astrocyte-restricted ablation of IL-17 signaling impairs NF- κ B activation and ameliorates EAE (Kang et al., 2010).

5.7 Phosphorylation of CREB

Oligodendrocytes (OLGs) are a major cellular component of white matter, which are the myelin-forming cells in the brain. There are increased levels of cyclic adenosine monophosphate (cAMP) response element binding protein (CREB) in developing oligodendrocytes (C. Sato-Bigbee, Chan, & Yu, 1994). Previous experiments, which imply inhibition of CREB synthesis, have indicated that CREB is one of the mediators

of cAMP-dependent stimulation of OLG differentiation (Carmen Sato-Bigbee & DeVries, 1996).

The activation of CREB has been associated with signaling proteins such as MAPKs (Shin et al., 2003) as well as pro-inflammatory cytokines, including IFN- γ and TNF- α (Renno et al., 1994; Tanuma et al., 1997). CREB is a potential *in vivo* substrate for the MAPK pathway. In EAE lesions phosphorylation of CREB occurs in the inflammatory cells, astrocytes and neurons; this corresponds to the increased phosphorylation of MAPKs (Shin et al., 2003). Increased phosphorylation of CREB occurs in the spinal cord in the peak stage of EAE and contributes to the activation of inflammatory cells such as macrophages. This partially works in the generation of neuropathic pain during the course of rat EAE and possibly in human multiple sclerosis (Kim et al., 2007).

In our study spinal cord lysates showed significantly increased levels of CREB phosphorylation in MK2^{-/-} mice in the acute phase of EAE. There were no significant differences seen in the chronic phase of EAE suggesting that MK2^{-/-} played a role in CREB phosphorylation only in the early stages of the disease. Many reports suggest the role of cAMP in the maturation of oligodendrocytes, in the expression of myelin basic protein (MBP), P2, P0, proteolipid protein (PLP) and myelin-associated glycoprotein (MAG) (Anderson & Miskimins, 1994; Bharucha et al., 1993; Jensen et al., 1993). As noticed in the analyses the level of MBP also indicate a pattern towards increased levels in the acute phase of EAE. There are results in the similar pattern with histological data where the amount of demyelination indicated by LFB-PAS was significantly reduced in the acute phase of MK2^{-/-} mice. Further we will discuss the increase in myelin basic protein mRNA. Nevertheless is it now known that CREB is an important mediator of myelination and cell process outgrowth in OLGs (Carmen Sato-Bigbee & DeVries, 1996; Wegner, 2000).

5.8 Regulation of myelin proteins and inhibitors of remyelination

The myelin sheath is a major element of the white matter of the CNS, facilitating signal conduction in axons being its main function. Myelin has a unique molecular architecture and is highly specialized. It has a higher proportion of lipids (70-85%) as compared to the protein proportion (15-30%) (Morell P, 1999). It contains an array of

proteins such as proteolipid protein (PLP), myelin basic protein (MBP), 2',3'-cyclic nucleotide 3'-phosphodiesterase (CNPase), myelin-associated glycoprotein (MAG) and myelin oligodendrocyte glycoprotein (MOG). PLP and MBP constitute the majority of the total myelin proteins of about 70% (Baumann & Pham-Dinh, 2001, Morell P, 1999). CNPase is a specific enzyme localized in the cytoplasm of non-compacted myelin. We analyzed the mRNA levels of MBP, PLP and CNPase by RT-PCR. There was a trend towards increased levels of MBP mRNA in both acute and chronic phase of EAE of MK2^{-/-} mice, but not significant. Furthermore, we analyzed expression of 2',3'-cyclic nucleotide-3'-phosphohydrolase (CNPase), an enzyme specifically expressed in myelin and located in oligodendrocyte (Sospedra & Martin, 2005). The protein exists in two splice variants and constitutes 3-4% of total myelin protein. The levels of CNPase mRNA were significantly increased in the MK2^{-/-} mice of chronic phase of EAE. The significant increase in the CNPase levels in the chronic phase cannot be associated to be beneficial for the MK2^{-/-} mice.

Myelin sheath plays an indispensable role in signal conduction. Repeated loss of myelin may cause axonal injury that eventually leads to progressive functional deficits. Remyelination is the process where new myelin sheaths are created on demyelinated axons.

A molecule that correlates with the extent of oligodendrocyte maturation and myelination is Lingo-1, a transmembrane protein containing leucine-rich repeats expressed in neurons and oligodendrocytes (Carim-Todd et al., 2003). It is generally believed that Lingo-1 negatively regulates oligodendrocyte differentiation and myelination in vivo (Mi et al., 2005) and in vitro (Mi et al., 2007). The expression of Lingo-1 has been shown to increase diseases of CNS, such as spinal cord injury and MS (Mi et al., 2004); the overexpression of Lingo-1 also inhibits myelin formation (Bradl & Lassmann, 2010). Deletion of Lingo-1 exhibit increased remyelination, functional recovery from EAE and even low EAE scores (Mi et al., 2007). In our study Lingo-1 was significantly increased in MK2^{-/-} mice in the chronic phase of EAE. There were no differences seen in the acute phase of EAE though, if compared the expression of Lingo-1 increased by almost 2-folds from the acute phase to the chronic phase EAE in MK2^{-/-} mice. This increase in the expression of Lingo-1 can be associated to have a

deteriorating effect on the chronic phase of EAE.

5.9 Role of MK2 in glatiramer acetate mediated C17.2 neuronal cell proliferation/survival

The mechanisms involved in glatiramer acetate (GA) treatment in multiple sclerosis are not completely understood. Recent work suggested that the proliferation of monocytes is controlled by GA activating Akt and MEK/ERK pathways which are involved in cell proliferation and survival (Carpintero et al., 2010). GA elevates the proliferation of neural precursor cells (NPC) (Aharoni, 2014). Recent studies have shown that MK2 is crucial for STAT3 activation in response to LPS (Ehltting et al., 2011). STAT3 is activated by a wide variety of cytokines or growth factors, it translocates to the nucleus and regulates proliferation (Simeone-Penney et al., 2008).

The findings of this study suggest that proliferation/survival of C17.2 is mediated by the MK2 associated with decreased STAT3/Akt activation. GA treatment has no effect on pSTAT3 so there is no proliferative effect. The combined treatment of MK2^{-/-} and GA results in reduced STAT3/Akt activation which shows that MK2 is crucial for cell survival/proliferation. These data suggest that MK2 is required to mediate glatiramer acetate cell survival/proliferative effect.

6 Summary

Experimental allergic encephalomyelitis (EAE) is an antigen-driven inflammatory disease of the central nervous system (CNS), which has many pathological features in common with multiple sclerosis. Multiple sclerosis (MS) is an autoimmune, T-cell mediated inflammatory and degenerative disease.

Immunological processes play a major role in contributing to the initiation and continuation of the disease. Cytokines are secreted proteins, their role as important regulatory elements in the immune responses has been well established in EAE. TNF- α is found at high levels in cerebral spinal fluid (CSF) and active lesions of MS patients, which makes it a critical cytokine. MK2 signaling is known to be crucial for the biosynthesis of cytokines like TNF- α and IL-6, hence influencing the inflammatory responses. Yet, the role of MK2 signaling in MS and EAE is poorly understood. Hypothesizing that MOG₃₅₋₅₅EAE will cause milder symptoms in MK2 depleted mice, we performed EAE studies with MK2^{-/-} mice. No phenotypic changes were observed in MK2^{-/-} mice. The MK2^{-/-} mice showed milder symptoms of MOG₃₅₋₅₅EAE on day 12 and day 14 along with reduced inflammation and infiltration of macrophages, reduced total myelin loss and axonal loss and reduced TNF- α levels. CREB phosphorylation was increased in the acute phase along with reduced levels of phosphorylated NF- κ B. In the chronic phase of EAE, the mRNA levels of CNPase and Lingo-1 increased significantly. Taken together, our findings indicate that MK2 does not play a major role for in the pathology of MOG₃₅₋₅₅EAE. There were regulations associated with the acute phase while there was no pattern seen in the chronic phase. EAE model is often associated with variability; we also saw some variability between the studies. It can be safe to express thereafter that MK2 might not serve as a potential target in the treatment of EAE model.

6 Zusammenfassung

Experimentelle autoimmune Enzephalomyelitis (EAE) ist eine Antigen-vermittelte entzündliche Erkrankung des zentralen Nervensystems (ZNS), die viele pathologische Merkmale der Multiplen Sklerose (MS) zeigt. MS ist eine autoimmune T-Zell-vermittelte und degenerative Erkrankung des ZNS.

Immunologische Prozesse spielen eine wichtige Rolle bei der Induktion und Pathogenese. TNF- α ist in hohen Konzentrationen im Liquor und aktiven Läsionen von MS-Patienten nachzuweisen. Der MK2-Signalweg ist für die Biosynthese von Zytokinen wie TNF- α und IL-6 relevant. Die Rolle des MK2-Signalwegs in MS und EAE ist weitgehend unbekannt.

Unsere Hypothese war die, dass in der MOG₃₅₋₅₅EAE bei MK2-defizienten Mäusen zu milderen Symptomen kommt. MK2^{-/-} Mäuse zeigten aber nur an Tag 12 und Tag 14 nach EAE Induktion mildere Symptome als Kontrollen. Bei den MK2-defizienten Mäusen fand sich eine verminderte Infiltration von Makrophagen, ein geringere Schädigung des Myelins und weniger axonale Degeneration. CREB-Phosphorylierung war in der akuten Phase erhöht, das phosphorylierte NF- κ B war vermindert. In der chronischen Phase der EAE zeigten sich mRNA-Werte von CNPase und Lingo-1 signifikant erhöht. Zusammengefasst zeigte sich, dass MK2 in der Pathologie von MOG₃₅₋₅₅EAE keine wesentliche Rolle spielt. Es gibt Hinweise für eine Wirkung in der akuten Phase, nicht aber in der chronischen Phase der EAE. Die Variabilität von EAE Verläufen, wie sie dies in dieser Studie zu beobachteten war, ist bekannt. Eine Hemmung von MK2 scheint keine Behandlungsoption für Patienten mit MS darzustellen.

References

- Aggarwal, S., Ichikawa, H., Takada, Y., Sandur, S. K., Shishodia, S., & Aggarwal, B. B. (2005). Curcumin (Diferuloylmethane) Down-Regulates Expression of Cell Proliferation and Antiapoptotic and Metastatic Gene Products through Suppression of I κ B α Kinase and Akt Activation. *Molecular Pharmacology*, 69(1), 195–206. Retrieved from <http://molpharm.aspetjournals.org/content/69/1/195.abstract>
- Aharoni, R. (2014). Immunomodulation neuroprotection and remyelination – The fundamental therapeutic effects of glatiramer acetate: A critical review. *Journal of Autoimmunity*, 54, 81–92. <https://doi.org/10.1016/j.jaut.2014.05.005>
- Albrecht, P., Bouchachia, I., Goebels, N., Henke, N., Hofstetter, H. H., Issberner, A., ... Methner, A. (2012). Effects of dimethyl fumarate on neuroprotection and immunomodulation. *Journal of Neuroinflammation*, 9, 163. <https://doi.org/10.1186/1742-2094-9-163>
- Anderson, S., & Miskimins, R. (1994). Involvement of protein kinase C in cAMP regulation of myelin basic protein gene expression. *Journal of Neuroscience Research*, 37(5), 604–611. <https://doi.org/10.1002/jnr.490370507>
- Barr, T. A., Shen, P., Brown, S., Lampropoulou, V., Roch, T., Lawrie, S., ... Gray, D. (2012). B cell depletion therapy ameliorates autoimmune disease through ablation of IL-6-producing B cells. *The Journal of Experimental Medicine*, 209(5), 1001–1010. Retrieved from <http://jem.rupress.org/content/209/5/1001.abstract>
- Bauer, M., Brakebusch, C., Coisne, C., Sixt, M., Wekerle, H., Engelhardt, B., & Fässler, R. (2009). Beta1 integrins differentially control extravasation of inflammatory cell subsets into the CNS during autoimmunity. *Proceedings of the National Academy of Sciences of the United States of America*, 106(6), 1920–1925. <https://doi.org/10.1073/pnas.0808909106>
- Baumann, N., & Pham-Dinh, D. (2001). Biology of Oligodendrocyte and Myelin in the Mammalian Central Nervous System. *Physiological Reviews*, 81(2), 871–901. Retrieved from <http://physrev.physiology.org/content/81/2/871.abstract>
- Ben-Levy, R., Leighton, I. A., Doza, Y. N., Attwood, P., Morrice, N., Marshall, C. J.,

- & Cohen, P. (1995). Identification of novel phosphorylation sites required for activation of MAPKAP kinase-2. *The EMBO Journal*, *14*(23), 5920.
- Bender, R. A., Lauterborn, J. C., Gall, C. M., Cariaga, W., & Baram, T. Z. (2001). Enhanced CREB phosphorylation in immature dentate gyrus granule cells precedes neurotrophin expression and indicates a specific role of CREB in granule cell differentiation. *European Journal of Neuroscience*, *13*(4), 679–686. <https://doi.org/10.1046/j.1460-9568.2001.01432.x>
- Berger, T., Weerth, S., Kojima, K., Linington, C., Wekerle, H., & Lassmann, H. (1997). Experimental autoimmune encephalomyelitis: the antigen specificity of T lymphocytes determines the topography of lesions in the central and peripheral nervous system. *Laboratory Investigation; a Journal of Technical Methods and Pathology*, *76*(3), 355–364.
- Beutler, B., & Cerami, A. (1989). The Biology of Cachectin/TNF -- A Primary Mediator of the Host Response. *Annual Review of Immunology*, *7*(1), 625–655. <https://doi.org/10.1146/annurev.iy.07.040189.003205>
- Bharucha, V. A., Peden, K. W. C., Subach, B. R., Narayanan, V., & Tennekoon, G. I. (1993). Characterization of the cis-acting elements of the mouse myelin P2 promoter. *Journal of Neuroscience Research*, *36*(5), 508–519. <https://doi.org/10.1002/jnr.490360503>
- Bradl, M., & Lassmann, H. (2010). Oligodendrocytes: biology and pathology. *Acta Neuropathologica*, *119*(1), 37–53. <https://doi.org/10.1007/s00401-009-0601-5>
- Brambilla, R., Persaud, T., Hu, X., Karmally, S., Shestopalov, V. I., Dvorianchikova, G., ... Bethea, J. R. (2009). Transgenic Inhibition of Astroglial NF-κB Improves Functional Outcome in Experimental Autoimmune Encephalomyelitis by Suppressing Chronic Central Nervous System Inflammation. *The Journal of Immunology*, *182*(5), 2628 LP-2640. Retrieved from <http://www.jimmunol.org/content/182/5/2628.abstract>
- Brust, J. C. M. (2007). *Current Diagnosis and Treatment in Neurology*. New York: Lange Medical Books/McGraw-Hill Medical.
- Carim-Todd, L., Escarceller, M., Estivill, X., & Sumoy, L. (2003). LRRN6A/LERN1

- (leucine-rich repeat neuronal protein 1), a novel gene with enriched expression in limbic system and neocortex. *European Journal of Neuroscience*, 18(12), 3167–3182. <https://doi.org/10.1111/j.1460-9568.2003.03003.x>
- Carpintero, R., Brandt, K. J., Gruaz, L., Molnarfi, N., Lalive, P. H., & Burger, D. (2010). Glatiramer acetate triggers PI3K δ /Akt and MEK/ERK pathways to induce IL-1 receptor antagonist in human monocytes. *Proceedings of the National Academy of Sciences*, 107(41), 17692–17697. <https://doi.org/10.1073/pnas.1009443107>
- Chen, X., & Jensen, P. E. (2008). The role of B lymphocytes as antigen-presenting cells. *Archivum Immunologiae et Therapiae Experimentalis*, 56(2), 77. <https://doi.org/10.1007/s00005-008-0014-5>
- Clark, A. R., Dean, J. L. E., & Saklatvala, J. (2003). Post-transcriptional regulation of gene expression by mitogen-activated protein kinase p38. *FEBS Letters*, 546(1), 37–44. [https://doi.org/10.1016/S0014-5793\(03\)00439-3](https://doi.org/10.1016/S0014-5793(03)00439-3)
- Codarri, L., Gyulveszi, G., Tosevski, V., Hesske, L., Fontana, A., Magnenat, L., ... Becher, B. (2011). ROR[γ]t drives production of the cytokine GM-CSF in helper T cells, which is essential for the effector phase of autoimmune neuroinflammation. *Nat Immunol*, 12(6), 560–567. Retrieved from <http://dx.doi.org/10.1038/ni.2027>
- Colombo, E., Cordiglieri, C., Melli, G., Newcombe, J., Krumbholz, M., Parada, L. F., ... Farina, C. (2012). Stimulation of the neurotrophin receptor TrkB on astrocytes drives nitric oxide production and neurodegeneration. *The Journal of Experimental Medicine*, 209(3), 521–535. <https://doi.org/10.1084/jem.20110698>
- Colombo, E., & Farina, C. (2012). Star Trk(B): The astrocyte path to neurodegeneration. *Cell Cycle*, 11(12), 2225–2226. <https://doi.org/10.4161/cc.20798>
- Compston, A., & Coles, A. (2008). Multiple sclerosis. *The Lancet*, 372(9648), 1502–1517. [https://doi.org/10.1016/S0140-6736\(08\)61620-7](https://doi.org/10.1016/S0140-6736(08)61620-7)
- Darnay, B. G., & Aggarwal, B. B. (1997). Early events in TNF signaling: a story of associations and dissociations. *Journal of Leukocyte Biology*, 61(5), 559–566.

Retrieved from <http://www.jleukbio.org/content/61/5/559.abstract>

- Dimitrijević, M., Laban, O., Hoersten, S. Von, Marković, B. M., & Janković, B. D. (1994). Neonatal sound stress and development of experimental allergic encephalomyelitis in Lewis and DA rats. *International Journal of Neuroscience*, 78(1–2), 135–143.
- Dolei, A., Garson, J. A., Arru, G., Clerici, M., Geremi, R., Marche, P. N., & Perron, H. (2014). Multiple sclerosis-associated retrovirus and related human endogenous retrovirus-W in patients with multiple sclerosis. *Journal of Neuroimmunology*, 266(1), 87–88. <https://doi.org/10.1016/j.jneuroim.2013.11.009>
- Domingues, H. S., Portugal, C. C., Socodato, R., & Relvas, J. B. (2016). Oligodendrocyte, Astrocyte and Microglia Crosstalk in Myelin Development, Damage and Repair. *Frontiers in Cell and Developmental Biology*, 4, 71. <https://doi.org/10.3389/fcell.2016.00071>
- Ehltling, C., Ronkina, N., Böhmer, O., Albrecht, U., Bode, K. A., Lang, K. S., ... Bode, J. G. (2011). Distinct Functions of the Mitogen-activated Protein Kinase-activated Protein (MAPKAP) Kinases MK2 and MK3: MK2 MEDIATES LIPOPOLYSACCHARIDE-INDUCED SIGNAL TRANSDUCERS AND ACTIVATORS OF TRANSCRIPTION 3 (STAT3) ACTIVATION BY PREVENTING NEGATIVE REGULATORY EF. *Journal of Biological Chemistry*, 286(27), 24113–24124. <https://doi.org/10.1074/jbc.M111.235275>
- El-Behi, M., Ciric, B., Dai, H., Yan, Y., Cullimore, M., Safavi, F., ... Rostami, A. (2011). The encephalitogenicity of TH17 cells is dependent on IL-1- and IL-23-induced production of the cytokine GM-CSF. *Nat Immunol*, 12(6), 568–575. Retrieved from <http://dx.doi.org/10.1038/ni.2031>
- Engel, K., Kotlyarov, A., & Gaestel, M. (1998). Leptomycin B-sensitive nuclear export of MAPKAP kinase 2 is regulated by phosphorylation. *EMBO J.*, 17, 3363–3371. Retrieved from <http://dx.doi.org/10.1093/emboj/17.12.3363>
- Farina, C., Aloisi, F., & Meinl, E. (2007). Astrocytes are active players in cerebral innate immunity. *Trends in Immunology*, 28(3), 138–145. <https://doi.org/10.1016/j.it.2007.01.005>

- Fletcher, J. M., Lalor, S. J., Sweeney, C. M., Tubridy, N., & Mills, K. H. G. (2010). T cells in multiple sclerosis and experimental autoimmune encephalomyelitis. *Clinical & Experimental Immunology*, *162*(1), 1–11. <https://doi.org/10.1111/j.1365-2249.2010.04143.x>
- Fragoso, G., Haines, J. D., Roberston, J., Pedraza, L., Mushynski, W. E., & Almazan, G. (2007). p38 mitogen-activated protein kinase is required for central nervous system myelination. *Glia*, *55*(15), 1531–1541. <https://doi.org/10.1002/glia.20567>
- Freshney, N. W., Rawlinson, L., Guesdon, F., Jones, E., Cowley, S., Hsuan, J., ... Cowley, S. (1994). Interleukin-1 activates a novel protein kinase cascade that results in the phosphorylation of Hsp27. *Cell*, *78*(6), 1039–1049. [https://doi.org/10.1016/0092-8674\(94\)90278-X](https://doi.org/10.1016/0092-8674(94)90278-X)
- Fujinami, R. S., von Herrath, M. G., Christen, U., & Whitton, J. L. (2006). Molecular Mimicry, Bystander Activation or Viral Persistence: Infections and Autoimmune Disease. *Clinical Microbiology Reviews*, *19*(1), 80–94. <https://doi.org/10.1128/CMR.19.1.80-94.2006>
- Gaestel, M. (2006). MAPKAP kinases—MKs—two’s company, three’s a crowd. *Nature Reviews Molecular Cell Biology*, *7*(2), 120–130.
- Genain, C. P., Nguyen, M. H., Letvin, N. L., Pearl, R., Davis, R. L., Adelman, M., ... Hauser, S. L. (1995). Antibody facilitation of multiple sclerosis-like lesions in a nonhuman primate. *Journal of Clinical Investigation*, *96*(6), 2966–2974. Retrieved from <http://www.ncbi.nlm.nih.gov/pmc/articles/PMC186008/>
- Ghasemlou, N., Lopez-Vales, R., Lachance, C., Thuraisingam, T., Gaestel, M., Radzioch, D., & David, S. (2010). Mitogen-Activated Protein Kinase-Activated Protein Kinase 2 (MK2) Contributes to Secondary Damage after Spinal Cord Injury. *The Journal of Neuroscience*, *30*(41), 13750 LP-13759. Retrieved from <http://www.jneurosci.org/content/30/41/13750.abstract>
- Giavazzi, R., Garofalo, A., Bani, M. R., Abbate, M., Ghezzi, P., Boraschi, D., ... Dejana, E. (1990). Interleukin 1-induced Augmentation of Experimental Metastases from a Human Melanoma in Nude Mice. *Cancer Research*, *50*(15), 4771 LP-4775. Retrieved from

<http://cancerres.aacrjournals.org/content/50/15/4771.abstract>

Gold, R., Linington, C., & Lassmann, H. (2006). Understanding pathogenesis and therapy of multiple sclerosis via animal models: 70 years of merits and culprits in experimental autoimmune encephalomyelitis research. *Brain*, *129*(8), 1953–1971. Retrieved from <http://dx.doi.org/10.1093/brain/awl075>

Goldenberg, M. M. (2012). Multiple Sclerosis Review. *Pharmacy and Therapeutics*, *37*(3), 175–184. Retrieved from <http://www.ncbi.nlm.nih.gov/pmc/articles/PMC3351877/>

Gorska, M. M., Liang, Q., Stafford, S. J., Goplen, N., Dharajiyi, N., Guo, L., ... Alam, R. (2007). MK2 controls the level of negative feedback in the NF- κ B pathway and is essential for vascular permeability and airway inflammation. *The Journal of Experimental Medicine*, *204*(7), 1637 LP-1652. Retrieved from <http://jem.rupress.org/content/204/7/1637.abstract>

Greenfield JG, Love S, Louis DN, et al. (2008). *Greenfield's neuropathology*. London: Hodder Arnold.

Gurgis, F. M. S., Ziaziaris, W., & Munoz, L. (2014). Mitogen-Activated Protein Kinase–Activated Protein Kinase 2 in Neuroinflammation, Heat Shock Protein 27 Phosphorylation and Cell Cycle: Role and Targeting. *Molecular Pharmacology*, *85*(2), 345 LP-356. Retrieved from <http://molpharm.aspetjournals.org/content/85/2/345.abstract>

Haines, J. D., Fang, J., Mushynski, W. E., & Almazan, G. (2010). Mitogen-activated protein kinase activated protein kinase 2 (MK2) participates in p38 MAPK regulated control of oligodendrocyte differentiation. *Glia*, *58*(11), n/a-n/a. <https://doi.org/10.1002/glia.21014>

Haines, J. D., Fragoso, G., Hossain, S., Mushynski, W. E., & Almazan, G. (2008). p38 Mitogen-activated protein kinase regulates myelination. *Journal of Molecular Neuroscience*, *35*(1), 23–33.

Hale, G. (2001). The CD52 antigen and development of the CAMPATH antibodies. *Cytotherapy*, *3*(3), 137–143.

Han, J., Lee, J. D., Bibbs, L., & Ulevitch, R. J. (1994). A MAP kinase targeted by

- endotoxin and hyperosmolarity in mammalian cells. *Science*, 265, 808–811.
Retrieved from <http://dx.doi.org/10.1126/science.7914033>
- Hauser SL, G. D. (2008). Harrison's Principles of Internal Medicine (17th ed. I, pp. 2611–2621). New York: McGraw-Hill Medical.
- Heidenreich, O., Neining, A., Schratz, G., Zinck, R., Cahill, M. A., Engel, K., ... Nordheim, A. (1999). MAPKAP Kinase 2 Phosphorylates Serum Response Factor in Vitro and in Vivo . *Journal of Biological Chemistry* , 274(20), 14434–14443.
<https://doi.org/10.1074/jbc.274.20.14434>
- Henderson, A. P. D., Barnett, M. H., Parratt, J. D. E., & Prineas, J. W. (2009). Multiple sclerosis: Distribution of inflammatory cells in newly forming lesions. *Annals of Neurology*, 66(6), 739–753. <https://doi.org/10.1002/ana.21800>
- Herrero-Herranz, E., Pardo, L. A., Gold, R., & Linker, R. A. (2008). Pattern of axonal injury in murine myelin oligodendrocyte glycoprotein induced experimental autoimmune encephalomyelitis: Implications for multiple sclerosis. *Neurobiology of Disease*, 30(2), 162–173. <https://doi.org/10.1016/j.nbd.2008.01.001>
- Hohlfeld, R., & Wekerle, H. (2001). Immunological update on multiple sclerosis. *Current Opinion in Neurology*, 14(3), 299–304.
- Huang, C.-K., Zhan, L., Ai, Y., & Jongstra, J. (1997). LSP1 Is the Major Substrate for Mitogen-activated Protein Kinase-activated Protein Kinase 2 in Human Neutrophils. *Journal of Biological Chemistry* , 272(1), 17–19.
<https://doi.org/10.1074/jbc.272.1.17>
- Iglesias, A., Bauer, J., Litzenburger, T., Schubart, A., & Linington, C. (2001). T- and B-cell responses to myelin oligodendrocyte glycoprotein in experimental autoimmune encephalomyelitis and multiple sclerosis. *Glia*, 36(2), 220–234.
<https://doi.org/10.1002/glia.1111>
- Jensen, N. A., Smith, G. M., Garvey, J. S., Shine, H. D., & Hood, L. (1993). Cyclic AMP has a differentiative effect on an immortalized oligodendrocyte cell line. *Journal of Neuroscience Research*, 35(3), 288–296.
<https://doi.org/10.1002/jnr.490350308>
- Kang, Z., Altuntas, C. Z., Gulen, M. F., Liu, C., Giltiy, N., Qin, H., ... Li, X. (2010).

- Astrocyte-restricted ablation of interleukin-17-induced Act1-mediated signaling ameliorates autoimmune encephalomyelitis. *Immunity*, 32(3), 414–425. <https://doi.org/10.1016/j.immuni.2010.03.004>
- Karin, M. (2006). Nuclear factor- κ B in cancer development and progression. *Nature*, 441(7092), 431–436. Retrieved from <http://dx.doi.org/10.1038/nature04870>
- Karussis, D. (2014). The diagnosis of multiple sclerosis and the various related demyelinating syndromes: A critical review. *Journal of Autoimmunity*, 48–49, 134–142. <https://doi.org/http://dx.doi.org/10.1016/j.jaut.2014.01.022>
- Kassiotis, G., & Kollias, G. (2001). Uncoupling the Proinflammatory from the Immunosuppressive Properties of Tumor Necrosis Factor (Tnf) at the P55 TNF Receptor Level. *The Journal of Experimental Medicine*, 193(4), 427 LP-434. Retrieved from <http://jem.rupress.org/content/193/4/427.abstract>
- Kim, H., Moon, C., Ahn, M., Lee, Y., Kim, S., Matsumoto, Y., ... Shin, T. (2007). Increased phosphorylation of cyclic AMP response element-binding protein in the spinal cord of Lewis rats with experimental autoimmune encephalomyelitis. *Brain Research*, 1162, 113–120. <https://doi.org/10.1016/j.brainres.2007.05.072>
- Koritschoner RS, S. F. (1925). Induktion von Paralyse und Rückenmarksentzündung durch Immunisierung von Kaninchen mit menschlichem Rückenmarksgewebe. *Z Immunitätsf Exp Therapie*, 42, 217–283.
- Kornek, B., Storch, M. K., Weissert, R., Wallstroem, E., Stefferl, A., Olsson, T., ... Lassmann, H. (2000). Multiple Sclerosis and Chronic Autoimmune Encephalomyelitis. *The American Journal of Pathology*, 157(1), 267–276. [https://doi.org/10.1016/S0002-9440\(10\)64537-3](https://doi.org/10.1016/S0002-9440(10)64537-3)
- Körner, H., Cook, M., Riminton, D. S., Lemckert, F. A., Hoek, R. M., Ledermann, B., ... Sedgwick, J. D. (1997). Distinct roles for lymphotoxin- α and tumor necrosis factor in organogenesis and spatial organization of lymphoid tissue. *European Journal of Immunology*, 27(10), 2600–2609. <https://doi.org/10.1002/eji.1830271020>
- Kotlyarov, A., Neining, A., Schubert, C., Eckert, R., Birchmeier, C., Volk, H.-D., &

- Gaestel, M. (1999). MAPKAP kinase 2 is essential for LPS-induced TNF-[alpha] biosynthesis . *Nat Cell Biol*, 1(2), 94–97. Retrieved from <http://dx.doi.org/10.1038/10061>
- Kotlyarov, A., Yannoni, Y., Fritz, S., Laaß, K., Telliez, J.-B., Pitman, D., ... Gaestel, M. (2002). Distinct Cellular Functions of MK2. *Molecular and Cellular Biology*, 22(13), 4827–4835. <https://doi.org/10.1128/MCB.22.13.4827-4835.2002>
- Kruglov, A. A., Lampropoulou, V., Fillatreau, S., & Nedospasov, S. A. (2011). Pathogenic and Protective Functions of TNF in Neuroinflammation Are Defined by Its Expression in T Lymphocytes and Myeloid Cells. *The Journal of Immunology*, 187(11), 5660 LP-5670. Retrieved from <http://www.jimmunol.org/content/187/11/5660.abstract>
- Laban, O., Dimitrijević, M., von Hoersten, S., Marković, B. M., & Janković, B. D. (1995). Experimental allergic encephalomyelitis in adult DA rats subjected to neonatal handling or gentling. *Brain Research*, 676(1), 133–140. [https://doi.org/10.1016/0006-8993\(95\)00106-Z](https://doi.org/10.1016/0006-8993(95)00106-Z)
- Langowski, J. L., Zhang, X., Wu, L., Mattson, J. D., Chen, T., Smith, K., ... Oft, M. (2006). IL-23 promotes tumour incidence and growth. *Nature*, 442(7101), 461–465. Retrieved from <http://dx.doi.org/10.1038/nature04808>
- Langrish, C. L., Chen, Y., Blumenschein, W. M., Mattson, J., Basham, B., Sedgwick, J. D., ... Cua, D. J. (2005). IL-23 drives a pathogenic T cell population that induces autoimmune inflammation. *The Journal of Experimental Medicine*, 201(2), 233 LP-240. Retrieved from <http://jem.rupress.org/content/201/2/233.abstract>
- Lassmann, H. (2010). Axonal and neuronal pathology in multiple sclerosis: What have we learnt from animal models. *Experimental Neurology*, 225(1), 2–8. <https://doi.org/10.1016/j.expneurol.2009.10.009>
- Lee, J. C. (1994). A protein kinase involved in the regulation of inflammatory cytokine biosynthesis. *Nature*, 372, 739–746. Retrieved from <http://dx.doi.org/10.1038/372739a0>
- LEE, J. C., BADGER, A. M., GRISWOLD, D. E., DUNNINGTON, D., TRUNEH, A., VOTTA, B., ... BENDER, P. E. (1993). Bicyclic Imidazoles as a Novel Class of

- Cytokine Biosynthesis Inhibitors. *Annals of the New York Academy of Sciences*, 696(1), 149–170. <https://doi.org/10.1111/j.1749-6632.1993.tb17149.x>
- Lehky, T. J., Levin, M. C., Kubota, R., Bamford, R. N., Flerlage, A. N., Soldan, S. S., ... Jacobson, S. (1998). Reduction in HTLV-I proviral load and spontaneous lymphoproliferation in HTLV-I-associated myelopathy/tropical spastic paraparesis patients treated with humanized anti-tac. *Annals of Neurology*, 44(6), 942–947. <https://doi.org/10.1002/ana.410440613>
- Lehner, M. D., Schwoebel, F., Kotlyarov, A., Leist, M., Gaestel, M., & Hartung, T. (2002). Mitogen-Activated Protein Kinase-Activated Protein Kinase 2-Deficient Mice Show Increased Susceptibility to *Listeria monocytogenes*; Infection. *The Journal of Immunology*, 168(9), 4667 LP-4673. Retrieved from <http://www.jimmunol.org/content/168/9/4667.abstract>
- Linington, C., Bradl, M., Lassmann, H., Brunner, C., & Vass, K. (1988). Augmentation of demyelination in rat acute allergic encephalomyelitis by circulating mouse monoclonal antibodies directed against a myelin/oligodendrocyte glycoprotein. *The American Journal of Pathology*, 130(3), 443–454. Retrieved from <http://www.ncbi.nlm.nih.gov/pmc/articles/PMC1880661/>
- Linker, R. A., Lee, D.-H., Ryan, S., van Dam, A. M., Conrad, R., Bista, P., ... Gold, R. (2011). Fumaric acid esters exert neuroprotective effects in neuroinflammation via activation of the Nrf2 antioxidant pathway. *Brain*, 134(3), 678–692. Retrieved from <http://dx.doi.org/10.1093/brain/awq386>
- Liu, J., Marino, M. W., Wong, G., Grail, D., Dunn, A., Bettadapura, J., ... Bernard, C. C. A. (1998). TNF is a potent anti-inflammatory cytokine in autoimmune-mediated demyelination. *Nature Medicine*, 4(1), 78–83.
- Loma, I., & Heyman, R. (2011). Multiple Sclerosis: Pathogenesis and Treatment. *Current Neuropharmacology*, 9(3), 409–416. <https://doi.org/10.2174/157015911796557911>
- Lublin, F. D., & Reingold, S. C. (1996). Defining the clinical course of multiple sclerosis results of an international survey. *Neurology*, 46(4), 907–911.
- Luo, J.-L., Tan, W., Ricono, J. M., Korchynskyi, O., Zhang, M., Gonias, S. L., ... Karin,

- M. (2007). Nuclear cytokine-activated IKK[agr] controls prostate cancer metastasis by repressing Maspin. *Nature*, *446*(7136), 690–694. Retrieved from <http://dx.doi.org/10.1038/nature05656>
- Mahad, D. H., Trapp, B. D., & Lassmann, H. (2015). Pathological mechanisms in progressive multiple sclerosis. *The Lancet Neurology*, *14*(2), 183–193. [https://doi.org/10.1016/S1474-4422\(14\)70256-X](https://doi.org/10.1016/S1474-4422(14)70256-X)
- Mahtani, K. R., Brook, M., Dean, J. L. E., Sully, G., Saklatvala, J., & Clark, A. R. (2001). Mitogen-Activated Protein Kinase p38 Controls the Expression and Posttranslational Modification of Tristetraprolin, a Regulator of Tumor Necrosis Factor Alpha mRNA Stability. *Molecular and Cellular Biology*, *21*(19), 6461–6469. <https://doi.org/10.1128/MCB.21.9.6461-6469.2001>
- Mantovani, A., Allavena, P., Sica, A., & Balkwill, F. (2008). Cancer-related inflammation. *Nature*, *454*(7203), 436–444. Retrieved from <http://dx.doi.org/10.1038/nature07205>
- Matsushita, T., Yanaba, K., Bouaziz, J.-D., Fujimoto, M., & Tedder, T. F. (2008). Regulatory B cells inhibit EAE initiation in mice while other B cells promote disease progression. *The Journal of Clinical Investigation*, *118*(10), 3420–3430. <https://doi.org/10.1172/JCI36030>
- McDonald, W. I., Compston, A., Edan, G., Goodkin, D., Hartung, H.-P., Lublin, F. D., ... Wolinsky, J. S. (2001). Recommended diagnostic criteria for multiple sclerosis: Guidelines from the international panel on the diagnosis of multiple sclerosis. *Annals of Neurology*, *50*(1), 121–127. <https://doi.org/10.1002/ana.1032>
- McFarland, H. F., & Martin, R. (2007). Multiple sclerosis: a complicated picture of autoimmunity. *Nat Immunol*, *8*(9), 913–919. Retrieved from <http://dx.doi.org/10.1038/ni1507>
- Mi, S., Hu, B., Hahm, K., Luo, Y., Kam Hui, E. S., Yuan, Q., ... Wu, W. (2007). LINGO-1 antagonist promotes spinal cord remyelination and axonal integrity in MOG-induced experimental autoimmune encephalomyelitis. *Nat Med*, *13*(10), 1228–1233. Retrieved from <http://dx.doi.org/10.1038/nm1664>
- Mi, S., Lee, X., Shao, Z., Thill, G., Ji, B., Relton, J., ... Sands, B. (2004). LINGO-1 is

- a component of the Nogo-66 receptor/p75 signaling complex. *Nature Neuroscience*, 7(3), 221–228.
- Mi, S., Miller, R. H., Lee, X., Scott, M. L., Shulag-Morskaya, S., Shao, Z., ... Pepinsky, R. B. (2005). LINGO-1 negatively regulates myelination by oligodendrocytes. *Nat Neurosci*, 8(6), 745–751. Retrieved from <http://dx.doi.org/10.1038/nn1460>
- MILLER, S. D., MCMAHON, E. J., SCHREINER, B., & BAILEY, S. L. (2007). Antigen Presentation in the CNS by Myeloid Dendritic Cells Drives Progression of Relapsing Experimental Autoimmune Encephalomyelitis. *Annals of the New York Academy of Sciences*, 1103(1), 179–191. <https://doi.org/10.1196/annals.1394.023>
- Milo, R., & Kahana, E. (2010). Multiple sclerosis: Geoeidemiology, genetics and the environment. *Autoimmunity Reviews*, 9(5), A387–A394. <https://doi.org/http://dx.doi.org/10.1016/j.autrev.2009.11.010>
- Milo, R., & Miller, A. (2014). Revised diagnostic criteria of multiple sclerosis. *Autoimmunity Reviews*, 13(4–5), 518–524. <https://doi.org/http://dx.doi.org/10.1016/j.autrev.2014.01.012>
- Morell P, Q. R. (1999). Characteristic Composition of Myelin. In *Basic Neurochemistry: Molecular, Cellular and Medical Aspects*. Philadelphia: Lippincott-Raven. Retrieved from <https://www.ncbi.nlm.nih.gov/books/NBK28221/>
- Nakagawa, S., Kim, J.-E., Lee, R., Chen, J., Fujioka, T., Malberg, J., ... Duman, R. S. (2002). Localization of Phosphorylated cAMP Response Element-Binding Protein in Immature Neurons of Adult Hippocampus. *The Journal of Neuroscience*, 22(22), 9868 LP-9876. Retrieved from <http://www.jneurosci.org/content/22/22/9868.abstract>
- Namiki, K., Matsunaga, H., Yoshioka, K., Tanaka, K., Murata, K., Ishida, J., ... Kasuya, Y. (2012). Mechanism for p38 α -mediated Experimental Autoimmune Encephalomyelitis. *The Journal of Biological Chemistry*, 287(29), 24228–24238. <https://doi.org/10.1074/jbc.M111.338541>
- Nicol, B., Salou, M., Laplaud, D.-A., & Wekerle, H. (2015). The autoimmune concept

- of multiple sclerosis. *La Presse Médicale*, 44(4), e103–e112.
<https://doi.org/10.1016/j.lpm.2015.02.009>
- Nielsen, J. A., Berndt, J. A., Hudson, L. D., & Armstrong, R. C. (2004). Myelin transcription factor 1 (Myt1) modulates the proliferation and differentiation of oligodendrocyte lineage cells. *Molecular and Cellular Neuroscience*, 25(1), 111–123. <https://doi.org/10.1016/j.mcn.2003.10.001>
- Nikic, I., Merkler, D., Sorbara, C., Brinkoetter, M., Kreutzfeldt, M., Bareyre, F. M., ... Kerschensteiner, M. (2011). A reversible form of axon damage in experimental autoimmune encephalomyelitis and multiple sclerosis. *Nat Med*, 17(4), 495–499. Retrieved from <http://dx.doi.org/10.1038/nm.2324>
- Noubade, R., Kremontsov, D. N., del Rio, R., Thornton, T., Nagaleekar, V., Saligrama, N., ... Teuscher, C. (2011). Activation of p38 MAPK in CD4 T cells controls IL-17 production and autoimmune encephalomyelitis. *Blood*, 118(12), 3290 LP-3300. Retrieved from <http://www.bloodjournal.org/content/118/12/3290.abstract>
- Ortiz, G. G., Pacheco-Moisés, F. P., Macías-Islas, M. Á., Flores-Alvarado, L. J., Mireles-Ramírez, M. A., González-Renovato, E. D., ... Alatorre-Jiménez, M. A. (2014). Role of the Blood–Brain Barrier in Multiple Sclerosis. *Archives of Medical Research*, 45(8), 687–697. <https://doi.org/10.1016/j.arcmed.2014.11.013>
- Osiri, M., Shea, B., Robinson, V., Suarez-Almazor, M., Strand, V., Tugwell, P., & Wells, G. (2003). Leflunomide for the treatment of rheumatoid arthritis: a systematic review and metaanalysis. *The Journal of Rheumatology*, 30(6), 1182 LP-1190. Retrieved from <http://www.jrheum.org/content/30/6/1182.abstract>
- Papenfuss, T. L., Rogers, C. J., Gienapp, I., Yurrita, M., McClain, M., Damico, N., ... Whitacre, C. C. (2004). Sex differences in experimental autoimmune encephalomyelitis in multiple murine strains. *Journal of Neuroimmunology*, 150(1–2), 59–69. <https://doi.org/10.1016/j.jneuroim.2004.01.018>
- Paty, D. W., Oger, J. J. F., Kastrukoff, L. F., Hashimoto, S. A., Hooge, J. P., Eisen, A. A., ... Brandejs, V. (1988). MRI in the diagnosis of MS A prospective study with comparison of clinical evaluation, evoked potentials, oligoclonal banding and CT.

Neurology, 38(2), 180.

- Phan, T. G., Gray, E. E., & Cyster, J. G. (2009). The microanatomy of B cell activation. *Current Opinion in Immunology*, 21(3), 258–265. <https://doi.org/10.1016/j.coi.2009.05.006>
- Polman, C. H., Reingold, S. C., Banwell, B., Clanet, M., Cohen, J. A., Filippi, M., ... Wolinsky, J. S. (2011). Diagnostic criteria for multiple sclerosis: 2010 Revisions to the McDonald criteria. *Annals of Neurology*, 69(2), 292–302. <https://doi.org/10.1002/ana.22366>
- Polman, C. H., Reingold, S. C., Edan, G., Filippi, M., Hartung, H.-P., Kappos, L., ... Wolinsky, J. S. (2005). Diagnostic criteria for multiple sclerosis: 2005 revisions to the “McDonald Criteria.” *Annals of Neurology*, 58(6), 840–846. <https://doi.org/10.1002/ana.20703>
- Poser, C. M., Paty, D. W., Scheinberg, L., McDonald, W. I., Davis, F. A., Ebers, G. C., ... Tourtellotte, W. W. (1983). New diagnostic criteria for multiple sclerosis: Guidelines for research protocols. *Annals of Neurology*, 13(3), 227–231. <https://doi.org/10.1002/ana.410130302>
- Probert, L., Eugster, H.-P., Akassoglou, K., Bauer, J., Frei, K., Lassmann, H., & Fontana, A. (2000). TNFR1 signalling is critical for the development of demyelination and the limitation of T-cell responses during immune-mediated CNS disease. *Brain*, 123(10), 2005–2019.
- Raasch, J., Zeller, N., van Loo, G., Merkler, D., Mildner, A., Erny, D., ... Prinz, M. (2011). IκB kinase 2 determines oligodendrocyte loss by non-cell-autonomous activation of NF-κB in the central nervous system. *Brain*, 134(4), 1184–1198. Retrieved from <http://dx.doi.org/10.1093/brain/awq359>
- Raingeaud, J., Whitmarsh, A. J., Barrett, T., Derijard, B., & Davis, R. J. (1996). MKK3- and MKK6-regulated gene expression is mediated by the p38 mitogen-activated protein kinase signal transduction pathway. *Mol. Cell. Biol.*, 16, 1247–1255.
- Ramiscal, R. R., & Vinuesa, C. G. (2013). T-cell subsets in the germinal center. *Immunological Reviews*, 252(1), 146–155. <https://doi.org/10.1111/imr.12031>
- Reboldi, A., Coisne, C., Baumjohann, D., Benvenuto, F., Bottinelli, D., Lira, S., ...

- Sallusto, F. (2009). C-C chemokine receptor 6-regulated entry of TH-17 cells into the CNS through the choroid plexus is required for the initiation of EAE. *Nat Immunol*, *10*(5), 514–523. Retrieved from <http://dx.doi.org/10.1038/ni.1716>
- Redford, E. J., Smith, K. J., Gregson, N. A., Davies, M., Hughes, P., Gearing, A. J., ... Hughes, R. A. (1997). A combined inhibitor of matrix metalloproteinase activity and tumour necrosis factor-alpha processing attenuates experimental autoimmune neuritis. *Brain*, *120*(10), 1895–1905. Retrieved from <http://dx.doi.org/10.1093/brain/120.10.1895>
- Renno, T., Lin, J.-Y., Piccirillo, C., Antel, J., & Owens, T. (1994). Cytokine production by cells in cerebrospinal fluid during experimental allergic encephalomyelitis in SJL/J mice. *Journal of Neuroimmunology*, *49*(1), 1–7.
- Riley CS, T. M. (2010). Merritt's Neurology. In *Multiple sclerosis* (12th ed., pp. 903–918). Philadelphia: Wolters Kluwer/Lippincott Williams & Wilkins.
- Ronkina, N., Kotlyarov, A., & Gaestel, M. (2008). MK2 and MK3—a pair of isoenzymes. *Front Biosci*, *13*, 5511–5521.
- Rouse, J., Cohen, P., Trigon, S., Morange, M., Alonso-Llamazares, A., Zamanillo, D., ... Nishida, E. (1994). A novel kinase cascade triggered by stress and heat shock that stimulates MAPKAP kinase-2 and phosphorylation of the small heat shock proteins. *Cell*, *78*(6), 1027–1037. [https://doi.org/10.1016/0092-8674\(94\)90277-1](https://doi.org/10.1016/0092-8674(94)90277-1)
- Sato-Bigbee, C., Chan, E. L. P., & Yu, R. K. (1994). Oligodendroglial cyclic AMP response element-binding protein: A member of the CREB family of transcription factors. *Journal of Neuroscience Research*, *38*(6), 621–628. <https://doi.org/10.1002/jnr.490380604>
- Sato-Bigbee, C., & DeVries, G. H. (1996). Treatment of oligodendrocytes with antisense deoxyoligonucleotide directed against CREB mRNA: effect on the cyclic AMP-dependent induction of myelin basic protein expression. *Journal of Neuroscience Research*, *46*(1), 98–107.
- Schluesener, H. J., Sobel, R. A., Lington, C., & Weiner, H. L. (1987). A monoclonal antibody against a myelin oligodendrocyte glycoprotein induces relapses and demyelination in central nervous system autoimmune disease. *The Journal of*

Immunology, 139(12), 4016 LP-4021. Retrieved from <http://www.jimmunol.org/content/139/12/4016.abstract>

Schumacher, G. A., Beebe, G., Kibler, R. F., Kurland, L. T., Kurtzke, J. F., McDowell, F., ... Willmon, T. L. (2006). PROBLEMS OF EXPERIMENTAL TRIALS OF THERAPY IN MULTIPLE SCLEROSIS: REPORT BY THE PANEL ON THE EVALUATION OF EXPERIMENTAL TRIALS OF THERAPY IN MULTIPLE SCLEROSIS. *Annals of the New York Academy of Sciences*, 122(1), 552–568. <https://doi.org/10.1111/j.1749-6632.1965.tb20235.x>

Shin, T., Ahn, M., Jung, K., Heo, S., Kim, D., Jee, Y., ... Yeo, E.-J. (2003). Activation of mitogen-activated protein kinases in experimental autoimmune encephalomyelitis. *Journal of Neuroimmunology*, 140(1–2), 118–125. [https://doi.org/10.1016/S0165-5728\(03\)00174-7](https://doi.org/10.1016/S0165-5728(03)00174-7)

Simeone-Penney, M. C., Severgnini, M., Rozo, L., Takahashi, S., Cochran, B. H., & Simon, A. R. (2008). PDGF-induced human airway smooth muscle cell proliferation requires STAT3 and the small GTPase Rac1. *American Journal of Physiology - Lung Cellular and Molecular Physiology*, 294(4), L698 LP-L704. Retrieved from <http://ajplung.physiology.org/content/294/4/L698.abstract>

Simon, C., Goepfert, H., & Boyd, D. (1998). Inhibition of the p38 Mitogen-activated Protein Kinase by SB 203580 Blocks PMA-induced M_r 92,000 Type IV Collagenase Secretion and in Vitro Invasion. *Cancer Research*, 58(6), 1135 LP-1139. Retrieved from <http://cancerres.aacrjournals.org/content/58/6/1135.abstract>

Smith, K. A., Gilbride, K. J., & Favata, M. F. (1980). Lymphocyte activating factor promotes T-cell growth factor production by cloned marine lymphoma cells. *Nature*, 287(5785), 853–855.

Smith, K. J., & McDonald, W. I. (1999). The pathophysiology of multiple sclerosis: the mechanisms underlying the production of symptoms and the natural history of the disease. *Philosophical Transactions of the Royal Society of London. Series B: Biological Sciences*, 354(1390), 1649 LP-1673. Retrieved from <http://rstb.royalsocietypublishing.org/content/354/1390/1649.abstract>

- Sospedra, M., & Martin, R. (2005). Immunology of multiple sclerosis. *Annu. Rev. Immunol.*, 23, 683–747.
- Steinman, L. (2007). A brief history of TH17, the first major revision in the TH1/TH2 hypothesis of T cell-mediated tissue damage. *Nat Med*, 13(2), 139–145. Retrieved from <http://dx.doi.org/10.1038/nm1551>
- Steinman, L., & Zamvil, S. (2003). Transcriptional analysis of targets in multiple sclerosis. *Nat Rev Immunol*, 3(6), 483–492.
- Stokoe, D., Engel, K., Campbell, D. G., Cohen, P., & Gaestel, M. (1992). Identification of MAPKAP kinase 2 as a major enzyme responsible for the phosphorylation of the small mammalian heat shock proteins. *FEBS Letters*, 313(3), 307–313. [https://doi.org/10.1016/0014-5793\(92\)81216-9](https://doi.org/10.1016/0014-5793(92)81216-9)
- Storch, M. K., Stefferl, A., Brehm, U., Weissert, R., Wallström, E., Kerschensteiner, M., ... Lassmann, H. (1998). Autoimmunity to Myelin Oligodendrocyte Glycoprotein in Rats Mimics the Spectrum of Multiple Sclerosis Pathology. *Brain Pathology*, 8(4), 681–694. <https://doi.org/10.1111/j.1750-3639.1998.tb00194.x>
- Stromnes, I. M., & Goverman, J. M. (2006). Active induction of experimental allergic encephalomyelitis. *Nat. Protocols*, 1(4), 1810–1819. Retrieved from <http://dx.doi.org/10.1038/nprot.2006.285>
- Sutton, C., Brereton, C., Keogh, B., Mills, K. H. G., & Lavelle, E. C. (2006). A crucial role for interleukin (IL)-1 in the induction of IL-17-producing T cells that mediate autoimmune encephalomyelitis. *The Journal of Experimental Medicine*, 203(7), 1685–1691. <https://doi.org/10.1084/jem.20060285>
- Takenaka, K., Moriguchi, T., & Nishida, E. (1998). Activation of the protein kinase p38 in the spindle assembly checkpoint and mitotic arrest. *Science*, 280, 599–602. Retrieved from <http://dx.doi.org/10.1126/science.280.5363.599>
- Tan, Y., Rouse, J., Zhang, A., Cariati, S., Cohen, P., & Comb, M. J. (1996). FGF and stress regulate CREB and ATF-1 via a pathway involving p38 MAP kinase and MAPKAP kinase-2. *The EMBO Journal*, 15(17), 4629–4642. Retrieved from <http://www.ncbi.nlm.nih.gov/pmc/articles/PMC452194/>
- Tanuma, N., Kojima, T., Shin, T., Aikawa, Y., Kohji, T., Ishihara, Y., & Matsumoto,

- Y. (1997). Competitive PCR quantification of pro-and anti-inflammatory cytokine mRNA in the central nervous system during autoimmune encephalomyelitis. *Journal of Neuroimmunology*, 73(1), 197–206.
- Teuscher, C., Bunn, J. Y., Fillmore, P. D., Butterfield, R. J., Zachary, J. F., & Blankenhorn, E. P. (2004). Gender, Age and Season at Immunization Uniquely Influence the Genetic Control of Susceptibility to Histopathological Lesions and Clinical Signs of Experimental Allergic Encephalomyelitis. *The American Journal of Pathology*, 165(5), 1593–1602. [https://doi.org/10.1016/S0002-9440\(10\)63416-5](https://doi.org/10.1016/S0002-9440(10)63416-5)
- Thomas, G., Haavik, J., & Cohen, P. (1997). Participation of a Stress-Activated Protein Kinase Cascade in the Activation of Tyrosine Hydroxylase in Chromaffin Cells. *European Journal of Biochemistry*, 247(3), 1180–1189. <https://doi.org/10.1111/j.1432-1033.1997.01180.x>
- Thomas, T., Hitti, E., Kotlyarov, A., Potschka, H., & Gaestel, M. (2008). MAP-kinase-activated protein kinase 2 expression and activity is induced after neuronal depolarization. *European Journal of Neuroscience*, 28(4), 642–654. <https://doi.org/10.1111/j.1460-9568.2008.06382.x>
- Thomas, T., Timmer, M., Cesnulevicius, K., Hitti, E., Kotlyarov, A., & Gaestel, M. (2008). MAPKAP kinase 2-deficiency prevents neurons from cell death by reducing neuroinflammation – relevance in a mouse model of Parkinson’s disease. *Journal of Neurochemistry*, 105(5), 2039–2052. <https://doi.org/10.1111/j.1471-4159.2008.05310.x>
- Tietz, S. M., Hofmann, R., Thomas, T., Tackenberg, B., Gaestel, M., & Berghoff, M. (2014). MK2 and Fas Receptor Contribute to the Severity of CNS Demyelination. *PLoS ONE*, 9(6), e100363. <https://doi.org/10.1371/journal.pone.0100363>
- Trajkovic, V., Stosic-Grujicic, S., Samardzic, T., Markovic, M., Miljkovic, D., Ramic, Z., ... Lebecque, S. (2001). Interleukin-17 stimulates inducible nitric oxide synthase activation in rodent astrocytes. *Journal of Neuroimmunology*, 119(2), 183–191. [https://doi.org/10.1016/S0165-5728\(01\)00391-5](https://doi.org/10.1016/S0165-5728(01)00391-5)
- Tzartos, J. S., Friese, M. A., Craner, M. J., Palace, J., Newcombe, J., Esiri, M. M., &

- Fugger, L. (2008). Interleukin-17 Production in Central Nervous System-Infiltrating T Cells and Glial Cells Is Associated with Active Disease in Multiple Sclerosis. *The American Journal of Pathology*, 172(1), 146–155. <https://doi.org/10.2353/ajpath.2008.070690>
- Voronov, E., Shouval, D. S., Krelin, Y., Cagnano, E., Benharroch, D., Iwakura, Y., ... Apte, R. N. (2003). IL-1 is required for tumor invasiveness and angiogenesis. *Proceedings of the National Academy of Sciences*, 100(5), 2645–2650. Retrieved from <http://www.pnas.org/content/100/5/2645.abstract>
- Waldmann, T. A., Longo, D. L., Leonard, W. J., Depper, J. M., Thompson, C. B., Krönke, M., ... Greene, W. C. (1985). Interleukin 2 Receptor (Tac Antigen) Expression in HTLV-I-associated Adult T-Cell Leukemia. *Cancer Research*, 45(9 Supplement), 4559s LP-4562s. Retrieved from http://cancerres.aacrjournals.org/content/45/9_Supplement/4559s.abstract
- Wang, X. (1998). The phosphorylation of eukaryotic initiation factor eIF4E in response to phorbol esters, cell stresses and cytokines is mediated by distinct MAP kinase pathways. *J. Biol. Chem.*, 273, 9373–9377. Retrieved from <http://dx.doi.org/10.1074/jbc.273.16.9373>
- Wang, X., Xu, L., Wang, H., Young, P. R., Gaestel, M., & Feuerstein, G. Z. (2002). Mitogen-activated Protein Kinase-activated Protein (MAPKAP) Kinase 2 Deficiency Protects Brain from Ischemic Injury in Mice. *Journal of Biological Chemistry*, 277(46), 43968–43972. <https://doi.org/10.1074/jbc.M206837200>
- Wegner, M. (2000). Transcriptional Control in Myelinating. *Glia*, 29, 118–123.
- Weiner, H. L. (2005). Book Review. *New England Journal of Medicine*, 353(12), 1306–1307. <https://doi.org/10.1056/NEJMbkevr38300>
- Wilson, H. C., Scolding, N. J., & Raine, C. S. (2006). Co-expression of PDGF α receptor and NG2 by oligodendrocyte precursors in human CNS and multiple sclerosis lesions. *Journal of Neuroimmunology*, 176(1), 162–173. <https://doi.org/10.1016/j.jneuroim.2006.04.014>
- Włodarczyk, A., Løbner, M., Cédile, O., & Owens, T. (2014). Comparison of microglia and infiltrating CD11c+ cells as antigen presenting cells for T cell proliferation

and cytokine response. *Journal of Neuroinflammation*, 11(1), 57.
<https://doi.org/10.1186/1742-2094-11-57>

Wynn, D., Kaufman, M., Montalban, X., Vollmer, T., Simon, J., Elkins, J., ... Rose, J. W. (2010). Daclizumab in active relapsing multiple sclerosis (CHOICE study): a phase 2, randomised, double-blind, placebo-controlled, add-on trial with interferon beta. *The Lancet Neurology*, 9(4), 381–390.
[https://doi.org/10.1016/S1474-4422\(10\)70033-8](https://doi.org/10.1016/S1474-4422(10)70033-8)

Xia, M.-Q., Tone, M., Packman, L., Hale, G., & Waldmann, H. (1991). Characterization of the CAMPATH-1 (CDw52) antigen: biochemical analysis and cDNA cloning reveal an unusually small peptide backbone. *European Journal of Immunology*, 21(7), 1677–1684. <https://doi.org/10.1002/eji.1830210714>

Xia, M. Q., Hale, G., Lifely, M. R., Ferguson, M. A. J., Campbell, D., Packman, L., & Waldmann, H. (1993). Structure of the CAMPATH-1 antigen, a glycosylphosphatidylinositol-anchored glycoprotein which is an exceptionally good target for complement lysis. *Biochemical Journal*, 293(3), 633 LP-640. Retrieved from <http://www.biochemj.org/content/293/3/633.abstract>

Xia, Z., Dickens, M., Raingeaud, J., Davis, R. J., & Greenberg, M. E. (1995). Opposing effects of ERK and JNK-p38 MAP kinases on apoptosis. *Science*, 270, 1326–1331. Retrieved from <http://dx.doi.org/10.1126/science.270.5240.1326>

Yu, H., Pardoll, D., & Jove, R. (2009). STATs in cancer inflammation and immunity: a leading role for STAT3. *Nat Rev Cancer*, 9(11), 798–809. Retrieved from <http://dx.doi.org/10.1038/nrc2734>

ACKNOWLEDGEMENT

No duty is more urgent than that of returning thanks...

First and foremost, I bow the almighty for blessing me with strength, providing me endurance and giving me intelligence for the logics and conclusions that helped me to carry out this work.

*It is difficult to overstate my gratitude to my mentor **Prof. Dr. Martin Berghoff** for his supervision, exceptionally versatile guidance, valuable suggestions, critical appreciation and keen interest that brought this thesis to completion. I am extremely grateful to him for giving me an opportunity to work under his tutelage. I extend my gratitude of thanks to **Prof. Dr. Christine Stadelmann-Nessler** for being an important collaborator to pursue this project. I always felt motivated and encouraged every time I attended the meetings with her. Her suggestions were of great scientific importance and helped in materializing this project. I would like to express my heartfelt thanks to **Prof. Dr. Martin Diener**, who agreed to be my co-supervisor in the committee. His suggestions were valuable and encouraging.*

*I sincerely thank **Dr. Daniel Zahner** and the entire team of the animal facility for providing me with adequate facilities required for the entire research work. I extend my thanks to **Dr. Saskia Peters** for teaching and helping me with animal care and handling during my experiments.*

I am indebted to my lab colleagues Corny, Marita, Edith, Helga, Thomas, Dr. Siloia Tietz, Ranjithkumar, Backialakshmi and Salar for their assistance, cooperation and support during my work. I owe a special thanks to KishorKumar Sivaraj for being there and lending me his unconditional help and support whenever needed. I am thankful to my friends Harmandeep, Nora, Aarati, Andrej, Landry and Priyanka for giving me a family here away from home.

I am grateful to my husband Sudhanshu for his support and love. He always motivated to bring out the best in me.

I'm truly thankful to God for being blessed with such wonderful parents. My parents are my strength, all that I'm or ever hope to be, I owe to my Parents. No choice of words will suffice to adequately register my love for my Grandmother.

Lastly I acknowledge the sacrifice of meek creatures, without them this work would have been impossible.

Thank you everyone.....

Liza

Publications

Mittal L, Rajendran R, Berghoff M. Functional characterization of the protein kinase MK2 in the pathogenesis of Experimental autoimmune encephalomyelitis (EAE). 7th Annual Giessen Graduate school of Life sciences (GGL), Giessen, Germany. 2014

Mittal L, Rajenderan R, Berghoff M. Functional characterization of the protein kinase MK2 in the pathogenesis of Experimental autoimmune encephalomyelitis (EAE). 8th Annual Giessen Graduate school of Life sciences (GGL), Giessen, Germany. 2015

Mittal L, Rajenderan R, Berghoff M. MK2 is required for Glateramer acetate mediated C17.2 neuronal cell survival/proliferation. 31st ECTRIMS congress – Barcelona 2015